Unravelling the antimicrobial features of the incompatible solutes creatine and guanidino-ectoine

Dissertation

zur

Erlangung des Doktorgrades (Dr. rer. nat.)

der

Mathematisch-Naturwissenschaftlichen Fakultät

der

Rheinischen Friedrich-Wilhelms-Universität Bonn

vorgelegt von

Kati Christine Waßmann, geb. Sell

aus

Kamp-Lintfort

Bonn, Mai 2013

Angefertigt mit Genehmigung der Mathematisch-Naturwissenschaftlichen Fakultät der Rheinischen Friedrich-Wilhelms-Universität Bonn.

1. Gutachter: Prof. Dr. Erwin A. Galinski
2. Gutachter: apl. Prof. Dr. Christiane Dahl

Tag der Promotion: 19.07.2013
Erscheinungsjahr: 2013

Contents

List of Figures

List of Tables

List of abbreviations

Physical quantities and corresponding dimensions are abbreviated according to the International System of Units.

A_{260}	absorption at 260 nm
ADAM	1-amino-adamantane hydrochloride
approx.	approximately
B & D extraction	Bligh and Dyer extraction
BSA	Bovine Serum Albumin
Carb	carbenicillin
CH	Switzerland
DABA	L-2,4-diaminobutyric acid
DE	Germany
DSC	differential scanning calorimetry
dw	dry weight
EDTA	ethylenediaminetetraacetic acid
EtBr	ethidium bromide
exp.	exponential
FL	Finland
FLISE	flux measurements with ion selective electrodes
FMOC-Cl	fluorenylmethyloxycarbonyl chloride
GABA	γ-aminobutyrate
GC	gas chromatography
gd-ectoine	guanidino-ectoine (2-amino-3,4,5,6-tetrahydro-4-pyrimidine-carboxylate)
GFP	Green fluorescence protein
h	hour
HPLC	high performance liquid chromatography
Hz	hertz
INV	inverted membrane vesicles
Kan	kanamycin
kdp	potassium dependent uptake system
kup	potassium uptake system
LT	Lithuania
MeOX	O-methylhydroxylamine
MDa	mega Dalton
MIFE	microelectrode ion flux estimation

min	minute
MSTFA	N-acetyl-N-(trimethylsilyl)-trifuoroacetamide
Nha	sodium proton antiporter
OD_{600}	optical density at 600 nm
PLL	poly-L-lysine
poly(dA-dT)	poly(deoxyadenylic-deoxythymidylic) acid
R515/460	emission ratio of intracellular pH measurements (515 nm/460 nm)
TOF - MS	time of flight - mass spectrometry
TRIS	tris(hydroxymethyl)aminomethane
trk	transport of potassium
UK	United Kingdom
US	United States
UV	ultraviolet
V	Volt
VA	vitamine solution
v/v	volume per volume
w/v	weight per volume

1 Introduction

A life without bacteria?

Scientists agree on the fact that life on earth, the way we know it, would not be possible without bacteria. Most plants, all higher animals and the environment itself are dependent on bacteria, from which and with which life itself has evolved. Naturally, problems caused by microorganisms are not minor, but the fact that our life and a high proportion of medical and food productory applications depend on microorganisms is an adequate motive to discuss their advantages.

We live in close association with billions of bacteria. Most of them are harmless or even needed for our health. Approximately ten (non pathogenic) bacterial cells per one human cell can be found in and on the human body (Tannock, 1994) and are essential for survival, digestion of nutrition, protection from pathogens and disadvantageous environmental impacts as well as several more functions are featured by bacteria without us noticing. The same accounts for the earth's climate and environment. To give only two examples: Bacterial nitrogen fixation is fundamental for synthesis of our amino acids, and cycling of minerals such as carbon and sulphur is facilitated by decomposing microorganisms.

Apart from those very important tasks, bacteria have been used for industrial applications for a long period of time now. Besides applying them to our food for means of fermentation and thus preservation or simply diversification of the taste, various enzymes for molecular biological work or substances for cosmetics are isolated from bacteria. Biological clarification plants for reclaiming sewage, as well as biogas plants for biogas production out of renewable primary products, would be lost without bacterial activities to name but two examples of routine technical applications.

1.1 Environmental habitats and habits

The wide range of different species makes it possible to find adaptation experts amongst bacteria for almost every problem. Consequently, bacteria can be found at for human beings desperate environments such as the black smoker in the deep sea where species like the hyperthermophilic *Pyrolobus fumarii* grow at 113 °C (Blöchl *et al.*, 1997), or extremely cold environments like glaciers or the Arctic Sea where psychrophiles find their ecological niche with respect to growth temperature (Bowman *et al.*, 1997). Besides experimental research on organisms with tolerance towards extremely high or low temperatures, high or low pH and high pressure, a lot of research on halophilic bacteria and their way of adapting to osmotic pressure was performed during the last decades. They even became interesting for industrial applications.

1.2 Noteworthiness of halophilic and halotolerant microorganisms

Compared to hyperthermophilic, psychrophilic or barophilic organisms, cultivation of halophilic bacteria is fairly simple and requires low amounts of energy. Furthermore, the magnitude of habitats with high osmolarity is immense on earth. 70 % of the surface of the earth is covered with natural salt-water bodies. Additional to these habitats, artificial environments such as salinas or cured food serve as biotopes for a range of halophilic organisms (Vilhelmsson *et al.*, 1996). Adaptation of microorganisms has not only taken place to environments with constantly high osmolarity but also to locations with changing osmolarity like soils which are flooded regularly after periods of desiccation. Organisms living in such places must have strategies to adapt to changing water activities (Galinski & Trüper, 1994; Ventosa *et al.*, 1998). Without any adaptation strategies, a bacterial cell with its semi-permeable cytoplasmic membrane (Bovell *et al.*, 1963) would lose water and thus cell turgor which would lead to a breakdown of metabolism and growth in a hypertonic milieu (Brown, 1976). Cells adapted to hypertonic environments are named halotolerant (NaCl optimum of 3 %, growth until 10 % NaCl) or halophilic (growth at NaCl concentration above 10 %) (Oren, 2002) and the mechanisms evolved in maintaining the vitally important cell turgor at high extracellular osmolarity are termed osmoadaptation (Galinski, 1995). There are two different osmoadaptation strategies within bacteria, both decreasing the intracellular chemical potential of water until an osmotic equilibrium between intra- and extracellular milieu

is reached (Csonka, 1989).

1.2.1 Bacterial osmoadaptation

Salt-in-cytoplasm and organic-osmolyte strategy

Organisms using the salt-in-cytoplasm strategy, named by da Costa *et al.* (Da Costa *et al.*, 1998), accumulate inorganic ions, particularly potassium cations and chloride as counter ions (Oren, 1999) to molar concentrations (Oren, 2002). This in turn demands an adaptation of the whole cell machinery to high intracellular ionic strength (Oren, 1999). Salt-in-cytoplasm strategy is performed primarily by species of Halobacteriales and Halanaerobiales (Galinski & Trüper, 1994; Oren, 2002). In contrast to this, the organic-osmolyte strategy is more prevalent within microorganisms and has the great advantage of accomplishing rapid adaptation to environments of changing osmolarity (Da Costa *et al.*, 1998). This strategy is based on controlled accumulation of so called compatible solutes: organic, low-molecular, highly water soluble, osmotically active and at physiological pH electrically neutral compounds (Galinski, 1995). These solutes can either be taken up from the environment via specific transport systems or synthesized *de novo* by the bacterial cell (Kempf & Bremer, 1998). Since uptake requires less energy compared to *de novo* synthesis, uptake is favoured (Oren, 1999). As their name indicates, compatible solutes do not interfere with the metabolism up to molar concentrations (Brown, 1976). Compatible solutes can be found within sugars (e.g. trehalose), polyoles (e.g. glycerol), amino acids (e.g. proline) and also derivatives of these substance classes which can contain sulfate- or phosphate moieties (Galinski, 1995; Da Costa *et al.*, 1998). Apart from their role in osmoadaption, compatible solutes are important for the protection of macromolecules from other environmental stresses such as cold, heat or desiccation (Lippert & Galinski, 1992; Göller & Galinski, 1999; Borges *et al.*, 2002). Those extensive protecting features aroused the industry's interest in biotechnological applications many years ago and today some compatible solutes are already promoted in commercial products such as ectoine in cosmetics (Schwarz, 2005; Motitschke *et al.*, 2003). However, halotolerant and halophilic bacteria are not only interesting because of the compatible solutes they produce; uptake of those compounds from the environment can also turn to account, considering that e.g. waste waters arising from a wide variety of origins are loaded with, on the one hand, potentially valuable compounds or, on the other hand, harmful substances. Enzymatic reactions of bacteria might render those substances innocuous, which is naturally cheaper and less environmentally polluting than elaborated

conventional disposal.

1.2.2 Discovery of incompatible solutes

SESCOWA

The above announced idea of separating high value compounds from waste water with the help of halophilic bacteria has led to the so called SESCOWA-project ("Selective separation of high value compounds from complex waste waters by halophilic microorganisms" Application number: CRAF 1999 72246), which was set up in 2003 and was promoted by the EU. In her diploma thesis "Wertstoffgewinnung aus industriellen Prozess- und Abfallwässern mit Hilfe halophiler Bakterien", Sylvia Fassbender (Fassbender, 2004) dealt with marine waste waters, which mainly contained betaine as a solute for potential accumulation by bacteria. Betaine occurs in many places in nature; therefore, it is not surprising to find a range of bacteria featuring transport systems for this solute. Furthermore, betaine seems to be a relatively effective compatible solute. This quality caused some problems in detecting other solutes which could potentially be taken up by halophilic bacteria. Investigations of waste waters incurring during the processing of mackerels resulted in the surprising finding of only low amounts of betaine but high amounts of a different substance, which had not been detected in waste waters before. This substance was identified as creatine by NMR analysis (Amendt *et al.*, 2007) and assumed to be a further compatible solute with protecting features on salt stressed cells.

Creatine

Eugène Chevreul, a French scientist, was the first one to discover the substance creatine (Greek: *kreas* = meat) while investigating the composition of bouillon in 1834. About 10 years later the German chemist, Justus von Liebig, provided evidence of creatine being a constituent of mammalian meat. Today it is well known that creatine is a zwitterionic nitrogenous organic acid, which is synthesised mainly in the liver but also in the pancreas and the kidneys of vertebrates from the amino acids glycine, L-arginine and L-methionine. Phosphocreatine serves as an energy supplier, increasing the rate of regeneration of ATP from ADP whereupon creatine is generated. 95 % of total creatine in the human body can be found in skeletal muscle cells. Besides its role in skeleton muscles, creatine is essential for brain- and nerve functions. A full-grown human body contains 100 - 150 g creatine (depending on nutrition) whereof only half is synthesized *de novo*; residual amounts are taken up with food, especially from meat and fish products

(van der Knaap *et al.*, 2000; Kreider, 2003). An schema on the creatine metabolism in mammals is given in figure 1.1. The scheme derives from Patricia Allen (Allen, 2012).

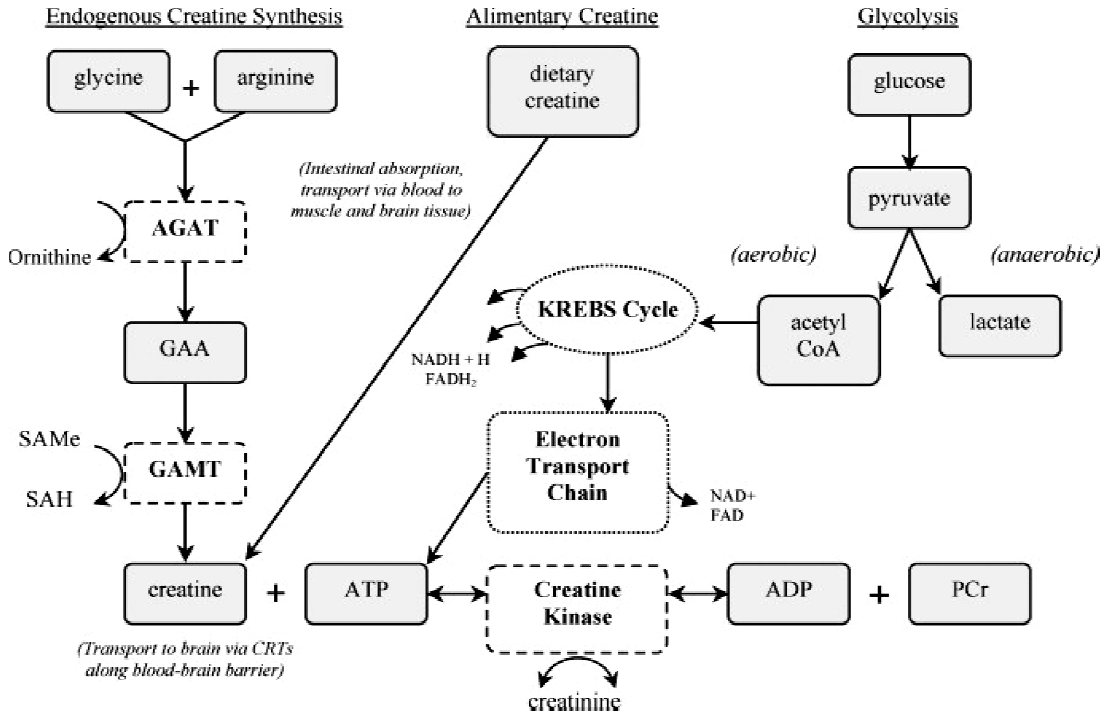

Figure 1.1: The figure as well as the following desctiption are taken from Allen, 2012. "*De novo* synthesis of creatine and relation to ATP. The machinery needed to produce endogenous creatine (dashed boxes) and ATP (dotted boxes) is expressed within neurons, oligodendrocytes, and astrocytes, but it is unknown to what extent this arrangement contributes to total brain creatine content. ATP synthesis from carbohydrate (glucose) occurs via three series of metabolic pathways: glycolysis, citric acid cycle (Krebs), and the electron transport chain. When ATP is rapidly depleted, creatine kinase catalyzes the donation of a phosphate group from phosphocreatine (PCr) to ADP, producing more ATP to buffer energy needs. Conversely, when energy is released, an individual phosphate group is cleaved from ATP and bound to creatine to rejoin the PCr pool. This reversible reaction causes a spontaneous byproduct (creatinine) that is excreted from the body, which is why creatine must be replenished daily (AGAT = arginine:glycine amidino transferase; CRT, creatine transporter; GAMT, guanidinoacetate methyltransferace; GAA, guanidinoacetate; SAMe, s-adenylmethionine; SAH, s-adenosylhomocysteine)."

In the field of body building it is not unusual to ingest creatine as dietary supplement to enhance muscle formation (Kreider, 1999). Occasionally creatine is also used in therapy

against musculoskeletal disorders (Schröter, 2008). But apart from that, it has so far not been established in many applications in the field of medicine. During the last decades, especially degradation and utilization of creatine by microorganisms have been studied. Enzymes involved in four different degradation pathways of creatine have been detected in bacteria isolated from chicken excrements, human urine and stomach (Dunn *et al.*, 1997; Gauglitz, 1988; Kopper & Beard, 1947; Kwon-Chung *et al.*, 1982). Those enzymes enable microorganisms to metabolise nitrogen and carbon from creatine and can be found within *Arthrobacter- Bacillus-*, *Clostridium-*, *Corynebacterium-*, *Escherichia-*, *Micrococcus* and *Pseudomonas*-species (Kaplan & Naugler, 1974; Polacheck & Kwon-Chung, 1980; Möller *et al.*, 1986).

Characterization of the impact of creatine on bacterial growth

First growth experiments with the newly discovered creatine from mackerel waste waters in the course of the SESCOWA project have led to the surprising result of creatine not at all being a compatible solute which enhances growth at elevated salinities. On the contrary, it showed to be a solute with the opposite effect of decreasing growth (Amendt *et al.*, 2007). A comparison of the molecule structures of creatine and betaine (figure 1.2) exposes that they bear resemblance to each other with one major exception: While the nitrogen in betaine is linked to 3 methyl groups, creatine owns a guanidine-function at this position.

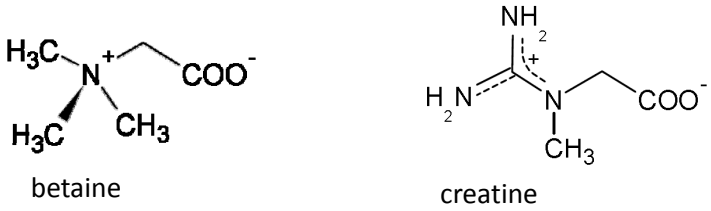

Figure 1.2: Chemical structures of the compatible solute betaine and the structurally related incompatible solute creatine.

Because of the structural relationship of betaine and creatine, it was assumed that creatine is being mistaken for the compatible solute betaine and taken up by transport systems for compatible solutes by mistake. The guanidine-function seems to be responsible for growth inhibition instead of an enhancing effect as it can be observed for compatible solutes in osmotic stress situations. Since creatine is not compatible with the metabolism, it was named an incompatible solute.

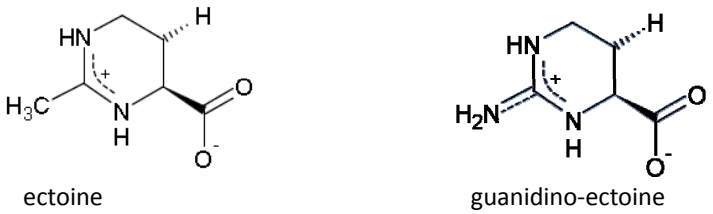

Figure 1.3: Chemical structures of the compatible solute ectoine and the structurally related incompatible solute guanidino-ectoine.

In his diploma thesis, Tobias Mann performed primary characterization experiments with creatine (Mann, 2008). Shortly after the first experiments it was clear that creatine is a specific growth inhibitor for Gram-negative bacteria: None of the tested Gram-positive strains was effected negatively, whereas nearly all tested Gram-negative strains showed reduced growth rates in the presence of creatine. In further studies it was shown that creatine also inhibits growth of some pathogenic organisms belonging to *Enterobacteriaceae* such as *Salmonella*- and *Yersinia*- species (Sell, 2009). Since growth experiments with deletion mutants of *E. coli* MC4100, which are deficient in *proU* and/or *proP*, showed no effect and no uptake of creatine, the hypothesis of creatine being taken up via the typical compatible solute transport systems ProP and ProU was successfully confirmed.
The assumption of the presence of the guanidino-function resulting in growth inhibition, can be encouraged by the fact that other guanidine compounds such as arginine or gunanidinium chloride are known to denaturate proteins (Waldmann, 2005). Amiloride inhibits activity of mammalian sodium-proton-antiporters (Kleyman & Cragoe, 1988) and 2-aminoperimidine even inhibits activity of bacterial sodium-proton-antiporters (Dibrov *et al.*, 2005). Therefore, it is not far-fetched to conclude that creatine with its guanidino-function might as well interact with bacterial proteins, possibly sodium-proton-antiporters which could lead to a growth inhibitory effect.

Guanidino-ectoine

In order to investigate whether other compounds structurally similar to compatible solutes also lose their protecting feature when a guanidinium group is introduced, a new derivative of the compatible solute ectoine, 2-amino-3,4,5,6-tetrahydro-4-pyrimidine-carboxylate (abbreviated guanidino-ectoine), was synthesized. Structures of those compounds are shown in figure 1.3.

First experiments with *E. coli* indicated similar growth inhibitory effects as already observed for creatine (Sell, 2009), which led to the conclusion that the addition of the guanidine-function is indeed responsible for the harmful effect on bacterial growth and that with guanidino-ectoine, a new incompatible solute was found (Sell & Galinski, 2011).

1.3 Ion transport in response to hyperosmotic stress

Since it is long known that one of the most rapid and elemental adaptation steps to an osmotic up-shock in *E. coli* are the accumulation of K^+ (Dinnbier *et al.*, 1988) and the extrusion of Na^+ (Karpel *et al.*, 1991; Padan *et al.*, 1989) and H^+ (McLaggan *et al.*, 1994; Akopyan & Trchounian, 2006), it is conceivable that (in)compatible solutes, which are accumulated in salt stress situations, affect those fluxes.
Potassium and sodium are fundamental cations on earth, considering that they belong to the most frequent elements of the lithosphere and occur in seawater in concentrations at an average of 10 mM in the case of potassium and even 450 mM in the case of sodium. In freshwater K^+ and Na^+ concentrations are significantly lower (1 - 2 mM). Interesting differences between the two ions arise when intra- and extracellular milieus of living cells are regarded. While K^+ is often actively transported into bacterial cells where it serves as a cofactor for a range of proteins (Médicis de, 1986) and is used to counteract high extracellular water potentials (Laimins *et al.*, 1981; Epstein & Laimins, 1980; Epstein & Schultz, 1965) the necessity to exclude sodium from the cytoplasm is so severe that different effective export systems have evolved. Several facts argue for the preferential accumulation of K^+ compared to Na^+. For instance, some energy dependent transport processes are known to use the electro chemical potential of Na^+ over the cytoplasmic membrane as driving force (Ventosa *et al.*, 1998; Tsuchiya *et al.*, 1977; MacDonald *et al.*, 1977; Stewart *et al.*, 1985). This system is virtually safe from breakdown since Na^+ is ubiquitous in natural environments, but it essentially requires the maintenance of an inwardly directed Na^+ gradient and thus the extrusion of sodium ions from the cytoplasm. Low intracellular Na^+ concentrations are also beneficial concerning macromolecule stabilisation. K^+ has a bigger ionic radius and is a rife cofactor and second messenger (Sutherland *et al.*, 1986; Higgins *et al.*, 1987) as well as an important cation to counter balance negative charges of anionic macromolecules, such as proteins and nucleic acids (Wiggins 1990). Na^+ on the other hand, with its smaller ionic radius is known to compete with K^+ but is often incompatible with maintenance of protein conformation and enzyme activity Both, K^+ accumulation and Na^+ extrusion are active

transport processes that are carried out against the concentration gradient and thus are energy requiring.

1.3.1 Potassium transport systems

Besides the functions mentioned above, potassium also plays an important role in bacteria when it comes to osmotic stress. The first instance to increase intracellular osmolarity to restore turgor after an osmotic up-shock is uptake and accumulation of K^+ (Epstein & Schultz, 1965). Shortly after that, further adaptation steps are induced, such as glutamate accumulation. Here again K^+ becomes essential, since it counterbalances the negative charge of glutamate (Tempest *et al.*, 1970). Subsequently compatible solutes are synthesized or taken up and the intracellular K^+ and glutamate levels decrease (Reed & Stewart, 1985; Dinnbier *et al.*, 1988; Whatmore *et al.*, 1990). Interestingly, K^+ also seems to be involved in regulation of respiration in osmotic stress situations (Meury, 1994). Those diverse functions of potassium necessitate strictly regulated uptake and efflux systems of which some will be introduced in the next paragraphs.

K^+ ATPases

Kdp (K^+-dependent) transport systems (Epstein & Davies, 1970) can be found amongst Gram-positive and Gram-negative Bacteria but not in the domain of Archaea (Durell *et al.*, 2000; Walderhaug *et al.*, 1989). Kdp is a specific and high affinity K^+ uptake system with a K_m in *E. coli* of 2 µM and a V_{max} which is only 1/3 as high as that of Trk (Stumpe & Bakker, 1997) (introduced in the next paragraph). Induction is carried out in K^+ limitation situations (Sutherland *et al.*, 1986; Laimins *et al.*, 1981) with K^+ concentrations below 200 µM (Stumpe & Bakker, 1997). It also comes into account for a short time after a hyperosmotic shock in response to changes in turgor pressure (Laimins *et al.*, 1981). Regulation of Kdp is based on transport activity and enzyme expression. Kdp consists of 4 components: KdpFABC. KdpF and KdpC accomplish structural functions (Gassel Altendorf 2001), whereas KdpA was described as the K^+ translocation unit of the system. It is a membrane protein with 10 transmembrane helices (Stumpe *et al.*, 1996). KdpB features ATPase function. The transport system translocates K^+ over the cytoplasmic membrane using ATP. It belongs to the superfamily of P-type ATPases, which indicates that in each translocation cycle one can observe a phosphorylated protein intermediate (Pederson & Carafoli, 1987).

Trk uptake systems

Trk systems (transport of K^+) (Epstein & Kim, 1971) are prevalent in the domain of Bacteria, Archaea (Durell *et al.*, 1999; Macario *et al.*, 1993) and Eukarya. Trk is characterised as a low affinity but high capacity system with a K_m in *E. coli* of 1 - 6 mM. It is constitutively expressed and its activity is osmoregulated. All known bacterial Trk systems comprise two essential components: TrkH, a K^+ translocating membrane protein and TrkA, a cytoplasmic membrane associated protein (Bossemeyer *et al.*, 1989; Schlösser *et al.*, 1995). TrkA owns a KTN domain (K^+ transport, nucleotide binding) and binds NADH and NAD^+ (Schlösser *et al.*, 1993). Such a KTN-domain is typical for many K^+ transport related systems and is also found in K^+ channels and K^+ efflux systems (Roosild *et al.*, 2002). Trk systems of Prokaryotes often contain only one membrane protein (TrkH). Here *E. coli* K-12 is an exception, meaning that two different K^+ translocating membrane proteins, which differ in substrate affinity and specificity, have been discovered: TrkH and TrkG. Therefore, *E. coli* K-12 owns two different Trk systems (Dosch *et al.*, 1991; Schlösser *et al.*, 1995). Interestingly, a further component, essential for TrkH function in *E. coli* has been discovered: *sapD* codes for TrkE, a membrane protein with ATP binding feature within the walker motives A and B. Trk is a K^+ H^+ symporter, dependent on high ATP level (Stewart *et al.*, 1985; Harms *et al.*, 2001), but independent on ATP hydrolysis. Contrary to TrkG, TrkH is not functional without TrkE. The unusual low GC content of TrkG and the location of the corresponding gene in the prophage region rec (recombinant activation) (Schlösser *et al.*, 1991) lead to the suspicion that the gene has been induced into the genome of *E. coli* K-12 via phagen and is therefore not an original *E. coli* protein and for this reason independent of TrkE.

Kup system

The Kup system (K^+ uptake, former TrkD) (Epstein & Kim, 1971) can be found in the domains of bacteria, plants and fungi. It consists of only one component and is, like Trk, a K^+ H^+ symporter. Kup is constitutively expressed and transports K^+ mainly at low osmolarity (Schleyer *et al.*, 1993), after hyperosmotic shock at low pH (Trchounian & Kobayashi, 1999) and when Trk and Kdp are not functioning or are not sufficiently effective. Compared to Trk, it reveals a slightly higher substrate affinity but lower transport rate (Bossemeyer *et al.*, 1989; Dosch *et al.*, 1991).

Efflux systems, Mechanosensitive channels

KefB, KefC In 1987 Bakker *et al.* already identified KefC and KefB to be the two major K^+ H^+ antiporters, which extrude K^+ from the cytoplasm (Bakker *et al.*, 1987). While KefB can be found within a wide range of bacteria, KefC is only found in Gram-negative ones, with the exception of the Gram-positive *Staphylococcus aureus* (Douglas *et al.*, 1991). K^+ extrusion is activated under certain conditions, such as increase in cell turgor (Bakker *et al.*, 1987), alkalisation of the cytoplasm (Nakamura *et al.*, 1984) and addition of dinitrophenol (Booth, 1985) or N-ethylmaleimide (Meury *et al.*, 1980). Experiments show that activation of K^+ efflux via KefB and KefC is always triggered by the reaction of glutathione with N-ethylmaleimide (not naturally occuring) which forms the activator N-ethyl-succinimidi-S-glutathione (Meury & Kepes, 1982) or alternatively the reaction of glutathione with other compounds that react with the sulphhydrylgroup of glutathione. It is proposed that natural activators simultaneously activate efflux and decrease activity of the uptake systems (Elmore *et al.*, 1990). Early research also shows that glutathione inhibits activity of KefB and KefC (Meury & Kepes, 1982; Bakker *et al.*, 1987; Elmore *et al.*, 1990), so that an increased glutathione level at high osmolarities protects cells from disadvantageous K^+ loss. This activation mechanisms of KefB and KefC via glutathione adducts is ubiquitous in Gram-negative bacteria (Douglas, Booth irgendwann nach 1990). A further interesting finding is the absence of a phenotype of $\Delta kefA$ $\Delta kefB$ mutant strains. Those two K^+ efflux systems are therefore not essential for growth, at least under the conditions tested by Booth (Booth, 1985).

KefA Apart from KefB and KefC, Gram-negative bacteria own a third K^+ efflux system which works as a mechanosensitive channel and is called KefA. KefA is responsible for balancing ion homoeostasis and hence turgor pressure during growth at high osmolarity (Levina *et al.*, 1999). According to growth experiments with *kefA* mutant strains, the encoded efflux system is not essential for survival, but mutation of the corresponding gene region leads to cell damage and lowered growth rates (Levina *et al.*, 1999), probably caused by prolonged opening times of the channels (Cui *et al.*, 1995). Compatible solutes, such as betaine, evoke K^+ efflux via KefA, either caused by the molecule itself or by increased turgor pressure due to accumulation of those osmotically active compounds to high cytoplasmic concentrations (Bakker *et al.*, 1987; Cui *et al.*, 1995).

1.3.2 Sodium transport systems

Sodium extrusion systems are mainly sodium proton antiporters (Nha), which are involved in Na^+ as well as in pH homoeostasis, not only in bacteria but in almost all species on earth. *E. coli* owns at least two of those Nha antiporters: NhaA and NhaB. Both are formed by 10 - 12 extensive alpha helical membrane spanning structures and both are electrogenic with a stoichiometry of 2 H^+ transported inside for every Na^+ which is expelled from the cytoplasm (Taglicht *et al.*, 1993). Purified membrane vesicles of an *E. coli* strain deficient in genes encoding for NhaA and NhaB did not reveal any Na^+ H^+ antiport activity, which leads to the assumption that those two are the exclusive specific antiporters in the membrane of *E. coli*. However, it is still possible that *E. coli* has silent antiporters. Interestingly, those double deletion mutants grow similar to wild type strains as long as Na^+ is absent.

NhaA NhaA is a high capacity but low affinity system, which is essential for adaptation to high salinity caused by NaCl and for growth at alkaline pH in the presence of Na^+. NhaA was observed to be sensitive to pH: At pH 7 it shows 3 times lower activity than at pH 9. NhaA functions as pH sensor and pH titrator but, nevertheless, contrary to Na^+ and Li^+, pH alone does not stimulate the expression of NhaA. Its inducibility increases with rising pH, though.

NhaB NhaB is a low capacity but high affinity transport system that is expressed constitutively. Compared to NhaA it features higher affinity to Na^+ but lower affinity to Li^+. NhaB grants the cell only low tolerance to Na^+ and is required when activity of NhaA limits growth. Based on the just named properties, NhaB provides additional protection in high Na^+ situations, but it cannot compensate complete loss of NhaA activity.

1.3.3 Maintenance of the electrochemical membrane potential

Hyperosmotic shock leads to a cascade of several adaptation reactions in bacteria, of which some are already announced above. The first and most rapid step to maintain turgor pressure after an osmotic up-shock in *E. coli* usually is the uptake of K^+ and the accumulation of glutamate. To sustain the fundamental electrochemical membrane potential, positive charges have to be transported out in exchange with K^+. This is done by extrusion of different positively charged molecules, such as putrescine^{2+} but mainly

by actively pumping out H^+ ions. For a long time it was unknown how this is achieved, but in 2006 Akopayan and co-workers (Akopyan & Trchounian, 2006) discovered that ATPases perform the extrusion of H^+, at least under fermentative conditions, in *E. coli*, which leads to alkalinisation of the cytoplasm after osmotic up-shock (Dinnbier *et al.*, 1988) or, as already observed much earlier, acidification of external milieu of e.g. *Aerogenes aeruginosa* (Tempest *et al.*, 1970).

1.4 Incentive to investigate function of incompatible solutes

As the last paragraphs indicate, osmoadaptation in bacteria, especially function of compatible solutes and corresponding ion fluxes, is a complex and not at all completely understood task. This makes investigation of the function of incompatible solutes all the more interesting. First of all, the new perspective of observing osmotic stress responses in the presence of incompatible solutes might gain new general insights into stress response of Gram-negative bacteria and into function of compatible solutes, as well. As indicated in the beginning, bacteria are naturally not only supporting for human life, but interaction with some of them can be unwanted, harmful or even life-threatening. Prevalent application of antibiotics throughout the last decades have resulted in continuous extension of bacteria being resistant to a wide range of established therapies, which makes it more and more important to search for new strategies to diminish unwanted bacteria. Eventually, incompatible solutes represent a new substance class for selective growth inhibitors of Gram-negative bacteria in the food industry or even medicine. To meet this aim, it is necessary to understand in which way those substances affect bacterial cells and to prove they are harmless for eukaryotes. The aim of this work is to enlighten the complex mode of action of creatine and guanidino-ectoine on the metabolism of *E. coli* as a representative of Gram-negative bacteria.

2 Materials and methods

2.1 Materials

2.1.1 Microorganisms

Organism	**Genotype**	**Reference**
Bacillus subtilis DSM 675^{T}	wild type	Cohn, 1972 described in (Smith & Gordon, 1957)
Escherichia coli DH5α	F^-, *sup*E44, *rec*A1, *end*A1, *rel*A1, *hsd*R17 (rk^-, mk^-), *gyr*A96, λ^-, *thi*-1, Δ(*lac*U169), (ϕ80*lacZ*ΔM15)	(Hanahan, 1983)
Escherichia coli DH5α-pRSET B-deGFP1	*E. coli* DH5α + plasmid pRSET B-deGFP1	(Sell, 2009)
Escherichia coli DH5α-pUC-deGFP1	*E. coli* DH5α + plasmid pUC19(Kan)-6His-deGFP1	this work
Escherichia coli DH5α-pUC19(Kan)-6His-pHluorin(pYEX)	*E. coli* DH5α + plasmid pUC19(Kan)-6His-pHluorin(pYEX)	provided by Ludwig, University of Bonn
Escherichia coli EP432	*mel*BLid, Δ(*nha*B1), Δ(*nha*A1), Δ(*lac*ZY), *thr*1	(Pinner *et al.*, 1993)

Organism	**Genotype**	**Reference**
Escherichia coli K-12 DSM 498	wild type	Castellani & Chalmers, 1919 described in (Ørskov, 1984)
Escherichia coli MC4100	*ara*D139, Δ(*arg*F-*lac*U169), *deo*C1, *flb*B5301, *rel*A1, *rps*L150, *pts*F25, *rsr*R	(Casadaban, 1976)
Escherichia coli MC4100 Δ(*ots*B)	*ara*D139 Δ(*arg*F-*lac*U169), *deo*C1, *flb*B5301, *rel*A1, *rps*L150, *pts*F25, *rsr*R, Δ(*ots*B)	(Meffert, unpublished)
Escherichia coli MKH13	MC4100, Δ(*put*PA101), Δ(*pro*P2), Δ(*pro*U608), [Spc^{r}]	(Haardt *et al.*, 1995)
Escherichia coli MKH17	MC4100, Δ(*put*PA101), *pro*P^{+}, Δ(*pro*U608), [Spc^{r}]	(Haardt *et al.*, 1995)
Escherichia coli NM81	*mel*BLid, *nha*B^{+}, Δ(*nha*A1),*kan*$^{+}$, Δ(*lac*ZY), *thr*1	(Padan *et al.*, 1989)
Escherichia coli TK2691	F^{-}*rha*, Δ(*kdp*FABC5), *trk*D1, *trk*H1, *trk*G90, *thi nadA*	(Dosch *et al.*, 1991)
Staphylococcus carnosus DSM 20501^{T}	wild type	(Schleifer & Fischer, 1982)

2.1.2 Culture media

All media were prepared in H_2O_{demin}. If not expressed otherwise, pH values of growth media and buffer were adjusted with 1 M KOH (for sodium free media), NaOH (for all media except sodium free media) or HCl. For the growth of strains carrying resistant genes, the corresponding antibiotic was added to the medium after autoclaving. Liquid media were stored at room temperature, agar plates at 4 °C. The percentaged NaCl concentrations are noted as a number at the end of the medium name (e.g. MM63-3 means MM63 medium with 3 % NaCl (w/v)).

Complex media

AB-medium (Antibiotic Broth Medium No. 3)	(L^{-1})
Antibiotic Broth Medium	17.5 g
NaCl	variable
pH 7.2	

Antibiotic Broth Medium contains 3.5 g NaCl per litre, which was considered during preparation of the medium. AB-medium was used for agar plates as well as for pre-cultures. For the latter, 2 % agar (w/v) were applied to the medium before autoclaving.

LBG-medium (Luria Bertani Medium)	(L^{-1})	(Bertani, 1951)
Caseine (enzymatically hydrolysed)	10 g	
Yeast extract	5 g	
Glucose	10 g	
NaCl	variable	
pH 7.5		

LBG-medium was used for growth experiments in complex medium and growth of *E. coli* K-12 prior to ribosome purification.

2 × YT-medium	(L^{-1})	(Sambrook *et al.*, 1989)
Caseinhydrolysate (Tryptone)	16 g	
Yeast extract	10 g	
NaCl	5 g	
pH 7.2		

2 × YT-medium served as growth medium for bacteria before chemically inducing competence and for regeneration of bacteria after transformation.

INV-medium	(L^{-1})
Peptone	10 g
Yeast extract	10 g
0.5 M K_2HPO_4	166 mL
0.5 M KH_2PO_4	41 mL
25 % glucose (w/v)	41 mL
pH 7.2	

INV-medium was used for growth of *E. coli* prior to purification of inside-out vesicles.

Synthetic media

Synthetic media were used for growth experiments. If not pronounced differently, osmotic stress was set with NaCl, KCl or sucrose according to announcements in the experiments to a total strength of 1,03 osmol/L (equivalent to 3 % NaCl (w/v)).

MM63	(L^{-1})	(Larsen *et al.*, 1987)
KH_2PO_4	13.61 g	
KOH	4.21 g	
$(NH_4)_2SO_4$	1.98 g	
$MgSO_4$ × 7 H_2O	0.25 g	
$FeSO_4$× 7 H_2O	0.0011 g	
NaCl	variable	
Glucose × H_2O	5 g	
pH 7.1		

Glucose was autoclaved separately in 50 - 100 mL H_2O_{demin} and transferred to the sterile medium after cooling to room temperature.

NaMM63	(L^{-1})
Na_2HPO_4	10 g
$(NH_4)_2SO_4$	1.98 g
$MgSO_4 \times 7\ H_2O$	0.25 g
$FeSO_4 \times 7\ H_2O$	0.0011 g
NaCl	variable
Glucose $\times\ H_2O$	5 g
pH 7.1	

Na_2HPO_4 and NaCl were dissolved before pH was adjusted to 7.1. pH was controlled by indicator paper to avoid intrusion of K^+ leaking from the pH-probe of the pH-meter. Further preparation was performed the same way as for the MM63-medium. Glucose was autoclaved separately in 50 - 100 mL H_2O_{demin} and transferred to the sterile medium after cooling to room temperature. Since this medium was used for potassium limitation experiments, ultra pure water was applied and all apparatuses were rinsed with ultra pure water before usage.

KMM63	(L^{-1})
KH_2PO_4	13.61 g
KOH	4.21 g
$(NH_4)_2SO_4$	1.98 g
$MgSO_4 \times 7\ H_2O$	0.25 g
$FeSO_4 \times 7\ H_2O$	0.0011 g
KCl	variable
Glucose $\times\ H_2O$	5 g
pH 7.1	

Glucose was autoclaved separately in 50 - 100 mL H_2O_{demin} and transferred to the sterile medium after cooling to room temperature. In contrast to MM63 medium, in the sodium free KMM63 medium osmolarity was increased with KCl instead of NaCl and ultra pure water was used.

K5	(L^{-1})	(Epstein & Kim, 1971), modified
Na_2HPO_4	6.50 g	
NaH_2PO_4	3.17 g	
$(NH_4)_2SO_4$	1.98 g	
$MgSO_4 \times 7\ H_2O$	0.25 g	
$FeSO_4 \times 7\ H_2O$	0.0017 g	
KCl	0.30 g	
NaCl	variable	
Glucose $\times\ H_2O$	5 g	
pH 7.1		

Glucose was autoclaved separately in 50 - 100 mL H_2O_{demin} and transferred to the sterile medium after cooling to room temperature. K5-medium contains similar compounds as MM63-medium but only 5 mM potassium. It was used for growth experiments where low potassium concentrations were required.

Spizizens-medium	(L^{-1})	(Spizizen, 1958)
$(NH_4)_2SO_4$	2 g	
K_2HPO_4	14 g	
KH_2PO_4	6 g	
$MgSO_4 \times 7\ H_2O$	0.2 g	
Tri-sodium citrate $\times\ 2\ H_2O$	1 g	
NaCl	variable	
Glucose $\times\ H_2O$	5 g	
pH 7.0		

Glucose was autoclaved separately in 50 - 100 mL H_2O_{demin} and transferred to the sterile medium after cooling to room temperature.

Media supplements

VA-solution (vitamin solution)	(L^{-1})	(Imhoff & Trüper, 1977)
Nicotinamide	0.35 g	
Calcium-DL-pantothenate	0.1 g	
Thiamine dichloride	0.3 g	
Biotin	0.1 g	
p-Aminobenzoic acid	0.2 g	
Pyridoxal chloride	0.1 g	
Vitamin B12	0.05 g	

Vitamin solution was sterilised by filtering through a filter with a pore size of 0.22 µM and stored at 4 °C in the dark. If needed, vitamin solution was diluted 1:1000 with sterile growth medium.

Antibiotics Organisms carrying plasmids were grown in presence of antibiotics to maintain selection pressure. Sterile stock solutions of 50 mg/mL Kanamycin in H_2O_{demin} or 100 mg/mL Carbenicillin in H_2O_{demin} were transferred to sterile media to a final concentration of 50 µg/mL (Kanamycin) or 100 µg/mL (Carbenicillin), respectively. Stock solutions were stored at -20 °C.

Supplementation with (in)compatible solutes Compatible solutes were added to growth media as sterile stock solutions. Incompatible solutes used in this work are poorly water soluble and have therefore been directly autoclaved in culture vessels

2.1.3 Buffers and solutions

If not expressed otherwise, ultra pure water was used to prepare the following buffers and solutions.

Buffers and solutions for HPLC analysis

Microextraction	
Bligh & Dyer Reagent (modified according to Galinski, 1986)	methanol/chloroform/ultra-pure H_2O (10:5:4, (v/v))
Isocratic HPLC	
Solvent Acetonitrile was recycled by distillation.	80 % (v/v) Acetonitrile
FMOC HPLC	
Borat buffer	0.5 M boric acid, pH 7.7 (adjusted with 1 N NaOH)
FMOC reagent	1 mM FMOC in acetone
ADAM reagent	40 mM ADAM in borat buffer, 1:1 dilution with acetone
Sodium acetate buffer	5 mM sodium acetate, pH 4.2
Solvent A	80 % sodium acetate buffer (v/v), 20 % acetonitrile (v/v), 0.5 % tetrahydrofurane (v/v)
Solvent B	20 % sodium acetate buffer (v/v), 80 % acetonitrile (v/v)

Buffers and solutions for preparation of inverted membrane vesicles and acridine orange measurements

Buffer A	50 mM Triethylamin acetate, 250 mM Sucrose, 1 mM EDTA, 1 mM Dithiotreitol
INV-Buffer	50 mM Triethylamin acetate, 250 mM Sucrose, 1 mM Dithiotreitol
Vesicle buffer	10 mM TRIS-HCl pH 8, 140 mM Choline chloride, 5 mM $MgCl_2$

Buffer for fluorescence measurements of deGFP1 (calibration)

Depending on required pH, solutions were buffered with MES (pH 6, 6.5), HEPES (pH 7.0) or TRIS (pH 7.5, 8.0, 8.5, 9.0), respectively. pH was adjusted with 1 M HCl or KOH.

Calibration-buffer (in H_2O_{demin})	
MES/HEPES/TRIS	75 mM
NaCl	140 mM

Buffers and solutions for purification of ribosomes

Resuspension buffer	10 mM TRIS-HCl, pH 7.6, 10 mM $MgCl_2$
Sucrose buffer	10 mM TRIS-HCl, pH 7.6, 10 mM $MgCl_2$, 1 M NH_4Cl, 37.8 % (w/v) sucrose
Storage buffer	10 mM TRIS-HCl, pH 7.6, 10 mM $MgCl_2$, 50 mM NH_4Cl

Buffers, solutions and material for MIFE and FLISE measurements

MIFE reference electrode	Electrolyte: 1 M NaCl, 2 % agar (w/v)
FLISE reference electrode	$MgSO_4$ CITSens Ion mini-reference electrode (C-CIT, Wädenswil/CH)
MIFE measuring electrode	
Backfilling solution	0.2 M NaCl
Frontfilling solution	Potassium ionophore I (Valinomycin)
FLISE measuring electrodes	
Potassium flux	CITSense Ion Potassium (K^+) selective mini-tube electrode (C-CIT, Wädenswil/CH)
Proton flux	Single Cell, Thin Stemmed, pH Glass Electrode for AgCl (Auchtermuchty, Scotland/UK)
Measuring solution	pH 7.0 adjusted with 2 mM MES/TRIS 0.1 mM $(NH_4)_2HPO_4$, 0.1 mM $MgSO_4$, 0.2 mM KCl, 1 % NaCl (w/v), 10 mM glucose, autoclaved
Shock solution	Measuring solution + 46 % sucrose (w/v)
Calibration buffer	
Potassium flux	Measuring solution with different KCl concentrations (0.1 mM - 10 mM)
Proton flux	1 mM KCl + 50 mM TRIS-HCl (pH 8.0)/ + 50 mM HEPES (pH 7.0)/ + 50 mM MES (pH 6.0)/ + 50 mM Acetate (pH 4.0 - 5.0)

Buffers and solutions for DNA thermal melting curve analysis

K^+-acetate buffer (in H_2O_{demin})	
Acetic acid	50 mM
EDTA	1 mM
pH 6.8 adjusted with 1 M KOH	

Buffers and solutions for molecular biology

Preparation of plasmid DNA	
Buffer P1	50 mM TRIS-HCl, 10 mM EDTA, 10 % RNase A (w/v), pH 8.0
Buffer P2	200 mM NaOH, 1 % SDS (w/v), pH 12.5
Buffer P3	3 M potassium acetate
Agarose gel electrophoresis	
Electrophoresis buffer(1 × TAE buffer)	40 mM TRIS-HCl, 10 mM EDTA, 0.6 % glacial acetic acid (v/v), pH 8.0
6 × Sample buffer (in H_2O_{demin})	60 mM EDTA, 0.09 % bromophenol blue (w/v), 60 % Glycerol (v/v)
EtBr solution (in H_2O_{demin})	10 µg/mL Ethidium bromide
GelRed™ solution (in H_2O_{demin})	3,300 fold dilution of 10,000 × stock solution
Transformation	
$CaCl_2/MgSO_4$ solution	70 mM $CaCl_2$ x 2 H_2O 20 mM $MgSO_4$ × 7 H_2O Autoclaved separately

2.1.4 Chemicals

Chemical	Manufacturer
1 kb DNA-ladder #SM0321	MBI Fermentas, Vilnius/LT
100 bp+ DNA-ladder #SM0311	MBI Fermentas, Vilnius/LT
Acetic acid (for synthesis)	Merck, Darmstadt/DE
Acetonitrile (LiChrosolv)	Merck, Darmstadt/DE
Acridine orange	Sigma, Deisenhofen/DE
1-Amino-adamantane hydrochloride (ADAM)	Sigma, Deisenhofen/DE
Adenosintriphosphate (ATP)	Roth, Karlsruhe/DE
Agarose	Roth, Karlsruhe/DE
Antibiotic Broth Medium No. 3	Oxoid LTD., Hampshire/UK
BCA-Assay: Protein Quantification Kit	Uptima, Montluçon/FR
Betaine ($\geq$ 98 %)	Fluka, Buchs/CH
Biotin (99 %)	Sigma, Deisenhofen/DE
Bradford reagent	Sigma, Deisenhofen/DE
Bovine serum albumin (BSA)	Uptima, Montluçon/Frankreich
$CaCl_2 \times 6\ H_2O$	Merck, Darmstadt/DE
Calf thymus DNA	Sigma, Deisenhofen/DE
Ca-DL-Panthothenate	Sigma, Deisenhofen/DE
Carbenicillin	Roth, Karlsruhe/DE
Caseinhydrolysat (Trypton)	Oxoid LTD., Hampshire/UK
Chloroform (LiChrosolv)	Merck, Darmstadt/DE
Choline chloride	Sigma, Deisenhofen/DE
Creatine monohydrate ($\geq$ 99 %)	Fluka, Buchs/CH
Creatinine	Fluka, Buchs/CH
Creatinine-HCl	Sigma, Deisenhofen/DE
Cyanocobalamin (Vitamin B12) (for biochemistry)	Merck, Darmstadt/DE
Dehysan Z 2111 (Antifoam)	Cognis, Düsseldorf/DE
D-Glucose $\times\ H_2O$ (for biochemistry)	Merck, Darmstadt/DE
1,4-Dithiotreitol	Roth, Karlsruhe/DE
DNase I	MBI Fermentas, Vilnius/LT
dNTP-Mix (2 mM)	MBI Fermentas, Vilnius/LT
Elektrophoresis buffer (1 $\times$ TAE)	MBI Fermentas, Vilnius/LT
Ethanol (p.a.)	Roth, Karlsruhe/DE

Chemical	Manufacturer
Ethidiumbromide	Fluka, Buchs/CH
Ethylenediaminetetraacetic acid (EDTA) (p. a.)	Serva, Heidelberg/DE
FastAP^{TM} Thermosensitive alkaline phosphatase	MBI Fermentas, Vilnius/LT
$FeSO_4 \times 7\ H_2O$ (p.a.)	Merck, Darmstadt/DE
Fluorenylmethyloxycarbonyl chloride (FMOC-Cl)	Sigma, Deisenhofen/DE
GelRed^{TM}	BIOTREND, Köln/DE
L-Glutamate	Fluka, Buchs/CH
Glycerine (99.5 %)	Serva, Heidelberg/DE
Guanidino-ectoine	own synthesis, Bonn/DE
4-(2-hydroxyethyl)-1-piperazineethanesulfonic acid (HEPES)	Roth, Karlsruhe/DE
High Yield Plasmid Mini Kit	SLG Süd-Laborbedarf GmbH, Gauting/DE
Isopropanol ($\geq$ 99.95 %)	Merck, Darmstadt/DE
Isopropyl-1-thio-β-D-galactopyranoside (IPTG)	MBI Fermentas, Vilnius/LT
K_2HPO_4	Roth, Karlsruhe/DE
KCl (ultra pure)	Merck, Darmstadt/DE
KH_2PO_4 (p.a.)	Merck, Darmstadt/DE
KOH (p.a.)	Roth, Karlsruhe/DE
L-2,4-Diaminobutyric acid $\times$ 2 HCl (97 %)	Fluka, Buchs/CH
Lysozym	MBI Fermentas, Vilnius/LT
Methanol (LiChrosolv)	Roth, Karlsruhe/DE
$MgCl_2 \times 6\ H_2O$ (ultra pure)	Merck, Darmstadt/DE
$MgSO_4 \times 7\ H_2O$ (p.a.)	Merck, Darmstadt/DE
$MnSO_4 \times 4\ H_2O$	Merck, Darmstadt/DE
2-(N-morpholino)ethanesulfonic acid (MES)	Roth, Karlsruhe/DE
Na_2PO_4	Merck, Darmstadt/DE
Na-Acetate $\times$ 3 H_2O (ultra pure)	Merck, Darmstadt/DE
NaCl (p.a.)	Fluka, Buchs/CH
NaH_2PO_4	Merck, Darmstadt/DE
NaOH (p.a.)	Merck, Darmstadt/DE
$(NH_4)_2SO_4$ (ultra pure)	Merck, Darmstadt/DE
Nicotinamide	Fluka, Buchs/CH
Nigericin	Sigma, Deisenhofen/DE

Chemical	Manufacturer
Norvaline	Sigma, Deisenhofen/DE
O-Methylisourea bisulfate (99 %)	Sigma Aldrich, St-Louis/US
p-Aminobenzoic acid	Fluka, Buchs/CH
Peptone from casein (for microbiology)	Merck, Darmstadt/DE
peqlab peqGOLD Gel Extraction Kit	Peqlab, Erlangen/DE
Phenol/Chloroform/Isopentyl alcohol (25:24:1)	Roth, Karlsruhe/DE
Phusion™High-Fidelity DNA Polymerase	Finnzymes, Espoo/FI
Polydesoxyadenylic-Thymidylic Acid (Poly(dA-dT))	Sigma, Deisenhofen/DE
Potassium ionophore I (Valinomycin)	Fluka, Buchs/CH
Pyridoxin × HCl (Vitamin B6) (for biochemistry)	Merck, Darmstadt/DE
Restriction endonucleases	MBI Fermentas, Vilnius/LT; New England Biolabs, Schwalbach/DE
RNase A	MBI Fermentas, Vilnius/LT
Select Agar	Gibco BRL, Paisly/UK
Sucrose	Roth, Karlsruhe/DE
Taurin	Fluka, Buchs/CH
T4-DNA-Ligase	MBI Fermentas, Vilnius/LT
Thiamin × HCl (Vitamin B1) (≥ 99 %)	Fluka, Buchs/CH
Tributylchlorosilane	Fluka, Buchs/CH
Triethylamine : acetate 1:1 (2 M : 2 M)	Fluka, Buchs/CH
Tris-(hydroxymethyl)-aminomethan (TRIS) (p.a.)	Roth, Karlsruhe/DE
Valinomycin	Sigma Aldrich, St-Louis/US
Yeast extract	Roth, Karlsruhe/DE

2.1.5 Software

- Clone Manager, Version 9, Scientific & Educational Software
- Plasmid Map Enhancer, Version 3.1, Scientific & Educational Software
- Primer Designer, Version 3.0, Scientific & Educational Software
- NCBI (national center for biotechnology information), http://ncbi.nlm.nih.gov (State: 21.May 2012)
- HPLC: ChromQuest 5.0 (Version 3.2.1, Thermo Quest Cooperation)
- MIFE: CHART, MIFEFLUX

- FLISE: Realview 3.0
- Analytic Jena, Specord 210: WinASPECT 2.2
- Perkin Elmer, LS 50 B: FL-WinLAB
- MicroCal, VP-DSC Microrcalorimeter: Microcal Origin
- Data analysis: Microsoft Office Excel 2007
- Text processing: LaTeX, distribution miktex-2.9.4521

2.2 Methods

2.2.1 Synthesis of the zwitterionic guanidino compound guanidino-ectoine

With the guanidine function, guanidino-ectoine holds the same functional group as the incompatible solute creatine. Since guanidino-ectoine is not purchasable, it was synthesized in this work according to standard procedures from L-2,4-Diaminobutyric acid and O-Methylisourea , as already described by Meffert (Meffert, 2012).

2.2.2 Culture conditions

An appropriate growth medium was inoculated with colonies from AB-agar plates and incubated overnight at optimal growth temperature in a shaking incubator (Fa. Infors AG, Bottmingen/Switzerland) at 180 rpm. 100 ml of growth medium (where required supplemented with (in)compatible solutes) were inoculated with the overnight culture to an optical density at 600 nm (OD_{600}) of 0.025 – 0.1 and incubated under the same conditions as the pre-culture. Information about growth conditions for the different strains are listed in table 2.3.

Table 2.3: Growth conditions for strains used in this work

organism	medium	temperature
B. subtilis	LBG, Spezizens-medium	30 °C
E. coli DH5α	AB-1	37 °C
E. coli DH5α-pRSET B-deGFP1	AB-1	37 °C
E. coli DH5α-pUC-deGFP1	AB-1 + Kan, MM63-1 + Kan, MM63-3 + Kan	37 °C
E. coli DH5α-pUC19(Kan)-6His-pHluorin(pYEX)	AB-1 + Kan	37 °C
E. coli EP432	MM63-2	37 °C
E. coli K-12	INV-medium	37 °C
E. coli MC4100	synthetic media (see respective experiments) + VA, LBG	37 °C
E. coli MC4100 Δ(*ots*B)	MM63-2 + VA	37 °C
E. coli MKH13	MM63-3 + VA	37 °C
E. coli MKH17	MM63-3 + VA	37 °C
E. coli NM81	MM63-2	37 °C
E. coli TK4623	MM63-3	37 °C
S. carnosus	LBG	30 °C

To observe the effect of (in)compatible solutes on bacterial growth, OD_{600} was monitored with a spectrophotometer (Novaspec II, Pharmacia, Uppsala/Switzerland) directly in side-arm flasks or in cuvettes with appropriate dilutions, depending on whether growth took place in side-arm flasks or mini-fermentation units.

2.2.3 Mini fermentation

Cultivations which required constant external pH values were performed in mini fermentation units. Preparation of pre-cultures and inoculation of main cultures was performed as described above (chapter 2.2.2). Mini fermentation units used in this work (DASGIP Technology, Jülich) are shown in figure 2.1.

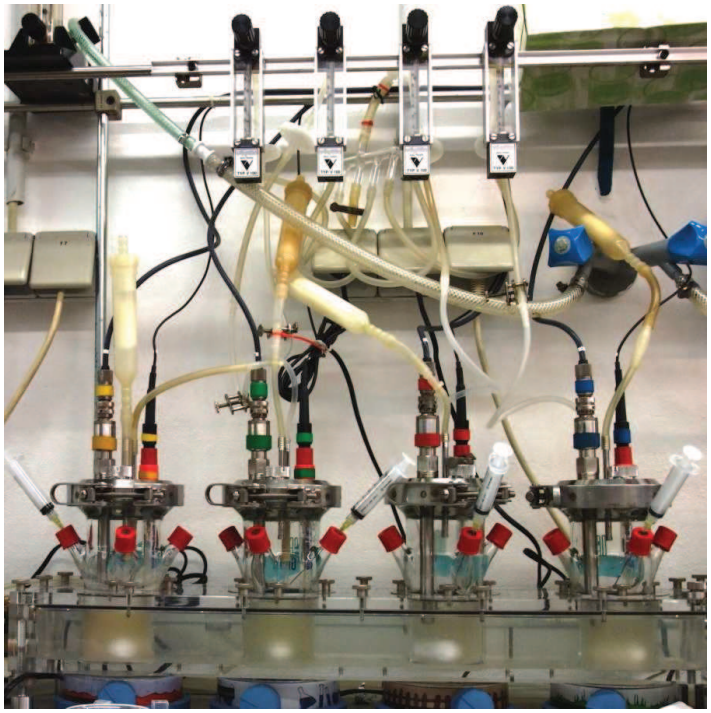

Figure 2.1: Composition of mini fermentation units. Mini fermentation units are embedded in a water bath and probes for pH value and temperature are connected to a data acquisition software. Oxygenation is accomplished through a sparger and a magnetic stirrer.

The cylindrical glass apparatuses with a volumetric capacity of 250 mL are equipped with probes for temperature, pH-measurement and spargers for oxygenation as well as magnetic stir bars for improved oxygenation. Sample drawing and adjustment of pH were performed with the help of sterile hollow needles and syringes, which were placed in silicone fixtures in the metal lids of the fermenters. If foaming occurred, antifoam (Dehysan Z 2111, Cognis, Düsseldorf/DE) was injected in the same way. Probes were connected to the Software DASGIP, which facilitated data acquisition and graphic demonstration of the different parameters of the fermentation process. Regulation of temperature was achieved with the help of a water bath in which the mini fermentation units were embedded.

2.2.4 Cell harvest

For determination of intracellular solute composition, stationary phase cells were harvested (20 min, 11,300 g) in a Beckmann centrifuge (Avanti^{TM} J-20XP, JA-10 rotor) and

freeze-dried with a full vacuum of 0.05 mbar at 20 - 30 °C (Heraeus Christ, Alpha 1-6) for 12 - 24 hours. Solutes were extracted from freeze-dried cells in chloroform/methanol/water (10:5:4, by volume) using a modified Bligh & Dyer technique (chapter 2.2.5).

2.2.5 HPLC (high performance liquid chromatography)

Bligh & Dyer - Microextraction of cytoplasmic compounds

The Bligh & Dyer technique (Bligh & Dyer, 1959) exploits the 2-phase separation of cellular components in a mixture of water, methanol and chloroform. At the same time macromolecular compounds (proteins, cell wall fragments) are precipitated at the interface between the polar layer (water/methanol) and the chloroform layer.
The extraction was performed as follows:
30 mg of freeze-dried and crushed cell material was transferred to a 1.5 mL reaction tube and 500 µL Bligh & Dyer solution was added. The mixture was shaken for at least 5 minutes at room temperature (IKA® VIBRAX®-VXR) before 130 µL chloroform and 130 µL H_2O_{demin} were added. After shaking for another 5 minutes, followed by a 5 minute centrifugation step at 9,300 g (Eppendorf Centrifuge 5415 R), the polar upper phase, which contained solutes and ions, was transferred to a fresh 1.5 mL reaction tube and stored at -18 °C until used for HPLC analysis.

HPLC

HPLC was used to detect and quantify (in)compatible solutes and amino compounds produced or accumulated by microorganisms.
Substances of interest in the Bligh & Dyer extracts were determined by comparing the retention time with a standard of this substance. The area of the signal-peak is used as a measure for the concentration of the particular substance. By comparing the area values of identified signals to those of the reference compounds of known concentration, the concentration of the substances of interest in the samples were determined. Measurements and analysis were facilitated by the software ChromQuest 4.2.34.

Isocratic aminopropyl phase HPLC

To determine the solute spectrum in the Bligh & Dyer extracts, the water soluble fraction was analysed via isocratic HPLC using a Nucleosil® aminopropyl-phase column (Macherey & Nagel, Düren, Germany) with acetonitril/water (80:20, (v/v)) as solvent.

Separation of solutes was monitored with a refractive index monitor and a UV-detector. This method allows the separation of polar solutes of different substance classes, such as sugars, polyoles, amino acids and derivatives. Hydrophilic compounds gain a stronger interaction with the terminal polar amino groups of the stationary phase which results in a decelerated elution from the column compared to hydrophobic compounds. Bligh & Dyer extracts were diluted 1:4 - 1:10 with acetonitril/water (80:20, (v/v)), mixed and centrifuged for 1 minute at 10,000 g (Thermo Scientific, Heraeus Christ Biofuge A) and injected into the injection valve. The isocratic NH_2-column HPLC system contained the following constituents:

- degasser (Spectra System SCM1000, Thermo Scientific)
- pump (Spectra System P100, Thermo Separation Products)
- injection valve for samples (Rheodyne Injector Nr. 7125, sample loop 20 µL, Rheodyne Inc.)
- Pre-column (LiChrospher 100-NH_2, 5 µm, Merck)
- separating column (CC 125/4 Nucleosil 100-3 NH_2, Macherey-Nagel)
- UV detector (Spectra System UV1000, 210 nm, Thermo Separation Products)
- RI detector (Shodex RI-71, Showa Denko K.K.)

Separation of substances was achieved by applying a flow rate of 1 mL/min at room temperature. Appropriate solute standards with defined concentrations enabled the calculation of intracellular solute concentrations in mmol/g dw.

FMOC/ADAM-HPLC

Identification and quantification of amino acids and other N-reactive compounds was performed by gradient HPLC with prior precolumn derivatisation using FMOC/ADAM (9-fluorenyl-methoxycarbonyl chloride/1-aminoadamantane). In this technique, amino-compounds are derivatised with FMOC, which allows the indirect detection of those compounds with a fluorescence detector. Bligh & Dyer extracts were diluted 1:20 - 1:100 with ultra-pure water. For pre-column derivatisation the following steps were performed: 40 µL of the diluted Bligh & Dyer extract or standard substance (25 µM) were mixed with 40 µL borat buffer, which contained 25 µM norvaline or taurine as internal standard, and 80 µL FMOC reagent for 45 seconds on a rotation shaker. 100 µL ADAM reagent were added before shaking for another 45 seconds. Derivatisation process was completed by adding 140 µL solvent A and mixing for a few more seconds. The internal standard served as a measure for quality of the derivatisation. Excessive FMOC was eliminated by binding to ADAM to prevent a reaction of FMOC with H_2O, which would otherwise

result in a large peak overlaying peaks of interest. The FMOC/ADAM HPLC system contained the following constituents:

- degasser (Spectra System SCM1000, Thermo Scientific)
- pump (Spectra System P2000, Thermo Separation Products)
- injection valve for samples (Autosampler Spectra Systems AS3000, sample loop 100 µL, sample volume 10 µL, specimen holder 4 °C, Thermo Separation Products)
- separating column (Merck Superspher 60 RP-8, 4 µm, 125 × 4 mm, LiChrocart-System)
- column oven (45 °C, Alltech Grom GmbH)
- fluorescence detector (Spectra System FL2000, 254 nm (exc.), 315 nm (em.), Thermo Separation Products)

Separation of substances was achieved by applying a flow rate of 1.25 mL/min and a solvent gradient, which is given in table 2.4. Appropriate solute standards with defined concentrations enabled calculation of intracellular concentrations in mmol/g dw.

Table 2.4: Solvent gradient during FMOC-HPLC

solvent gradient								
time [min]	0	15	30	40	42	47	49	51
solvent B [%]	0	9	30	60	100	100	0	0

2.2.6 Metabolomics

In collaboration with Jochem Gätgens of the Forschungszentrum Jülich, Germany, the metabolome of *E. coli* after growth with different (in)compatible solutes was investigated via GC/TOF-MS (gas chromatography/time of flight-mass spectrometry).

Preparation for GC/TOF-MS

E. coli MC4100 was cultured in MM63-3 + VA in side-arm flasks as described in chapter 2.2.2 until the end of exponential growth phase (OD_{600} of 0.8 - 0.9). Cultures were supplemented with 2 mM betaine, ectoine, creatine or guanidino-ectoine, respectively. To compare metabolome of salt stressed to that of osmotically unstressed cells, *E. coli* MC4100 was cultivated in MM63-1 + VA, additionally. Harvest of cells was performed as described in chapter 2.2.4. After centrifugation cell pellets were shortly dried on Whatman-filters and transferred to 1.5 mL Eppendorf caps, which were immersed in

liquid nitrogen, immediately. By this means time from centrifugation stop to freeze of cells fell below three minutes which was important for the reduction of changes in metabolome during preparation of cells for later analysis. Frozen cells were stored at -20 °C until freeze-drying (Heraeus Christ, Alpha 1-6) over night which was followed by Bligh & Dyer extraction as described in chapter 2.2.5. 400 µL of every Bligh & Dyer extract were transferred to 2 mL screw cap tubes and sent to Forschungszentrum Jülich, where GC/TOF-MS measurements were to be performed. The remaining 100 µL of the different Bligh & Dyer extracts were prepared for HPLC analysis (see chapter 2.2.5).

GC/TOF-MS

GC/TOF-MS measurements were performed by Jochem Gätgens of the Forschungszentrum Jülich according to the following protocol:

Sample preparation 130 µL of the sample were frozen in liquid nitrogen and freeze-dried over night (Heraeus Christ, LT-105). Dry samples were stored at -20 °C.

Derivatisation The freeze-dried samples were derivatised with 50 µL O-methyl-hydroxylamine in pyridine (MeOX, 20 mg/mL) for 90 minutes at 30 °C in a thermomixer (Eppendorf) at 600 rpm. After addition of 80 µL MSTFA (N-acetyl-N-(trimethylsilyl)-trifuoroacetamide) incubation took place for another 90 minutes at 40 °C at 600 rpm.

GC/ToF-MS measurements Derivatised metabolites were separated and determined using a gas chromatograph (Agilent 6890N) equipped with a 30 m Varian FactorFour VF-5ms + 10 m guard column. The GC was coupled to a high resolution time of flight mass spectrometer (Waters Micromass GCT Premier). Data acquisition and control of the measuring system were accomplished by the software Waters MassLynx 4.1.

Identification of peaks Already established metabolites were identified by comparing fragment patterns to recordings in different data base such as the commercial database NIST08 (National Institute of Standards and Technology, USA), the free available database GMD (MPI of Molecular Plant Physiology, Golm) and the in-house database JuPoD. Fragments of unknown substances were identified by combining elemental compositions.

2.2.7 Analysis of ion transport activity

Preparation of inverted membrane vesicles

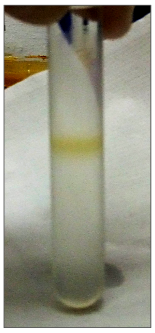

Figure 2.2: Appearance of centrifugation tube after sucrose gradient centrifugation during purification of inside-out vesicles. The membrane fraction is visible as a brown band in the upper third of the gradient and can be removed with a cannula and a syringe for further preparation steps.

Preparation of inverted membrane vesicles (INV) was performed according to Müller and co-workers (Müller & Blobel, 1984) with slight modifications. All preparation steps (except cultivation of *E. coli*) were performed on ice or with technical equipment cooled to 4 °C.

E. coli K-12 was grown at 37 °C and 180 rpm in 2 × 0.5 L INV-medium in 1 L side-arm flasks until the end of exponential growth phase (OD_{600} 1.0) and harvested (Beckman Coulter Avanti™ J-20XP, JA-10 rotor, 10 min, 11,300 *g*, at 4 °C). Cell pellets were resuspended in Buffer A (chapter 2.1.3) followed by further centrifugation (Beckman Coulter Avanti™ J-20XP, JA-25-50 rotor, 10 min, 7730 *g*, at 4 °C). After discarding supernatant, cell pellets of different centrifugation tubes were resuspended in Buffer A with 0.5 mM PMSF and 10 µg/mL DNase and combined. To get inverted vesicles, cells were passed through a French press (Thermo Spectronic, French® Pressure Cell Press) 1 - 2 times at 1020 psi. To separate cell debris and not disrupted cells from inverted vesicles a further centrifugation step followed (Beckman Coulter Avanti™ J-20XP, JA-25-50 rotor, 7730 *g*, 20 min, at 4 °C), and the resulting supernatant was centrifuged at 150,000 *g* for 2 hours at 4 °C (Beckman Coulter Optima™ LE-804, rotor 70Ti). The pellet which contained inverted vesicles was resuspended in Buffer A.

During a subsequent sucrose gradient ultra centrifugation, outer membrane-free INV were prepared. Therefore centrifugation tubes were filled with 4 mL 2.02 M sucrose in Buffer A followed by 3.3 mL 1.44 M sucrose in Buffer A followed by 3.3 mL 0.77 M sucrose in Buffer A. This sucrose gradient was overlayed with approx. 2 mL of the resuspended cell pellet. Ultra centrifugation was performed in a swing-bucket rotor (Beckman Coulter Optima™ LE-804, rotor SW41) at 82,705 *g* for 17 hours at 4 °C. After centrifugation 2 interphases were visible, as shown in figure 2.2. The upper, darker one contained the inverted vesicles and was carefully removed and transferred to a fresh centrifugation tube, using a hollow needle and a syringe. The membrane fraction was diluted approx. 1:4

with Buffer A without sucrose, and the inverted vesicles were finally pelleted at 150,000 *g* for 2 hours at 4 °C (Beckman Coulter Optima™ LE-804, rotor 70Ti). The pellet was resuspended in INV-buffer. 0.3 mL aliquots were frozen in liquid nitrogen and stored at -70 °C if not directly used for activity measurements.

Bradford protein test

Bradford-assay (Bradford, 1976) was used to determine protein concentration in solutions of purified inside-out vesicles. This protein concentration served as a measure of vesicle concentrations for later ion transport activity measurements. Albumin from bovine serum (BSA) with appropriate concentrations was used to generate a calibration curve from which protein concentrations of vesicle samples were calculated. The assay was performed as follows:
BSA stock solution (2 mg/mL) was diluted in H_2O_{demin} to final concentrations of 0.00, 0.25, 0.50, 0.75, 1.00, 1.25 and 1.50 mg/mL. 5 µL of diluted BSA-solutions were pipetted into a 96-well plate and mixed with 250 µL Bradford reagent. 5 µL H_2O_{demin} and 250 µL Bradford reagent served as reference. Vesicle solutions were diluted 1:2 in INV-buffer (see chapter 2.1.3) and 5 µL of diluted and undiluted samples were mixed with 250 µL Bradford reagent in the wells. After incubation at room temperature for 10 minutes absorbance was measured at 595 nm (Infinite M200, Tecan, Crailsheim). Each sample (BSA-, reference-, vesicle-solutions) was applied to four wells, and the arithmetic mean was used to calculate protein concentrations.

Performance of transporter activity tests

Acridine orange, a pH sensitive fluorescent dye, was used to measure Nha antiport- and potassium transport activity indirectly via pH changes outside the inverted membrane vesicles. Emission intensities were measured in 1 mL Suprasil® quartz glass cuvettes (HELLMA, Müllheim/DE) at 570 nm with an excitation wavelength of 430 nm in a fluorescence spectrometer (Perkin Elmer LS-50B). Measurement control and recording of data were achieved with the help of the spectrometer software FL WinLab.
According to Nies *et al.* (Nies, 1995), vesicles (50 - 100 µg membrane protein, beforehand measured and calculated with the help of Bradford protein test, chapter 2.2.7) were resuspended in vesicle buffer with 1 - 2 µM acridine orange and energized with 2 mM ATP. At an excitation wavelength of 430 nm and an emission wavelength of 570 nm changes in fluorescence intensity were monitored. After the resulting quenching reached

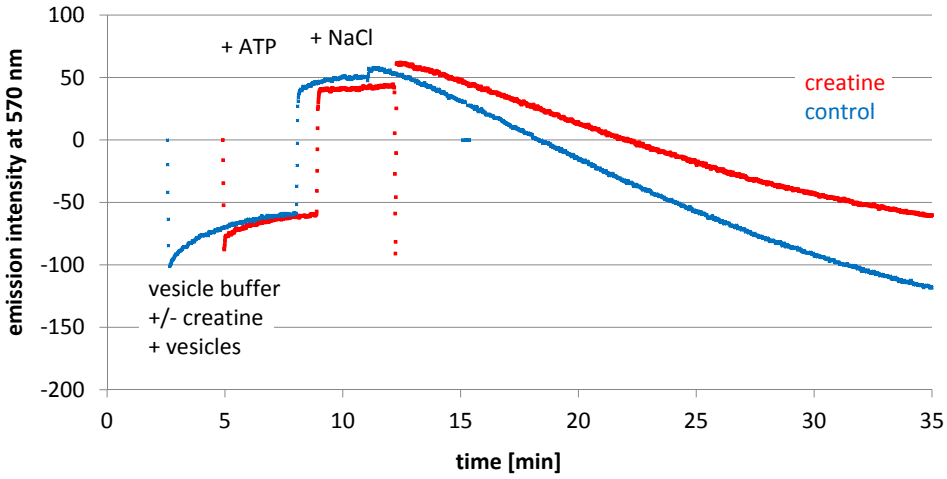

Figure 2.3: Representative patterns of Nha activity measurements on inverted membrane vesicles of *E. coli*. The steeper the slope after addition of NaCl, the faster the pH-change in the measuring buffer and the higher the activity of the Na^+/H^+ antiporters.

a steady state, NaCl or KCl was added to initiate ion transport. The respective salt concentration in the cuvette was 10 mM.

The change of proton concentration due to transport activity is indicated by change in fluorescence intensity. The influence of creatine, guanidino-ectoine and betaine on transport activity was determined by applying vesicle buffer containing different concentrations of these substances in the fluorescent measurements. Changes of emission intensities after NaCl/KCl addition reflected the extent of transporter activity and were compared to each other. Typical patterns of such measurements are shown in figure 2.3.

2.2.8 Intracellular pH measurements

To investigate the effect of creatine on changes of intracellular pH during growth, a pH sensitive GFP derivative, deGFP1 (Hanson *et al.*, 2002), was cloned into *E. coli* (chapter 2.2.12). The ratiometric deGFP provides a convenient method for intracellular pH measurements independently on cell mass which is a great advantage especially for determination of cytoplasmic pH during growth.

Measurements were performed in a fluorescence spectrometer (Perkin Elmer LS-50B) using Suprasil® quartz glass cuvettes (HELLMA, Müllheim/DE). Measurement control and the recording of data were facilitated by the spectrometer software FL WinLab. At an excitation wavelength of 400 nm, the typical dual emission of deGFP1 at 460 and

515 nm (with intensities depending on pH) was monitored.

Calibration

To calculate corresponding pH values, calibration curves of cell cultures were constructed according to the following method:
5 × 500 µL of stationary cell culture (*E. coli* DH5α-pUC-deGFP1 in AB-1 medium + kan) was harvested (10,000 rpm, 3 minutes, 20 °C) and washed in 500 µL calibration buffer each (chapter 2.1.3) with pH values of 7.0, 7.5, 8.0, 8.5 or 9.0, respectively.
The washed cell pellets were resuspended in the same calibration buffer as before and supplemented with 1 mM EDTA to increase membrane permeability or rather to disrupt the outer membrane of *E. coli*. During incubation at 30 °C for 4 minutes the samples were shaken several times. Cells were washed and resuspended again in 1 mL of the appropriate calibration buffer. Solutions were supplemented with 50 µM Nigericine as H^+ and K^+ ionophore and 50 µM Valinomycin as K^+ ionophore. At this point intra- and extracellular pH were assumed to be identical and fluorescence measurements were performed. Emission ratios (R515/460) were calculated and plotted versus pH values of the equilibrated cells in the pH range of 7.0 to 9.0.

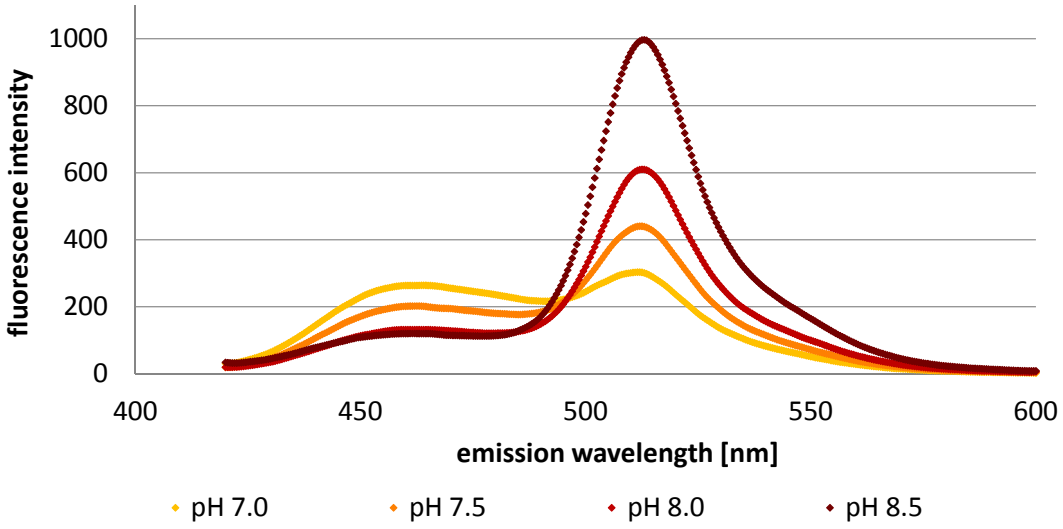

Figure 2.4: Emission spectra of purified ratiometric deGFP1 in buffers of increasing pH. Samples were excited at 400 nm and emission was monitored from 420 to 600 nm. Calculation of ratios between the two characteristic emission peaks at 460 and 515 nm allow construction of calibration curves which enable determination of pH values in samples of unknown pH.

In vivo pH measurements

Growth experiments of *E. coli* DH5α-pUC-deGFP1 in MM63-3 with supplementation of 4 mM creatine or no supplementation were performed in mini fermentation units (DASGIP Technology, Jülich) (chapter 2.2.3). Samples for emission measurements were taken every few hours and growth was observed measuring OD_{600}. pH of cultures was adjusted with sterile 1 M NaOH during growth.
For pH measurements, cell cultures were diluted with growth medium and emission was monitored after excitation at 400 nm. R515/460 was calculated and intracellular pH values were determined with the help of the calibration curve. Representative emission curves are shown in figure 2.4. Corresponding measurements were performed previous to this work on purified proteins (Sell, 2009).
Optimally, calibration curves are constructed before every measurement with the cells of the specific experiment, which was not practicable in this case. Calibration values of stationary cells of the pre-culture were used for the whole experiment.

2.2.9 Ion flux measurements

To determine the influence of incompatible and compatible solutes on the flux of monovalent cations after an osmotic up-shock, two different techniques were used: microelectrode ion flux estimation (MIFE) and flux measurements with ion selective electrodes (FLISE), which will be described in the following paragraphes.

MIFE

About 20 years ago Ian Newman from the University of Tasmania started to establish a system for non-invasive ion flux measurements across (plant) membranes: the MIFE system. Today MIFE is an expedient tool (albeit not yet used by many scientists) for studies of membrane-transport processes from eukaryotes to prokaryotes in living organisms. Technical background information as well as the mode of operation of the MIFE system are given in publications by Shabala and co-workers, especially from 1997 and 2006 (Shabala *et al.*, 1997; Shabala *et al.*, 2006). In figure 2.5 the MIFE system, similar to the one used in this work, is illustrated. The photograph and description of the figure are taken from the above cited paper of Shabala from 2006.
Principles of MIFE-measurements are displayed in figure 2.6, which is again taken from Shabala *et al.* 2006.

The following paragraphs explain preparation steps for MIFE measurements which were used in this work to determine potassium fluxes across the membrane of *E. coli*.

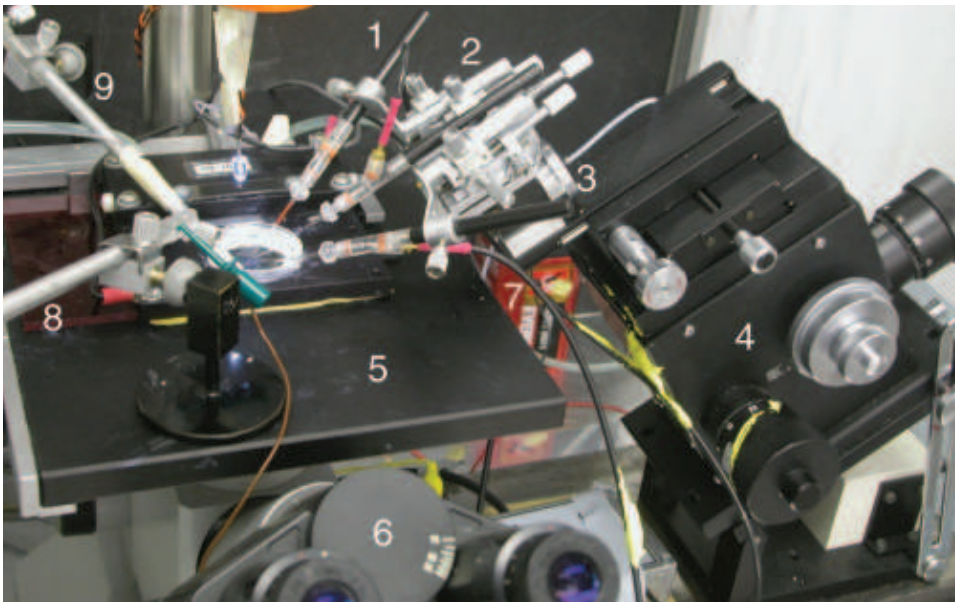

Figure 2.5: Assembly of the MIFE system similar to the one used in this work except for the number of measuring electrodes and (9). The photograph as well as the following description are taken from Shabala *et al.* 2006: "The cover slip containing the bacterial 'monolayer' is placed on the bottom of the Petri dish. Three ion-selective microelectrodes are mounted in electrode holders (1). Electrode holders are assembled on a MMT-5 micromanipulator (2), allowing fine electrode-tip adjustment. The manipulator is mounted on the cartridge (3) of the computer-driven hydraulics manipulator (not shown). The assembled electrode unit is mounted on a 3D mechanical manipulator (4), allowing precise positioning of electrode tips near the surface of the bacterial monolayer. All manipulations are performed under high ($\times 200$ or $\times 500$) magnification of the microscope (6). Microscope stage (5) also contains the reference electrode holder (8) and another holder with syringe needle (9), connected to a peristaltic pump and used for rapid solution replacement. The whole unit is located within the Faraday cage. To reduce electrical noise, a battery (7) and an LED are used for illumination instead of the normal microscope lighting system".

Immobilization of bacteria on cover slips

For ion flux measurements with MIFE, an immobilised monolayer of bacterial cells on cover slips is needed. Poly-L-Lysine (PLL), a polypeptide with positively charged moieties, is used to enhance the adhesion effect of bacteria to the glass surface. To accomplish such a monolayer several preparation steps are essential:

Cleaning and sterilization of cover slips To clean cover slips and remove organic residues they were placed in a glass beaker together with glass beads and 1 % HCl solution in H_2O_{demin}. The beaker was covered and the mixture was boiled and swirled for 30 minutes before the cover slips were washed with H_2O_{demin} 3 times. After dipping each cover slip into 100 % ethanol separately, 30 minutes treatment with UV rays followed. Clean and sterile cover slips were stored in sealed, sterile Petri dishes.

PLL treatment Prior to immobilisation, cover slips were treated with PLL to strengthen the subsequent adhesion effect of the cells to the glass surface. Approximately 300 µL of PLL solution (0.1 % (w/v) in H_2O_{demin}) were pipetted on top of cover slips which were covered afterwards. After several hours any remaining PLL solution was removed and the treated cover slips were carefully rinsed with sterile H_2O_{demin}.

Immobilisation of bacterial cells on PLL treated cover slips 30 µL of concentrated cell culture (harvested culture, resuspended in measuring solution (chapter 2.1.3)) was transferred onto the PLL treated side of a cover slip and left for 1 minute. By shortly dipping the cover slip into sterile measuring solution, unattached cells were removed. After successful immobilisation, the monolayer of cells was visible as a flimsy haze. Measurements were started immediately after immobilization.

Preparation of microelectrodes

Within the prearrangements for MIFE measurements, the preparation of measuring electrodes is the critical component determining the quality of each measurement. Unfortunately the success of producing an optimal measuring electrode for a specific measurement is based mainly on experience and cannot simply be achieved by following instructions of a text book. Nevertheless, the following paragraphs describe the principal preparation steps.

Preparation of Ag/AgCl-reference electrodes Glass electrodes (glass capillaries with 1.5 mm outer diameter, non-filamentous borosilicate (e.g. GC 150-10, Harvard Apparatus Ltd., UK)) were pulled with a self made electrode puller (by Sergey Shabala, University of Tasmania), comprising an electrode holder, which is connected to a metal weight and a heater coil which envelopes the glass electrode. The tips of those electrodes were broken to enlarge the diameter from 1 µm to approx. 50 µm. Appropriate reference electrode solution (chapter 2.1.3) was heated in a suitable beaker and the electrodes were

dipped slowly into the hot agar-solution. Ideally this lead to soakage of the agar into the electrode without any air bubbles. The electrodes were covered with the remaining agar solution, sealed with parafilm and stored at 4 °C. When required, agar filled electrodes were withdrawn and a chloride silver wire was inserted into the base hole of the electrode. Wire and electrode were stabilised by sealing the transition of those constituents with parafilm.

Preparation of measuring-electrodes Before usage of microelectrodes pulled from glass capillaries of non-filamentous borosilicate with 1.5 mm outer diameter, a series of drying and silanisation steps had to be performed. Pulled electrodes were placed carefully, base down into a heat resistant electrode rack and were dried in an oven at 200 °C. To attain a hydrophobic microelectrode surface 30 µL tributylchlorosilane were dropped into the electrode holder after 5 hours, which was carefully but promptly closed with a suitable cover. After 10 minutes of silanisation, the cover was removed, the oven was turned off and the electrodes were left in the oven for another 30 minutes until they were cooled down. The rack with the electrodes was covered and stored at room temperature up to 6 weeks.

Filling of microelectrodes

Enlargement of tip diameter A micro electrode and a crude glass capillary were positioned opposite to each other in electrode holders under a binocular microscope, the tips close to each other. The electrode was carefully moved towards the glass capillary until a little slice of the electrode tip was broken off, so that the tip diameter was increased from 1 µm to approx. 2 µm. At this point in time the electrode contained an optimal surface and shape for the MIFE measurements.

Back-filling of microelectrodes Appropriate back-filling solution (chapter 2.1.3) was inserted into the microelectrode through the base hole with the help of a back-filling pipette (syringe with a long needle, MF34G-5, WPI, Sarasota, FL). Electrodes were filled up to 2/3, necessarily without air bubbles.

Preparation of front-filling tube An electrode was pulled as described above (chapter 2.2.9) and the tip was broken off to increase the tip diameter to approx. 30 µm. The enlarged tip of the electrode was dipped into appropriate stock of ionophore (chapter 2.1.3) for a few seconds until the electrode contained an ionophore column of approx.

1 mm. Front-filling tubes were stored at room temperature in darkness.

Front-filling of measuring electrodes Front-filling tube and micro electrode with the back-filling solution were positioned opposite to each other in electrode holders under a binocular microscope, the two tips close to each other. The measuring electrode was carefully moved towards the front filling tube to a slight contact for 3 seconds (without breaking the electrode tip) which led to ionophore-uptake into the measuring electrode, which could be observed under the microscope.
The filled electrodes were used for calibration and subsequent measurements, immediately. Filled electrodes were used for up to 24 hours, sometimes even longer (possible changes in characteristics of electrode were checked from time to time by means of calibration).

Calibration of microelectrodes

To test the condition of the self-made electrodes as well as for later flux calculations, calibrations were performed after every electrode preparation and if used for several measurements, calibrations were also performed in between to exclude errors due to faulty electrodes. The measuring electrode was fitted to an electrode holder and a set of three standard solutions (chapter 2.1.3) with increasing concentrations of the ion to measure was prepared. The measuring electrode and reference electrode were placed in the different standard solutions for approx. 1 minute each, and all computing steps were performed according to the instructions of the CHART software and the corresponding manual. Electrodes with response of less than 50 mV per decade for monovalent ions and / or with correlation coefficients smaller than 0.999 were judged as useless and have therefore been discarded. Both, slope and intercept of calibration line, were used to calculate the concentrations of ions during the experiments. Features as electrode resistance (typically $1 - 4\,\mathrm{G\Omega}$) and length of ionophore-column in the electrode tip are critical for electrode signal-to-noise resolution (Shabala *et al.*, 2006) and offered opportunities for optimisation during the electrode preparation process.

MIFE measurements

After calibration of the electrode and immobilisation of the bacterial cells on the PLL-treated cover slips preparations for measurements were complete. A cover slip with the immobilised cells was now placed in a small Petri dish and fastened with a small glass tube. 3 mL of measuring solution (chapter 2.1.3) were added. The reference electrode

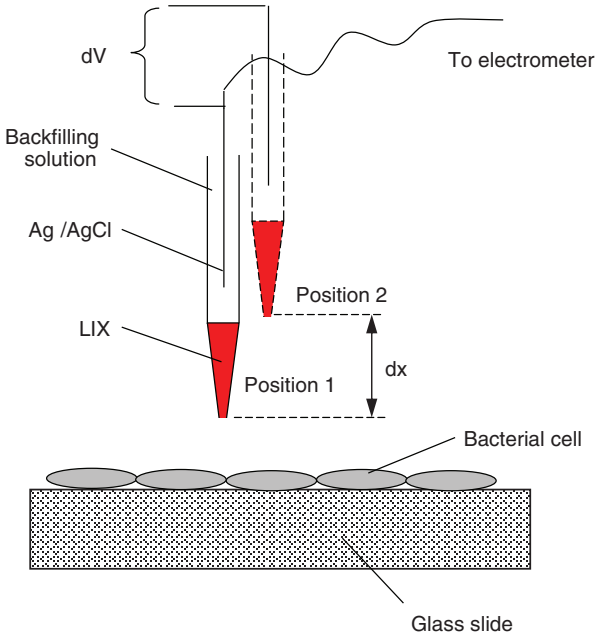

Figure 2.6: The picture as well as the following description are taken from Shabala *et al.* 2006: "Principles of the MIFE ion flux measurements. The microelectrode tip, filled with ionophore (LIX), is moved in a square-wave manner between two positions near a dense bacterial 'monolayer' or the biofilm surface. A voltage gradient (dV) is measured by the electrometer between two positions over the travel range dx. Net ion fluxes (nmol m^{-2} s^{-1}) are calculated using planar geometry diffusion equations (see (Newman, 2001) for details)."

was placed in the measuring solution next to the cover slip, whereas the measuring electrode was moved towards the cell surface (at a location of closed bacterial monolayer) as close as possible without touching the cell surface using a 3-dimensional manipulator. Optimal distance to the cell surface was estimated to be 30 µm. After positioning the measuring electrode, the motor was started with the first movement of the electrode away from the cell tissue. The electrode was moved away from the cell surface and back with a frequency of 0.05 Hz and the distance between the two positions was 50 µm. After measuring null-flux for 5 minutes, an osmotic shock was applied by adding measuring solution with sucrose. Fluxes were measured for 20 - 30 minutes after osmotic shock and data processing took place with the help of respective MIFE software programmes CHART and MIFEFLUX.

FLISE (flux measurements with ion selective electrodes)

FLISE is a convenient method to determine fluxes indirectly by measuring changes in ion concentrations in a cell suspension. During the last decade, the system has been established by Jost Ludwig from Rheinische Friedrich-Wilhelms University in Bonn (Ludwig, unpublished). Taking cell numbers, cell shape and size of the membrane surface into account, fluxes can be assessed on basis of concentration changes. Since an exact quantification of fluxes was not essential for this work, extracellular changes in ion concentration served as an indirect measure for altered uptake behaviour in presence and absence of incompatible solutes.
Concentration changes of ions of interest were measured with industrially manufactured ion selective electrodes (see chapter 2.1.3). Potassium concentrations were determined using a plastic electrode containing a PVC membrane, in which in turn the selective potassium ionophore valinomycin was embedded. To measure proton fluxes, a glass electrode with lithium and sodium ions in its solvated layer was used. Those ions are displaced by protons which induces building up of a voltage against a reference electrode. An Ag/AgCl electrode, containing $MgSO_4$ solution was used as reference electrode. The typical setup of the FLISE system is depicted in figure 2.7.

Calibration Electrodes were placed into the measuring cuvette and measuring solution with different proton or potassium concentrations was added. With the help of the software RealView 3.0, determined potentials were plotted against time. Calibration curves were generated and concentrations of later experiments were calculated with the help of the Nernst equation.

Preparation of cells for FLISE measurements *E. coli* MC4100 was grown in MM63 containing 1 % NaCl (w/v) until middle of exponential growth phase (OD_{600} of about 0.5) in 100 mL sidearm flasks. Cells were harvested (20 min, 11,300 g) in a Beckmann centrifuge (Avanti^{TM} J-20XP, JA-10 rotor) and washed in measuring solution (see chapter 2.1.3). Cell pellets were resuspended in 1 - 2 mL measuring solution and stored on ice until measurements started.

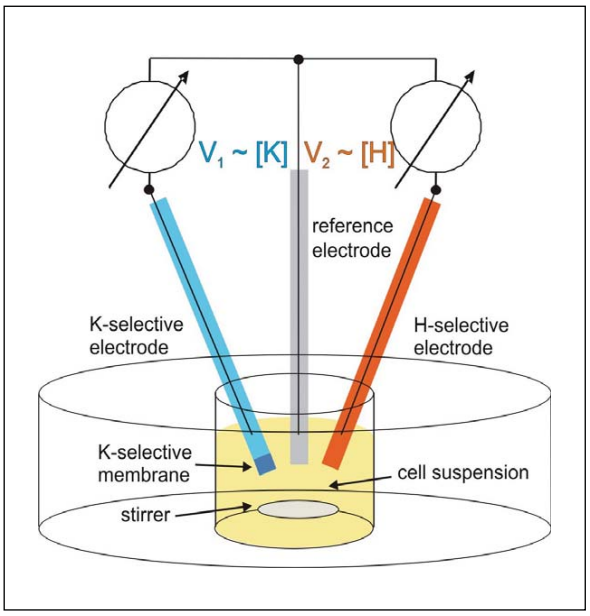

Figure 2.7: Assembly of the FLISE-system. The picture was provided by Jost Ludwig (Ludwig, unpublished). Measuring solution containing cells with an OD_{600} of 6 was stirred with the help of a magnetic stir bar. K^+ and H^+ selective electrodes, as well as the reference electrode, were positioned in approriate fixtures in the measuring cuvette and voltage was recorded.

FLISE measurements Measuring electrodes and the reference electrode were positioned into appropriate fixtures in the measuring cuvette and 1.5 mL measuring solution was added. Cells were injected to an OD_{600} of 12 before osmotic shock was applied by adding 1.5 mL of shock solution (measuring solution + 46 % sucrose (w/v)), which resulted in a final osmolaritiy of 1.03 osmol/L. Where required, solutes were added to a final concentration of 10 mM together with measuring solution in the beginning. Voltage was recorded and displayed by the software RealView.

2.2.10 Analysis of ribosome stability

For all preparation steps (except cultivation), material was autoclaved twice to reduce RNase contamination.

Cultivation and harvest of *E. coli* K-12

Precultures of *E. coli* K-12 in LBG were prepared as described in chapter 2.2.2. As maincultures *E. coli* K-12 was grown in 2 × 1 L side-arm flasks with 0.5 L LBG-medium

each. Harvest was performed as described in chapter 2.2.4 in the end of exponential growth phase (OD_{600} 0.8 - 1.0). Harvested cells were transferred to 50 mL Falcon tubes, cell wet weight was determined and cells were stored at -20 °C until purification of crude ribosomes was started.

Purification of crude 70S ribosomes

Purification was done according to Mackey 1991 (Mackey *et al.*, 1991) with slight modifications. All preparation steps were performed on ice or with cooled technical equipment and cooled buffers were used. Harvested cells were thawed and resuspended in 3 mL ribosome resuspension buffer/g wet cells (chapter 2.1.3). Cells were disrupted by sonification (BRANSON, Sonifier® cell disruptor B-15) for 1 min/mL cell suspension. With two ultracentrifugation steps (Beckman Coulter Optima™ LE-804, rotor 70Ti, 54,000 *g*, 20 min, 4 °C) cell debris was sedimented. 13 mL sucrose buffer (chapter 2.1.3) were transferred into clean centrifugation tubes and overlayed with 13 mL of the supernatant each. Ribosomes were sedimented during a further ultracentrifugation (rotor 70Ti, 110,000 *g*, 18 h, 4 °C). Supernatant and a brown pellet were removed carefully and the remaining clear ribosome pellet was resuspended in storage buffer (chapter 2.1.3). Resuspended ribosomes from different centrifugation tubes were combined, and unsolvable compounds were removed in another ultracentrifugation step (rotor 70Ti, 2,600 *g*, 10 min, 4 °C). A small volume of the supernatant was removed for determination of ribosome concentration in the buffer. The rest was frozen in liquid nitrogen and stored at -70 °C until use for calorimetric measurements.

Determination of ribosome concentration

Ribosomes consist of 2/3 RNA and 1/3 proteins. Since nucleic acids absorb at 260 nm, spectrophotometrical measurements can be performed to roughly determine the concentration of ribosomes after purification. Absorption at 260 nm (A_{260})(Specord 210, Analytik Jena, Jena, Germany) of storage buffer was used as reference. Ribosome solution was diluted 1:1000 with storage buffer and A_{260} was determined. Measurements for determination of concentration were repeated 4 times and mean average was calculated. 40 µg of pure RNA/mL show an A_{260} of 1. Ribosomes contain 2/3 RNA. Consequently an absorption of 1 at 260 nm equates to 60 µg ribosomes/mL. Since ribosomes exhibit an atomic mass of 2.5 MDa, which equals 2.5×10^6 g/mol, ribosome concentration can be calculated as follows:

$A_{260} = 1 \mathrel{\widehat{=}} 0.06\,\text{g/L} / (2.5 \times 10^6\,\text{g/mol}) = 2.4 \times 10^{-8}\,\text{mol/L}$

Comparing values from literature leads to the assumption that a concentration of 70S ribosomes of 24 pmol/mL is a suitable value for an absorption of 1 at 260 nm (e.g. Hill and co-workers announce 25 pmol (Hill *et al.*, 1970) whereas McNicholas and co-workers suggest 23 pmol/mL(McNicholas *et al.*, 2000)).

Differential scanning calorimetry (DSC)

DSC is a beneficial method to determine changes in quantity of heat such as specific heat capacity, latent heat due to phase transformation or heat of reaction and allows to characterise chemical and biological processes in respect of thermodynamic questions. As shown in figure 2.8, a differential scanning calorimeter consists of a reference cell and a sample cell. The reference cell usually contains the same buffer which is used to dissolve the compounds of interest which in turn are placed in the sample cell. The two cells are heated constantly according to a programmed heating rate as appropriate. If endo- or exothermic reactions take place in the sample cell, this will be detected as differences in thermic flow between the two measuring cells.
Before sample and buffer were injected (MicroCal, VP-DSC Microcalorimeter), the measuring cells were rinsed with RNase-free water repeatedly. Storage buffer was injected into the reference cell without air bubbles with the help of a special DCS-syringe. Ribosome solutions were diluted to 1 µmol/mL with storage buffer and subsequently injected into the sample cell the same way. (In)compatible solutes were added to required concentrations (see chapter 3.4).
For all measurements 1 µM ribosomes were applied and temperature was increased by 60 °C per hour from 25 - 85 °C. Two scans were performed successively; data of the second scan served as reference and was substracted from that of the first scan. Data was recorded and visualised by the DSC-software MicroCal Origin. Denaturation of ribosomal subunits and mRNA can be observed, at which maxima of peaks reflect 50 % denaturation of the respective ribosomal compound.

2.2.11 DNA thermal melting curve analysis

Thermal melting curve analysis of DNA facilitates the investigation of (in)compatible solute effects on DNA stability. Melting temperature (T_m) of DNA is defined as the temperature at which half of double stranded DNA is dissociated to single stranded DNA. This can easily be observed spectrophotometrically at 260 nm due to a higher UV absorbance of single stranded compared to double stranded DNA. Absorption of 20 µg

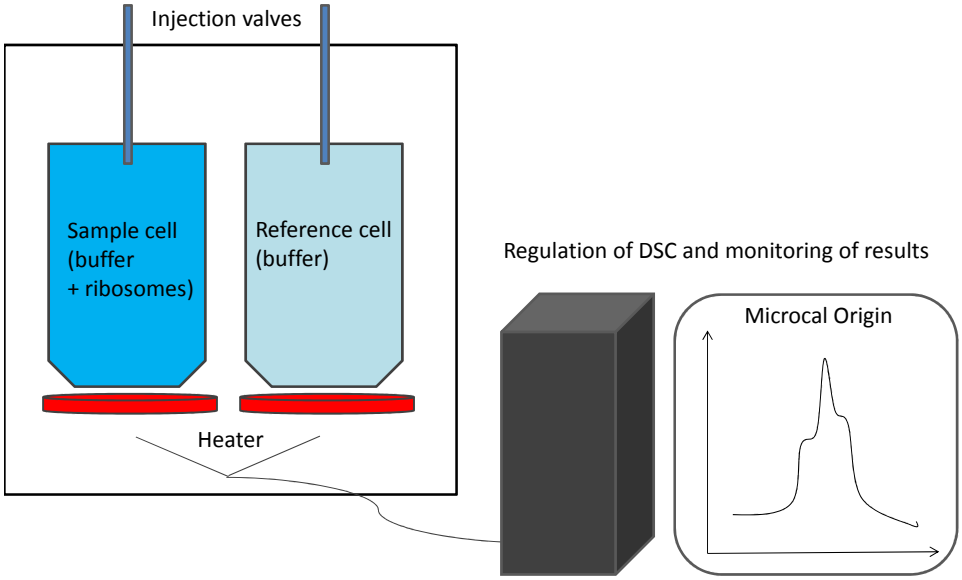

Figure 2.8: Setup of a differential scanning calorimeter. Differences of heat capacity between reference and sample cell are detected and visualised with the help of a special software.

calf thymus DNA or synthetic poly(dA - dT) in potassium-acetate buffer (chapter 2.1.3) (+/- (in)compatible solutes) was measured spectrophotometrically at 260 nm (Specord 210, Analytik Jena, Jena, Germany) over the time with a heating profile of 10 °C per hour from 40 °C - 90 °C and data acquisition took place at every 1 °C. DNA samples were degassed and covered with silicon oil to reduce evaporation during measurements.
Melting points were calculated according to Mergny *et al.* (Mergny & Lacroix, 2003) by calculating medians of the upper and lower baseline of the melting curve as shown exemplarily in figure 2.9.
Unfortunately, measurements with creatine were not meaningful because creatine is converted to creatinine in hot water solutions which leads to changes in absorbance during the measurement. Those changes cannot be correlated with either conversion of double stranded to single stranded DNA or conversion from creatine to creatinine.

2.2.12 Molecular work

During several cloning steps, deGFP1 (kindly provided by Hanson *et al.*, University of Oregon, also see diploma thesis Sell, K. 2009), a pH sensitive GFP (Hanson *et al.*, 2002), was inserted into the plasmid pUC19(Kan)-6His-pHluorin(pYEX) (constructed

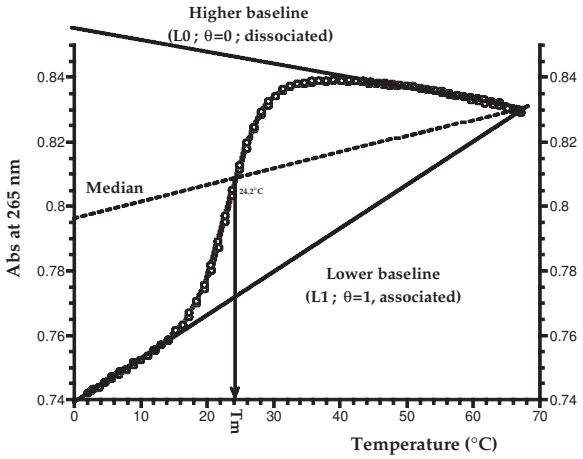

Figure 2.9: Calculation of thermal melting point according to Mergny *et al.* (Mergny & Lacroix, 2003). Representative melting curve with higher and lower baselines. By calculation of the median of the upper and lower baseline, the melting point of the tested DNA can be determined (source of figure: Mergny and Lacroix, 2003).

and kindly provided by Jost Ludwig and colleagues, Institut für zelluläre und molekulare Botanik, Rheinische Friedrich-Wilhelms Universität Bonn) by cutting the sequence of *degfp1* out of pRSET B-deGFP1 and cloning it into the pUC-vector in exchange with the gene for pHluorin. The single cloning steps are described in the following paragraphs.

Transformation

For means of duplication, pUC19(Kan)-6His-pHluorin(pYEX) was transformed into *E. coli* DH5α. Competence of *E. coli* DH5α was increased by chemical treatment with $CaCl_2$ according to Dagert & Ehrlich (Dagert & Ehrlich, 1979).

Production of competent *E. coli* DH5α cells The following steps (except cultivation of *E. coli*) were performed under sterile conditions on ice. Technical apparatuses and buffers were cooled to 4 °C.
70 mL 2 × YT-medium were inoculated with cells from a preculture of *E. coli* DH5α to an OD_{600} of about 0.05 and cultured at 37 °C at 180 rpm to an OD_{600} of approx. 0.3. After cell harvest (Beckman Coulter Avanti^{TM} J-20XP, JA-25-50 rotor, 4,000 *g*, 6 min, 4 °C), the cell pellet was resuspended in 10.5 mL $CaCl_2$ - $MgSO_4$-solution (see chapter 2.1.3) and incubated on ice for 30 minutes, followed by a further centrifugation step similar to the above described. The cell pellet was resuspended in 3.5 mL $CaCl_2$-$MgSO_4$-solution

before 875 µL sterile glycerine was added. The solution was mixed thoroughly and frozen and stored at -70 °C in 200 µL aliquots.

Transformation of the competent cells 200 µL competent *E. coli* DH5α cells were thawed on ice and mixed with 10 µL plasmid DNA (pUC19(Kan)-6His-pHluorin(pYEX)). After 30 minutes of incubation in iced water, the cells were transferred to a 42 °C water bath for 90 seconds. The heat shocked cells were then again placed into iced water for 2 minutes. For regeneration and development of kanamycin resistance, 600 µL preheated 2 × YT-medium (see chapter 2.1.3) was added and cells were incubated for 2 hours at 37 °C in a thermal mixer (Epppendorf, 500 rpm). 100 µL of transformation suspension as well as 10 µL of concentrated cell suspension were plated on selective agar plates (AB-2 + 50 µg/mL Kanamycin) and incubated at 37 °C over night.
Success of the transformation was visible by green colonies (due to GFP derivative pHlourin) and additionally proven by inoculating MM63-1 + Kan medium with colonies from selective agar plates and performing fluorescence measurements. The pH-sensitive GFP derivative pHluorin provides characteristic emission peaks at 508 nm after excitation at 390 nm and 485 nm, depending on pH value. A Calibration curve (see chapter 2.2.8) was constructed to prove pH-dependency.
Unfortunately, emission ratios of pHluorin only reflect pH values in acidic milieu reliably. Internal pH of *E. coli* has been shown to be slightly alkaline, so that pHlourin is not suitable for the purpose of this work. In 2009 first attempts to express the more suitable GFP derivative deGFP1 on the vectors pRSET B and pET-22b(+) in *E. coli* were made but without success (Sell, 2009). Since pHlourin is expressed on the vector pUC19 without difficulty, the gene for deGFP1 was cloned into this vector in exchange with the gene for pHlourin. Therefore, the plasmids pUC19(Kan)-6His-pHluorin(pYEX) and pRSET B-deGFP1 were isolated from corresponding *E. coli* DH5α strains.

Preparation of plasmid-DNA

Preparation of plasmid-DNA was performed with the method of alkaline lysis of cells according to the following protocol: *E. coli* DH5α cells with the plasmids pUC19(Kan)-6His-pHluorin(pYEX) and pRSET B-deGFP1 were grown in AB-1 + Kan (*E. coli* DH5α pUC19(Kan)-6His-pHluorin(pYEX)) or AB-1 + Carb (*E. coli* DH5α pRSET B-deGFP1) over night. 2 - 4 mL of those cultures were sedimented by short centrifugation. The supernatant was discarded and the pellet was resuspended in 200 µL buffer P1 (see chapter 2.1.3). Alkaline lysis was gained by adding 200 µL buffer P2 and gentle mixing.

During subsequent centrifugation (10,000g, 3 min) precipitated cell debris was separated from plasmid-DNA. The supernatant was transferred to 500 µL chloroform and centrifuged as above. To precipitate plasmid-DNA, the supernatant was mixed with 500 µL isopropanol. After a further centrifugation step (as above), supernatant was removed and the plasmid-DNA pellet was washed in 500 µL ice cold 70 % ethanol (v/v). Ethanol was removed carefully and plasmid-DNA pellets were dried at 60 °C for 20 - 30 minutes. The dried pellet was resuspended in 30 µL sterile ultra pure water.

Enzymatic modification of plasmid-DNA

Enzymatic hydrolysis of DNA For later ligation of deGFP1 with the pUC19-vector, hydrolysis of pUC19(Kan)-6His-pHluorin(pYEX) and of the amplified deGFP1 fragment (see chapter 2.2.12) is necessary. Therefore, aligned restriction enzymes hydrolyse DNA at specific palindromic recognition sequences of about 6 base pairs. Hydrolysis was carried out for 2.5 hours. Concentration of the different compounds as well as temperature, buffer and deactivation procedure were applied according to manufacturers' instructions. Compositions of reaction mixtures are listed in table 2.5.

Table 2.5: Composition of reaction mixture for enzymatic hydrolysis of pUC19(Kan)-6His-pHluorin(pYEX) and deGFP1 with different restriction enzymes

Compound	**pUC19**	**deGFP1**
DNA	15 µL	15 µL
Buffer 10 ×	8 µL	4 µL
Restriction enzymes (10 U/µL)	1 µL each	1 µL each
Ultra pure water	15 µL	19 µL
Deactivation	65 °C, 20 min	DNA purification (see chapter 2.2.12)

Dephosphorylation of plasmid-DNA Plasmid-DNA was dephosphorylated after hydrolysis by incubation with 1 U of FastAP^{TM}, an alkaline phosphatase which prevents religation of the linearised vector during ligation with deGFP1. After incubation at 37 °C for 10 minutes, enzymatic reactions were stopped at 65 °C for 20 minutes, followed by purification of linearised vector-DNA.

Purification of DNA after hydrolysis

Hydrolysed DNA was separated via agarose gel electrophoresis and respective bands were cut from the gel to extract DNA with the help of peqGOLD Gel Extraction Kit according to manufacturers' instructions. Corresponding gel slice was dissolved at 60 °C in binding buffer and washed several times with the different buffers offered by the Kit on a PerfectBind silica membrane and finally eluted with 30 µL elution buffer. To prevent excessive loss of DNA during agarose gel electrophoresis, hydrolysed DNA was, where applicable, purified directly with the peqGOLD Gel Extraction Kit. Therefore, hydrolysis mixtures were transferred to equal volumes of binding buffer and purification on silica membrane performed according to manufacturers' instructions.
Previous to ligation, the future insert *degfp1* needed to be amplified by polymerase chain reaction.

Polymerase chain reaction (PCR)

PCR is a method which allows selective amplification of DNA (Mullis & Faloona, 1987) with the help of two oligonucleotides (primer), which flank the DNA sequence of interest. Optimal conditions, coordinated with the needs of primers and enzymes used in the reaction, lead to high yield of amplified DNA fragments during cyclic reaction sequence of denaturation of DNA, annealing of primers and elongation of DNA. Components for PCR were mixed on ice (see table 2.6) and PCR was performed in a thermo cycler (BioRad, MyCycler) according to the temperature program shown in table 2.7. Sequences of the primers used to amplify *degfp1* are given in table 2.8

Table 2.6: Composition of reaction mixture for amplification of *degfp1*

Compound	**Amount**
10 × *Pfu*-buffer with $MgSO_4$	5.0 µL
dNTPs (2 mM)	5.0 µL
Betaine (5 M)	10.0 µL
Primer 5' (50 pmol/µL)	1.0 µL
Primer 3' (50 pmol/µL)	1.0 µL
Template DNA	1.0 µL
Pfu polymerase (2.5 U/µL)	0.5 µL
Ultra pure water	26.5 µL

Table 2.7: Temperature profile for amplification of *degfp1*

Step	**Temperature [°C]**	**Duration [min]**	**Repetition**
Initial denaturation	95	1	
Denaturation	95	0.5	
Annealing	45.9	0.5	2 ×
Extension	72	2	
Denaturation	95	0.5	
Annealing	51	0.5	30 ×
Extension	72	2	
Final extension	72	10	
Cooling	10	∞	

The two different annealing temperatures used in this PCR (first 2 cycles at 45.9 °C, following cycles at 51 °C) ensured a binding of the primers despite the fact that melting temperatures of the binding parts of the primers were significantly lower than those of complete primers (including overhanging bases).

Table 2.8: Sequences, melting temperatures (T_m) and restriction sites of primers used to amplify deGFP *degfp1*. Recognition sites for restriction enzymes are written in bold.

Denotation	nucleotide sequence (5'→3')	T_m [°C]	Restriction site
forw.-PET-deGFP1	aat**tcatga**gtaaaggagaagaac	55.9	*Pag*I
rev.-pRSET-deGFP	aagcttc**gaattc**catggta	53.2	*Eco*RI

To prove the success of the PCR and to purify deGFP1 fragments, agarose gel electrophoresis was performed, followed by DNA-purification and hydrolysis with the restriction enzymes *Pag*I and *Eco*RI (see chapter 2.2.12).

Ligation

Ligation of hydrolysed plasmid-DNA (pUC19(Kan)-6His) and insert-DNA (deGFP1) was achieved using T4-DNA-Ligase, which forms phosphodiester bonds between the 3' hydroxyl- and 5' phosphate termini. Success of ligation is dependent on the ratio of vector-DNA and insert-DNA. Concentration of DNA was determined by agarose gel electrophoresis.

Determination of DNA concentration DNA concentrations can be estimated by comparing fluorescence intensities of DNA-bands in the agarose gel and corresponding bands of a DNA size standard with known concentration.
For calculation of molarity, a molar mass of 660 g/mol was estimated for each base pair. The following formula provides a means of evaluating concentrations of plasmid- and insert-DNA:
x mol/µL DNA = (molarity of DNA [mol/µL] $\times 10^{-9}$)/(660 g/mol $\times$ number of base pairs of DNA fragment)

Ligation Plasmid- and insert-DNA were applied in molar ratio of 1:2 - 1:4 according to beforehand calculated concentrations. Reaction mixture is shown in table 2.9.

Table 2.9: Composition of reaction mixture for ligation of pUC19(Kan)-6His and deGFP1

Compound	Amount
Vector-DNA	60 ng
Insert-DNA	2:1 - 4:1 to vector-DNA
Ligase-buffer (10 ×)	2 µL
T4-ligase (5 U/µL)	0.5 µL
Ultra pure water	3.6 µL

The ligation reaction mixture was incubated for 1 hour at room temperature before reaction was stopped at 80 °C for 5 minutes.
The ligated vector was transformed into *E. coli* DH5α immediately as described in chapter 2.2.12. Success of transformation was tested by plasmid preparation, followed by test-restriction. Unfortunately, sequence of pUC19(Kan)-6His, constructed by a former master student of Jost Ludwig (Institut für molekulare und zelluläre Botanik, Universität Bonn), was not fully available. Furthermore, complete sequence of deGFP1 had not been published at the time of the cloning. To exclude all possibility of doubt, arising with indefinite fragment sizes after test restriction, fluorescence measurements were performed, which revealed strong expression of functional deGFP1 in *E. coli* DH5α.

Agarose gel electrophoresis

Agarose gel electrophoresis is a method to separate DNA or RNA molecules by size. This is achieved by moving negatively charged nucleic acid molecules through an agarose matrix with an electric field (electrophoresis). Shorter molecules move faster than longer ones. Agarose gel electrophoresis was used for several steps during cloning of *E. coli* DH5α-pUC19(Kan)-6His-deGFP1. Furthermore, gel-shift experiments, which were meant to prove interaction of incompatible solutes with ribosomes, were performed with the help of agarose gel electrophoresis.
Agarose gels were prepared by dissolving appropriate concentrations of agarose (1 % (w/v) for DNA fragments and 0.8 % (w/v) for ribosomal complexes) in 30 ml TAE-buffer (chapter 2.1.3) which was poured into a gel chamber. After polymerisation, the gel was submerged with TAE-buffer and the beforehand prepared samples (mixed with appropriate amounts of 6 × loading dye) were loaded on the gel. Electrophoresis was performed at 60 - 70 V for 1 - 2 hours for DNA fragments and at 50 V for 4 hours for

ribosomes. Gels were stained in gel red® solution for 20 minutes and washed for a few seconds in H_2O_{demin}. Using a UV transilluminator the DNA was visualised.

3 Results

As already shown in previous studies (Mann, 2008; Sell, 2009), the incompatible solute creatine leads to growth inhibition of γ-Proteobacteria. In the following chapters probable interaction-partners of the incompatible solutes creatine and guanidino-ectoine and their influences on ion homoeostasis will be examined. Attention will also be turned on the effect of creatinine (which is in equilibrium with creatine under certain conditions) on growth of different bacteria.

3.1 Characteristics of the guanidino-function and consequences for bacterial growth

3.1.1 Comparison of growth inhibition by creatine and guanidino-ectoine

In figure 3.1 relative growth rates of *E. coli* grown in MM63 containing 3 % NaCl and increasing concentrations of creatine or guanidino-ectoine are shown. While growth inhibition is enhanced with rising creatine concentrations, inhibition is not dependent on concentration with guanidino-ectoine (note that different concentrations were used for creatine and guanidino-ectoine).

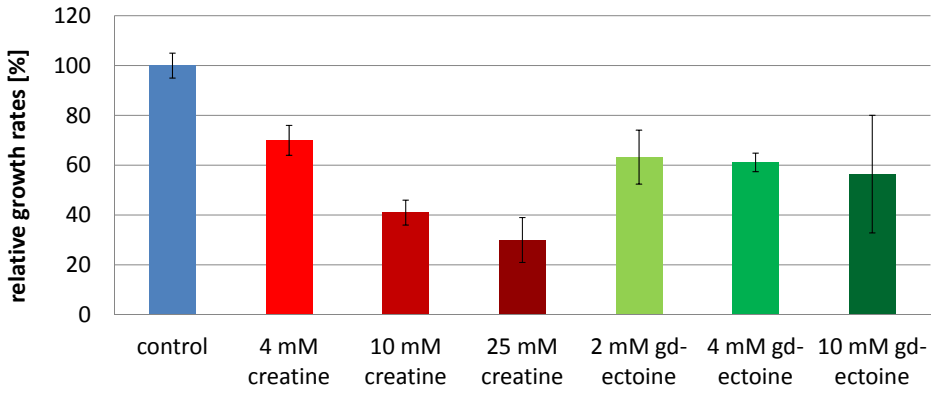

Figure 3.1: Effect of rising creatine and guanidino-ectoine concentrations on growth rate of *E. coli* MC4100 in MM63-3 at 37 °C. Control: no supplementation, set to 100 %. Each bar reflects the arithmetic mean of 3 cultures with error bars providing the standard deviation.

These results already indicate that although the guanidino function was shown to render compatible solutes incompatible, the two compounds investigated here appear to have different modes of action.

3.1.2 Ionic vs. non-ionic osmotic stress

To indicate if salinity or water activity is responsible for uptake of creatine and guanidino-ectoine and their inhibitory effect on growth, *E. coli* was grown in minimal medium containing 1 % NaCl and 23 % sucrose (*w/v*), which equates to a total osmolarity of 1.03 osmol/L (osmotically equivalent to 3 % NaCl). In figure 3.2 appropriate growth rates are shown. Corresponding growth curves are provided in the appendix (see figure 6.1).

When osmolarity was increased with sucrose, growth rates and OD_{600} were lower in all cultures compared to those of cells grown with 3 % NaCl. Both, creatine and guanidino-ectoine led to growth inhibition. While growth rates of creatine supplemented cultures were 20 % lower than those of control cultures, guanidino-ectoine led to a 30 % reduction of growth rates. Compared to MM63 medium containing 3 % NaCl (figure 3.1), creatine and guanidino-ectoine effects are lower in sucrose medium. To prove if those findings are consistent with intracellular concentrations of creatine and guanidino-ectoine, HPLC-analyses were performed. Results are compared to those of cells grown in MM63 containing 3 % NaCl in figure 3.3.

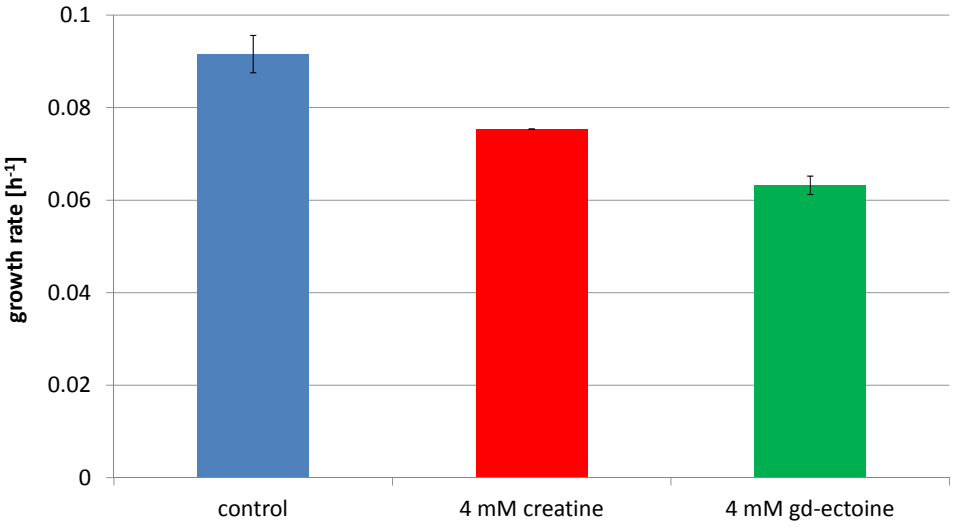

Figure 3.2: Growth rates of *E. coli* MC4100 during growth at 37 °C in MM63 containing 1 % NaCl and 23 % sucrose (*w*/*v*) (total osmolarity of 1.03 osmol/L). Cultures were supplemented with 4 mM creatine or guanidino-ectoine. Control cultures were not supplemented with any solute. Each measuring point reflects the arithmetic mean of 2 cultures with error bars providing the highest and lowest value.

Concentrations are given in mmol/g dry weight but one has to consider that dry weight does not only arise from cells but also from media compounds which is problematic for cultures grown with 23 % sucrose (*w*/*v*) with a molecular mass of 342.3 g/mol. Solute concentrations estimated for cells grown with sucrose are therefore even higher than given in figure 3.3.
Considering underestimated values for sucrose cultures, trehalose concentrations might be the same regardless of ionic or non-ionic osmotic stress. Despite of that, concentrations of the incompatible solutes are increased in sucrose medium. While it is 0.4 mmol/g dw creatine in NaCl medium, it is 0.7 mmol/g dw in sucrose medium. Increase of guanidino-ectoine concentration from 0.2 mmol/g dw to 0.25 mmol/g dw is, in contrast, less severe. In NaCl medium as well as in sucrose medium trehalose levels are decreased when incompatible solutes are present.
Results shown in this chapter already reveal some interesting findings. Despite the chemical similarity of the guanidino-function, which is responsible for growth inhibition, creatine and guanidino-ectoine behave differently by means of correlation between growth inhibition and concentration. Furthermore, it was proven that lowered water activity caused by osmotic stress, not salinity *per se*, induces incompatible solute uptake and its inhibitory effect.

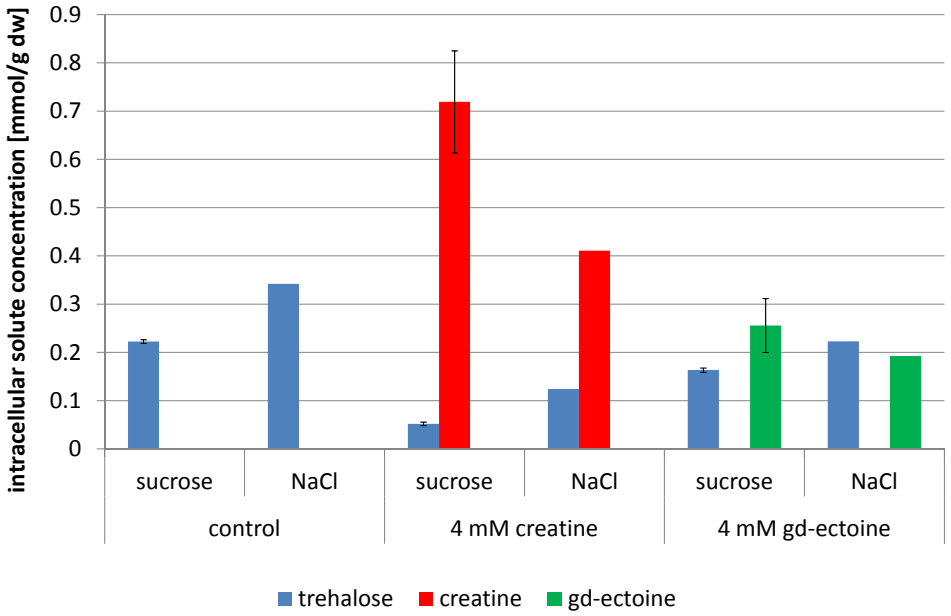

Figure 3.3: Comparison of intracellular solute concentration of stationary *E. coli* MC4100 after growth at 37 °C in MM63 containing 1 % NaCl and 23 % sucrose (w/v) or 3 % NaCl (total osmolarity of 1.03 osmol/L), respectively. Cultures were supplemented with 4 mM creatine or guanidino-ectoine. Control cultures were not supplemented with any solute. Solute concentrations of cells grown with sucrose were determined 2 times and the arithmetic mean is displayed, those of cells grown with NaCl only once. Error bars reflect the highest and the lowest values.

Before this will be considered more closely, intracellular solute composition of cells treated with (in)compatible solutes and their metabolome in principle will be object of investigation.

3.2 Metabolomics: Changes in the metabolome of *E. coli* due to presence of (in)compatible solutes

For metabolome studies the composition of cytoplasmic compounds of *E. coli* grown to end of exponential / beginning of stationary phase was determined by HPLC and GC/TOF-MS. Growth took place in presence of the incompatible solutes creatine or guanidino-ectoine or with their corresponding compatible solutes betaine and ectoine in concentrations of 2 mM each. The typical increase of trehalose synthesis with elevated salinity (1 % NaCl compared to 3 % (w/v)) as well as the absence of this compatible

solute when betaine or ectoine are present can be seen in figure 3.4. Interestingly, not only compatible solutes but also incompatible solutes decrease the trehalose level in *E. coli*. This effect is stronger with creatine than with guanidino-ectoine, but one has to note that the latter is accumulated to lower concentrations. Intracellular concentrations of compatible solutes are approx. 3 times higher than incompatible solute concentrations or the concentration of trehalose.

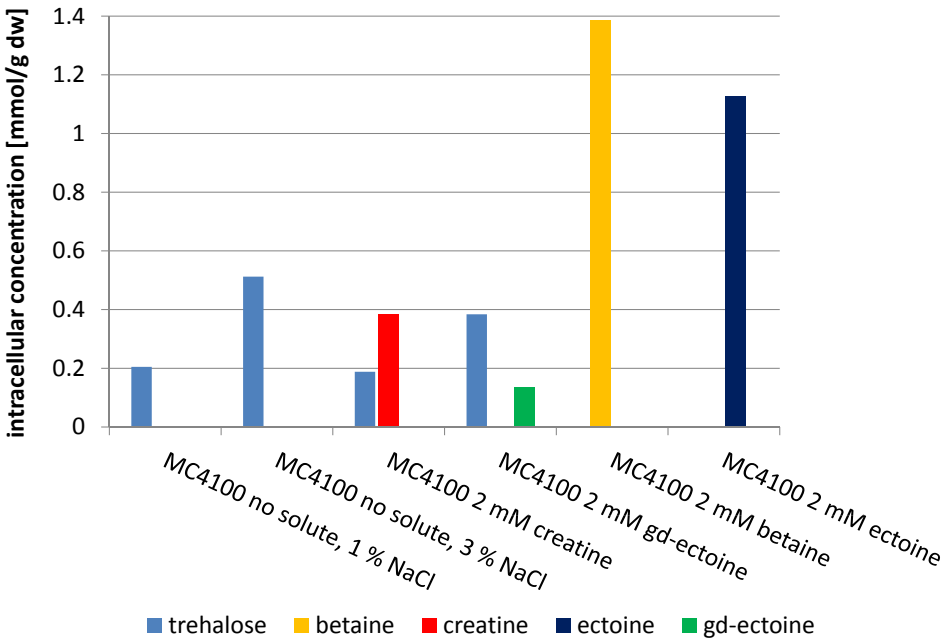

Figure 3.4: Intracellular solute concentration of *E. coli* MC4100 grown at 37 °C in MM63-1 without solutes and in MM63-3 with 2 mM creatine, guanidino-ectoine, betaine or ectoine and without supplementation. Cells were harvested at the end of exponential growth phase and solutes were analysed by aminopropyl phase HPLC.

Consistent with this is the observation that compatible solutes as well as incompatible solutes decrease intracellular glutamate and glutamine levels, which are similar in salt stressed supplemented cultures (3 % NaCl) and not salt stressed (1 % NaCl) but unsupplemented culture (figure 3.6).
In order to determine if other compounds than the afore cited ones are relevant to understand the effect of (in)compatible solutes on *E. coli*, metabolome analysis was performed using GC/TOF-MS. With the expertise of Jochem Gätgens of the Forschungszentrum Jülich, a high bandwidth of potentially affected compounds was detected (not shown), of which amino and diamino compounds, first of all 4-aminobutyrate, seemed to be particularly interesting. A typical mass spectrum is shown in figure 3.5. Peaks were attributed

to corresponding substances with the help of different databases (see chapter 2.2.6).

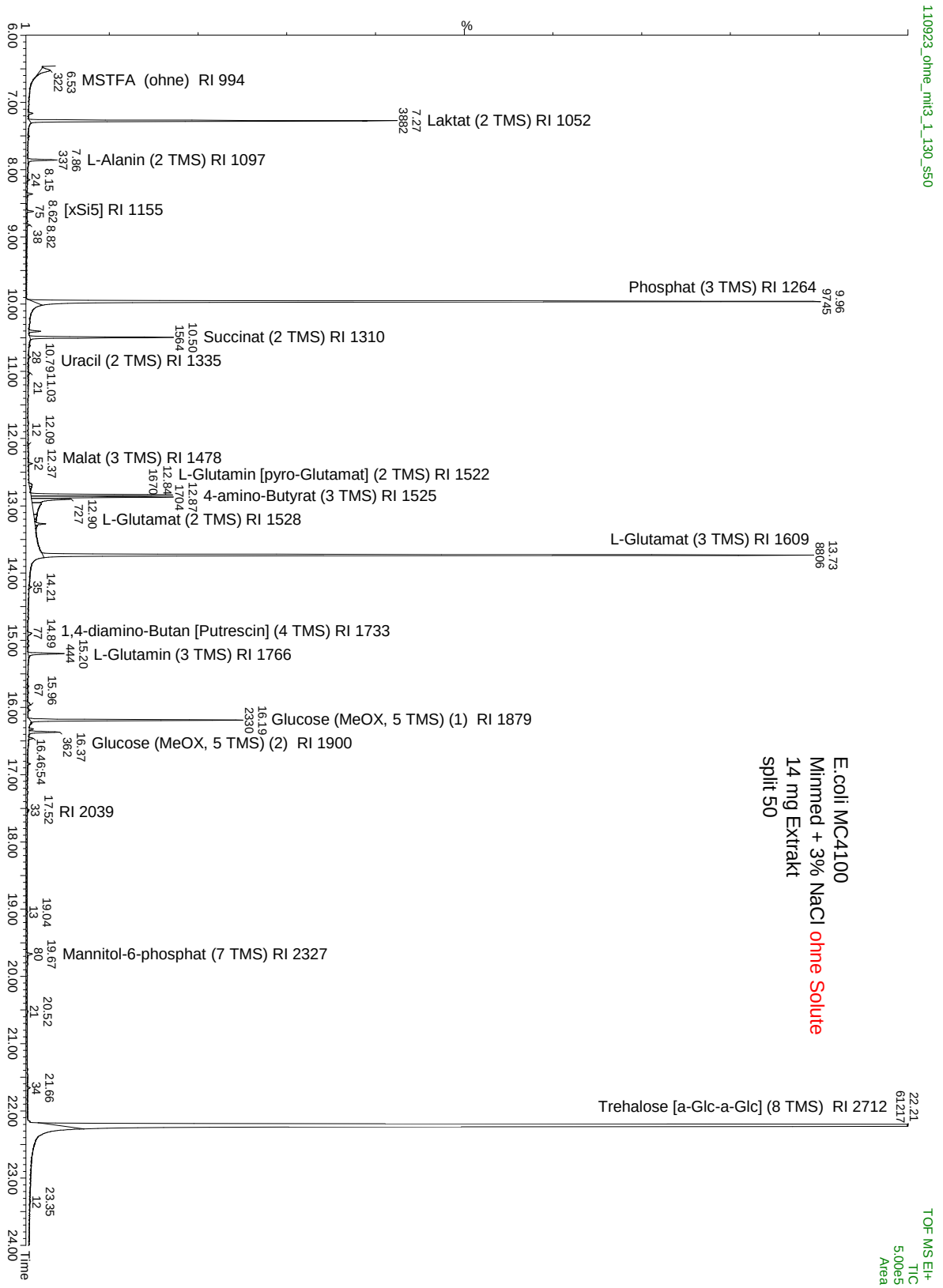

Figure 3.5: Representative mass spectrum of a Bligh & Dyer extract of *E. coli* MC4100 grown in MM63 containing 3 % NaCl.

Quantification of those identified substances was performed via FMOC-HPLC (see figure 3.6 and figure 3.7). Interestingly, 4-aminobutyrate was only found in unsupplemented cultures and the concentration rose with increasing salinity. Concentrations were in the range of glutamate concentrations. Further amino compounds were analysed but concentrations were relatively low compared to those of glutamate and 4-aminobutyrate. While concentrations of alanine and histidine increase with increasing salt concentration, 2,6-diamino pimelic acid concentration decreases. No strong salt dependent increase was observed for the other amino compounds tested.

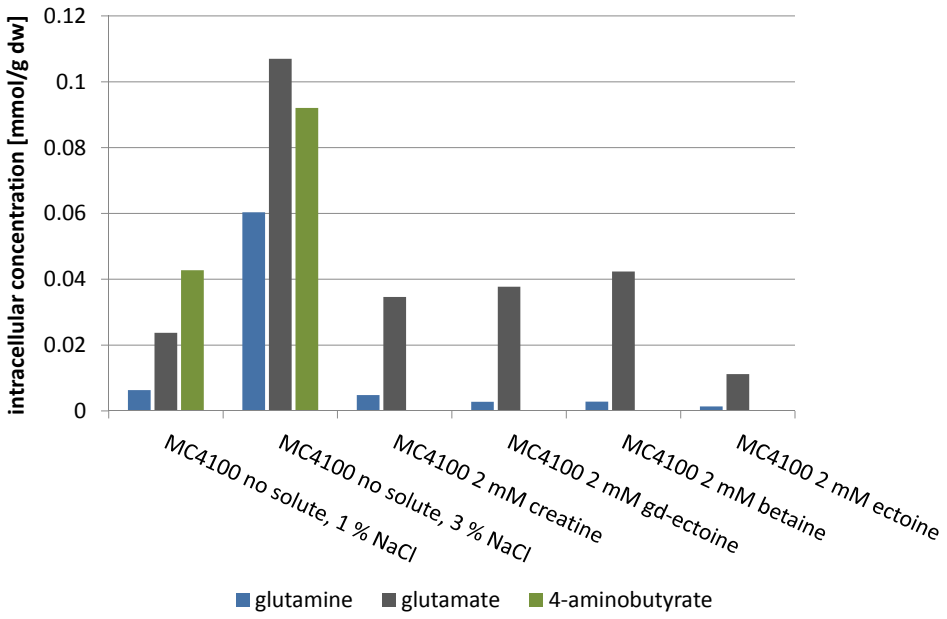

Figure 3.6: Intracellular concentration of glutamine, glutamate and 4-aminobutyrate in *E. coli* MC4100 grown in MM63-1 without solutes and in MM63-3 with 2 mM creatine, guanidino-ectoine, betaine or ectoine and without supplementation. Cells were harvested at the end of exponential growth phase and solutes were analysed by FMOC-HPLC.

Again, compatible solutes and incompatible solutes decreased intracellular concentrations of the amino compounds. Conspicuous differences were observed for 2,6-diamino pimelic acid and putrescine concentrations. While the amount of 2,6-diamino pimelic acid is not reduced with creatine, it is totally absent with guanidino-ectoine. Putrescine concentration is noticeably high in betaine supplemented cells.
Data shown in this paragraph relies on single determinations, but the principle trend of trehalose and glutamate reduction in presence of (in)compatible solutes was observed several times during other experiments of this work and can therefore be accepted as

authentic.

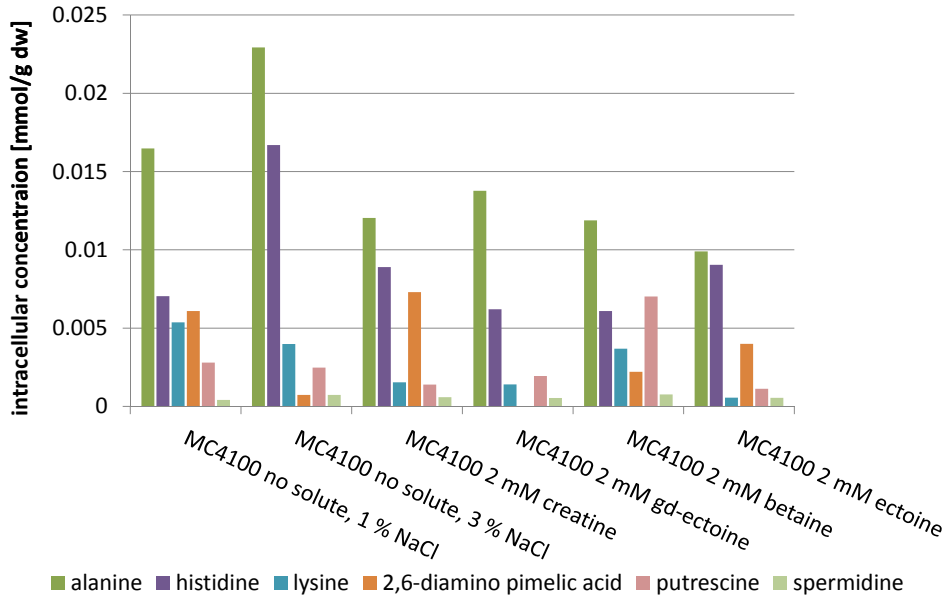

Figure 3.7: Intracellular concentration of (di)amino compounds in *E. coli* MC4100 grown in MM63-1 without solutes and in MM63-3 with 2 mM creatine, guanidino-ectoine, betaine or ectoine and without supplementation. Cells were harvested at the end of exponential growth phase and solutes were analysed by FMOC-HPLC.

3.2.1 Competition of creatine and betaine

The following experiments deal with the competitive effect of creatine and betaine. Previous experiments revealed that at simultaneous presence of the compatible solute betaine and the structurally related incompatible solute creatine, 40 times lower concentrations of betaine are enough to compensate the inhibitory effect of creatine (Mann, 2008). Without any evidence, the natural compatible solute betaine was postulated to have a higher affinity to the involved transport systems ProP and ProU than creatine. But does the competition really occur at the transport systems or are processes inside the cell responsible for the phenomenon described above? To obtain first answers, the intracellular solute pool of bacteria grown in media supplemented with both the compatible and the incompatible form was investigated. Growth rates of *E. coli* MC4100 grown in MM63 medium containing 3 % NaCl with betaine and/or creatine or no supplementation can be compared in figure 3.8. Growth curves are provided in the appendix (see figure 6.2). Betaine concentration (0.1 mM) was 20 times lower than creatine concentration (2 mM).

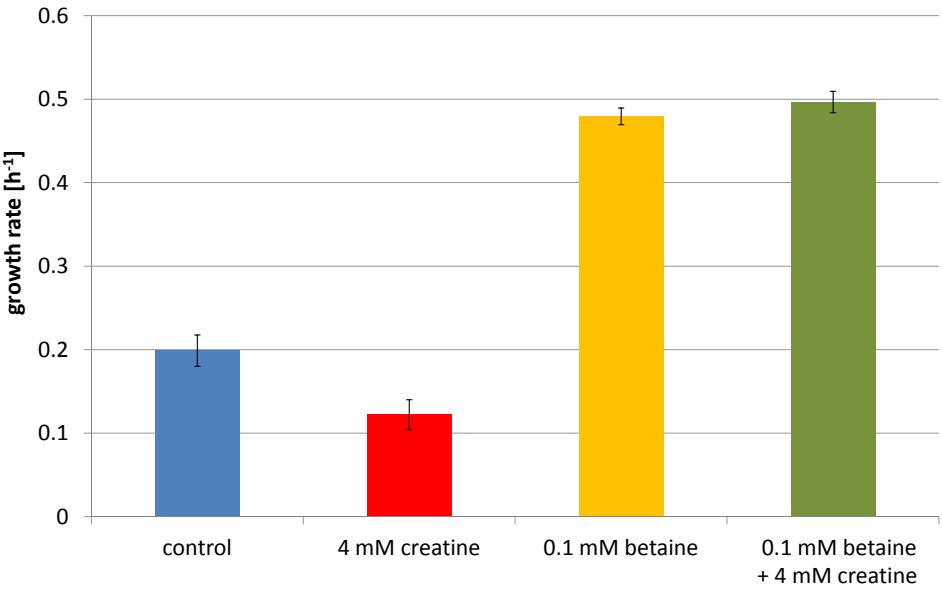

Figure 3.8: Growth rates of *E. coli* MC4100 in MM63 containing 3 % NaCl. Control: no solutes added, betaine: growth medium supplemented with 0.1 mM betaine, betaine + creatine: growth medium supplemented with 0.1 mM betaine and 2 mM creatine, creatine: growth medium supplemented with 2 mM creatine. Values derive from single determinations.

As expected, creatine does not inhibit growth of *E. coli* in the presence of 20 times lower betaine concentration. Growth rate was approx. 2 times higher compared to control cultures and nearly 5 times higher than that of cultures supplemented with creatine only. If the "location" of competition of the two substances were the transport systems, one would expect them to take up betaine preferred to creatine. Thus, if supplemented simultaneously, creatine was accumulated only to low concentrations whereas betaine levels would be similar to cells which were supplemented with betaine only.
But interestingly, HPLC measurements of stationary phase cells revealed that creatine concentration in cultures supplemented only with creatine was as high as the concentration in cultures supplemented with creatine and betaine simultaneously (figure 3.9).
In addition to that, betaine concentration was much higher when creatine was not present. When supplemented together, creatine concentrations were twice as high as betaine concentrations. Surprisingly, the same growth rates as with only betaine were attained in this situation. From these results it becomes clear that selectivity of the transport systems is not responsible for competition of betaine and creatine.
It can be concluded that incompatible solutes behave like compatible solutes with respect

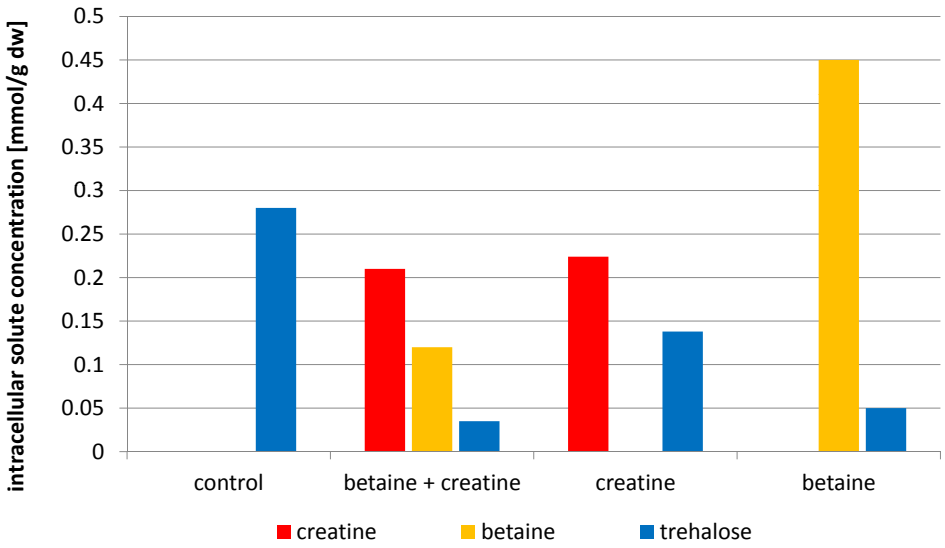

Figure 3.9: Solute concentration in *E. coli* MC4100 after growth in MM63 containing 3 % NaCl. Control: cells without supplementation, betaine + creatine: growth medium supplemented with 0.1 mM betaine and 2 mM creatine, creatine: growth medium supplemented with 2 mM creatine, betaine: growth medium supplemented with 0.1 mM betaine.

to various aspects. They are actively taken up and reduce the intracellular concentration of trehalose, glutamate and other amino compounds. Additionally, betaine compensates the growth inhibitory effect of creatine, although both solutes are accumulated simultaneously. Clarification of reasons can only be made if the mode of action of incompatible solutes is discovered. Therefore, the following chapters will address main cell machineries, such as ion-homoeostasis, ribosome stability and interaction with DNA, as probable targets for incompatible solutes in *E. coli*.

3.3 Examination of the impact of incompatible solutes on ion-homoeostasis of *E. coli*

A well regulated ion-homoeostasis is fundamental for unrestricted life of bacterial cells. Depending on the particular ion, its disruption will for example lead to problems in generation of energy, to disadvantageous intracellular pH or to hindered transport processes. Growth inhibition as a result of each of those factors is conceivable. Therefore, investigation of probable changes in ion-homoeostasis due to presence of creatine and guanidino-ectoine was performed in several experiments. Corresponding results are described in the following paragraphs.

3.3.1 Influence of creatine and guanidino-ectoine on Nha activity

The effect of the incompatible solutes creatine and guanidino-ectoine on activity of Nha-type Na^+ H^+ antiporters from *E. coli* was investigated. Inside-out membrane vesicles of *E. coli* K-12 were used to measure the antiport activity with the help of acridine orange, a fluorescent probe for pH difference across the membrane. With the acridine orange method Na^+ H^+ antiport activity was determined indirectly. In living cells Na^+ H^+ antiporters simultaneously extrude Na^+ from the cytoplasm and import H^+. In inside-out vesicles those ions are transported in the opposite direction which results in an acidification of the measuring buffer when the antiporters are active. The decline in emission intensity after NaCl addition gives information about the Na^+ H^+ antiport activity. A steep slope reflects a fast acidification of the vesicle buffer. The flatter the slope, the slower the pH change, the slower the H^+ transport and the lower the Na^+ H^+ antiport activity. Emission intensities were measured at 570 nm with an excitation wavelength of 430 nm in a fluorescence spectrometer (Perkin Elmer, LS 50 B). Typical patterns of such measurements are shown in chapter 2.2.7, figure 2.3.
Results of measurements are shown in figure 3.10. Increasing creatine concentrations led to decreased Nha activities. Very low concentrations already revealed a strong effect: Only 10 µM creatine are enough to reduce Nha-activity by 50 %. Guanidino-ectoine on the contrary does not seem to affect antiport activity.
These experiments demonstrate that creatine clearly inhibits Nha activity at µM concentrations while neither its corresponding compatible solute betaine nor ectoine-type solutes affected antiport activity (results not shown).
Although the guanidino group is believed to be the critical function for the inhibitory

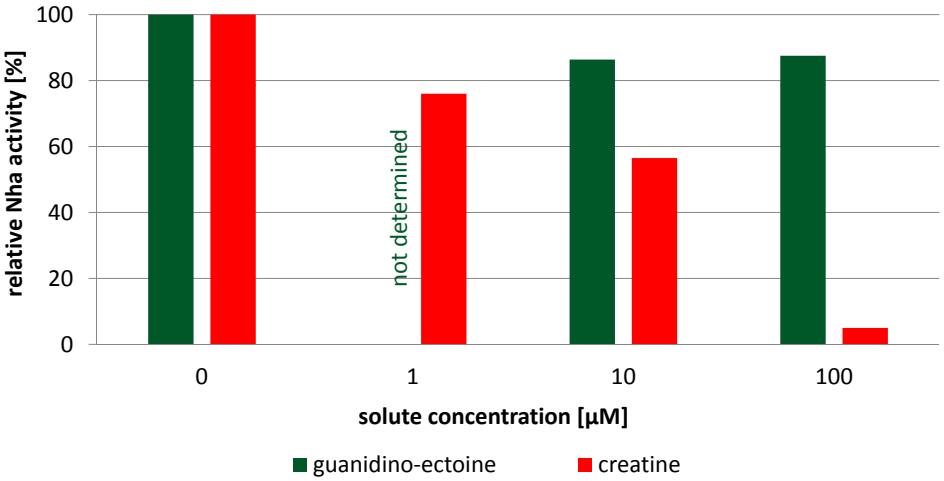

Figure 3.10: Comparison of Na^+ H^+ antiport activities in inverted membrane vesicles of *E. coli* in the absence and presence of increasing guanidino-ectoine and creatine concentrations. Slopes of emission intensities after addition of NaCl served as a measure of Na^+ H^+ antiport activity. Activity in absence of solutes was set to 100 %.

effect on sodium-proton antiporters, it must again be concluded that guanidino-ectoine has a different mode of action.

Constriction of Nha activity must inevitably affect growth, especially when Na^+ is available excessively. Growth patterns of *E. coli* grown in a modified MM63 medium (NaMM63), which contains Na^+ abundantly but only traces of K^+ due to impurity of chemicals, water and glassware, are shown in figure 3.11.

Growth was very slow in all cultures (0.05 - 0.1 h^{-1}) and optical density did not exceed 0.3. Cultures supplemented with creatine grew half as fast as control cultures but reached the same but low optical density at the end of the experiment. Guanidino-ectoine on the other hand, led to nearly complete halt of growth which resulted in a final OD_{600} of only 0.2. Comparing these results to growth inhibition in MM63 medium (see figure 3.1) reveals that growth inhibition by creatine is 15 - 20 % stronger in the presence of extremely high amounts of Na^+.

Results of Nha activity measurements are also consistent with growth experiments of an *E. coli* mutant strain which is deficient in both classes of Nhas in *E. coli*: NhaA and NhaB. While creatine does not lead to growth inhibition in the absence of those antiporters, growth of cultures supplemented with guanidino-ectoine is highly reduced (figure 3.12).

HPLC-analysis demonstrated the absence of trehalose in supplemented as well as in

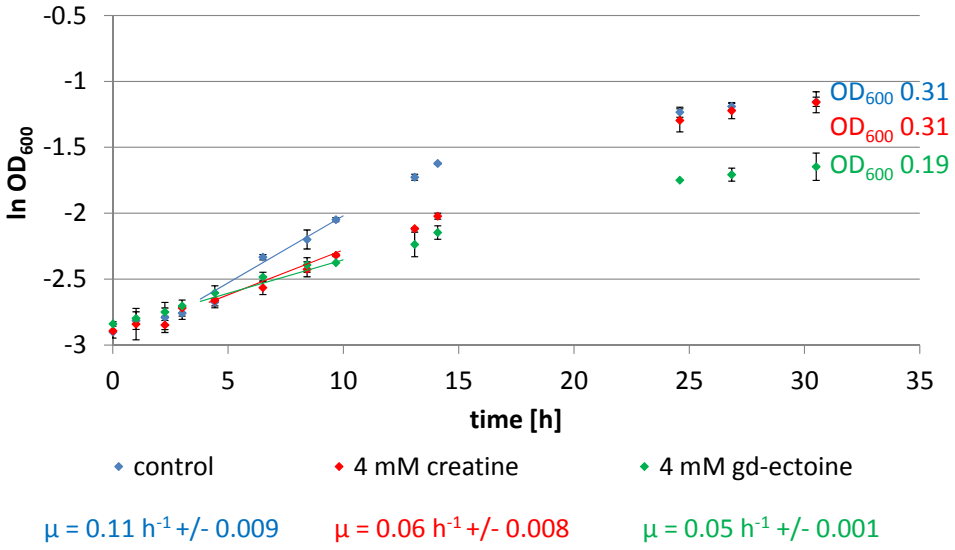

Figure 3.11: Growth of *E. coli* MC4100 in NaMM63 containing 3 % NaCl (*w*/*v*). Cultures were supplemented with 4 mM creatine or guanidino-ectoine. Unsupplemented cultures served as control. Growth rates (μ) are given in corresponding colours and the range of values from which μ was calculated is indicated by lines in the graphs.

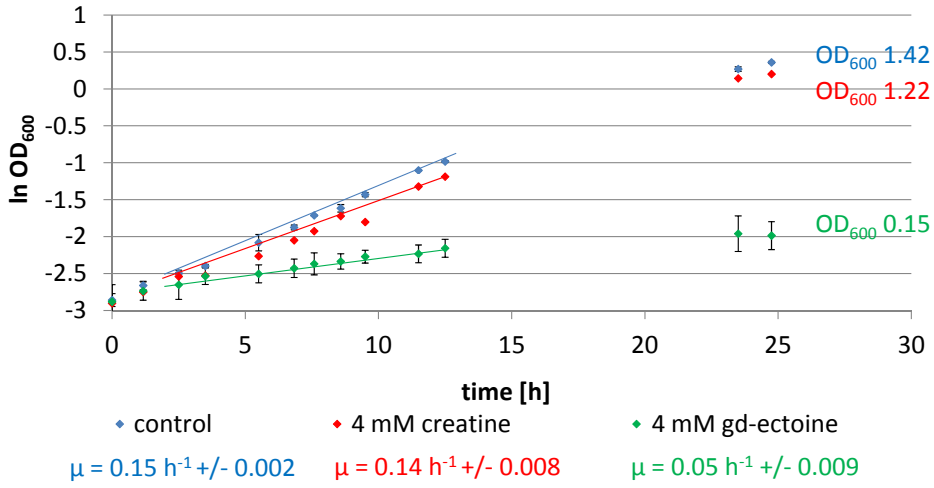

Figure 3.12: Growth of *E. coli* EP432 (Δ*nha*A Δ*nha*B) in MM63-2 in the absence and presence of 4 mM guanidino-ectoine or creatine. Unsupplemented cultures served as control. Growth rates (μ) are given in corresponding colours and the range of values from which μ was calculated is indicated by lines in the graphs.

unsupplemented cultures of *E. coli* EP432. This is not mentioned in literature but might be responsible for the very strong growth inhibition by guanidino-ectoine (much stronger than on *E. coli* wild type). A possibility for this strain to adapt to increased osmolarity (2 % NaCl) is the increased accumulation of K^+ and glutamate compared to *E. coli* wild type. If that could be disrupted by guanidino-ectoine, cells would suffer from turgor loss which would lead to cessation of growth. To investigate whether this suspicion is founded, potassium homoeostasis will be the object of investigation in the next paragraphs.

3.3.2 Influence of creatine and guanidino-ectoine on K^+-homoeostasis in *E. coli*

K^+-fluxes in response to hyperosmotic shock

Evidence for change of K^+ balance by the incompatible solutes creatine and guanidino-ectoine are provided by *in vivo* K^+ flux measurements with ion selective electrode (FLISE) technique (Ludwig, unpublished) and microelectrode ion flux estimation (MIFE) technique (Shabala *et al.*, 1997).
Preparation of measurements and cells were performed as described in chapter 2.2.9.
In figure 3.13 fluxes over membranes of *E. coli* MC4100 determined using the MIFE technique are shown.
Osmotic up-shock led to uptake of potassium (positive change of net K^+ flux), immediately to a maximum of 100 nmol m^{-2} s^{-1}. Shortly after the maximum was reached, net flux slowly decreased. When cells were treated with betaine from beginning of measurements, a completely different reaction was observed. With more than 1000 nm m^{-2} s^{-1}, cells extruded large amounts of potassium (negative change of net K^+ flux). Cells treated with creatine, showed a strong immediate uptake, which was 2.5 fold higher than without creatine, but subsequent decrease was also stronger than in control cells. These results indicate, that creatine influences potassium flux but in a different way than the compatible solute betaine.
To get a better idea of what the procedure for creatine interaction with K^+ transport systems is, measurements were repeated with cells of *E. coli* MKH13, which is deficient in genes encoding for the creatine and betaine uptake systems ProU and ProP. As shown in figure 3.14, K^+ uptake after sucrose shock in control cells is comparable to that observed for *E. coli* MC4100 cells: A maximum of 80 nmol m^{-2} s^{-1} was reached shortly after addition of sucrose, followed by a slow decline.

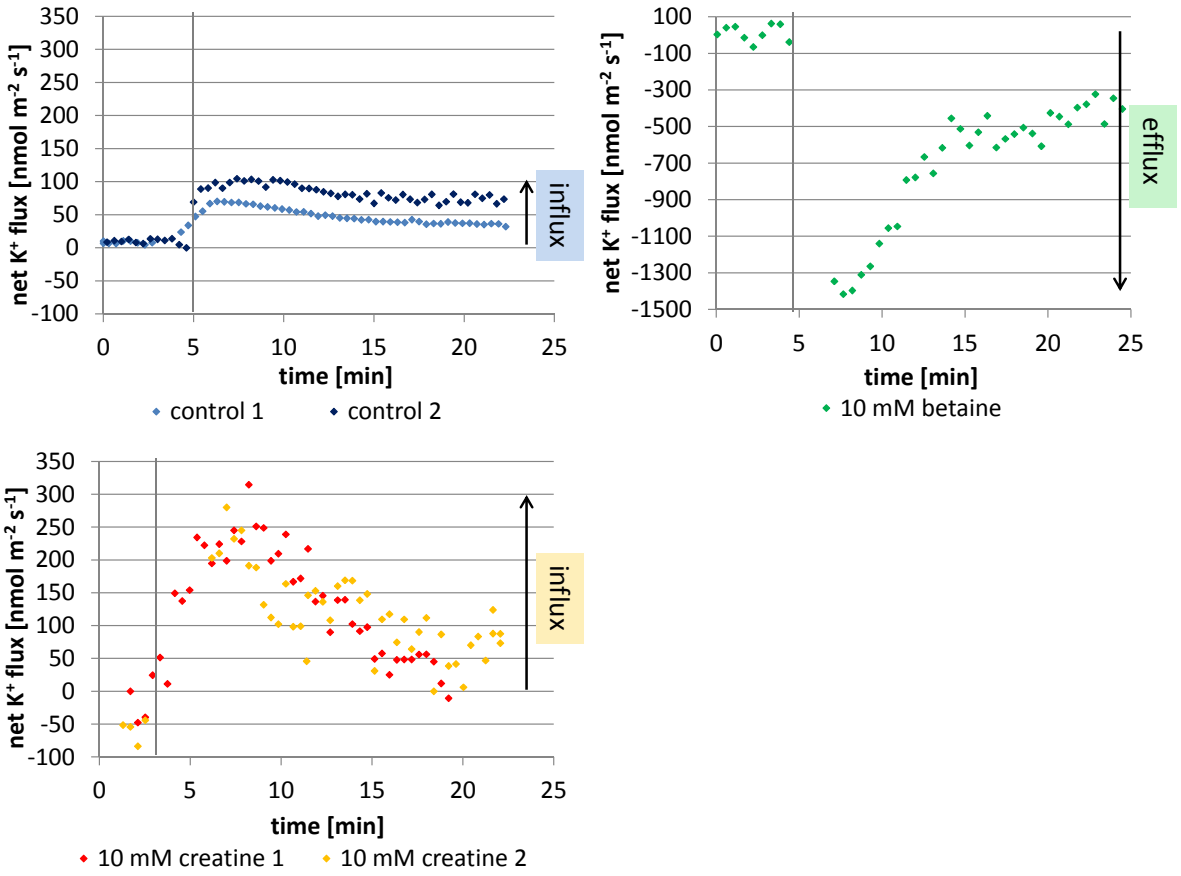

Figure 3.13: K^+ fluxes over membranes of *E. coli* MC4100, observed by using MIFE-technique. Cells were adhered to a glass cover slip as a monolayer and were adapted to conditions in measuring solution containing 1 %NaCl (w/v) for several minutes prior to flux measurements. 2 - 5 minutes after start of measurements, cells were shocked with sucrose (grey line) to a final osmolarity of 1.03 osmol/L.

Addition of 2 mM betaine led to decreased influx of only 20 nmol m^{-2} s^{-1}, which seems different to the reaction of *E. coli* MC4100 cells, but might be due to lower concentration (2 mM compared to 10 mM). Nevertheless, K^+ flux is changed, even if betaine is not taken up. Concentration dependency gets more likely when fluxes observed for different creatine concentration are considered: With 1 mM creatine, sucorse shock leads to an immediate and strong influx of K^+, which, compared to control cells, declines relatively fast. Presence of 10 times higher creatine concentration changed cell response completely. Net K^+ efflux was observed whereas values for efflux were similar to those observed for influx with 1 mM creatine (change of 120 nmol m^{-2} s^{-1}). Interestingly, presence of 10 mM creatine led to similar result in stationary phase *E. coli* MC4100 cells (not shown).

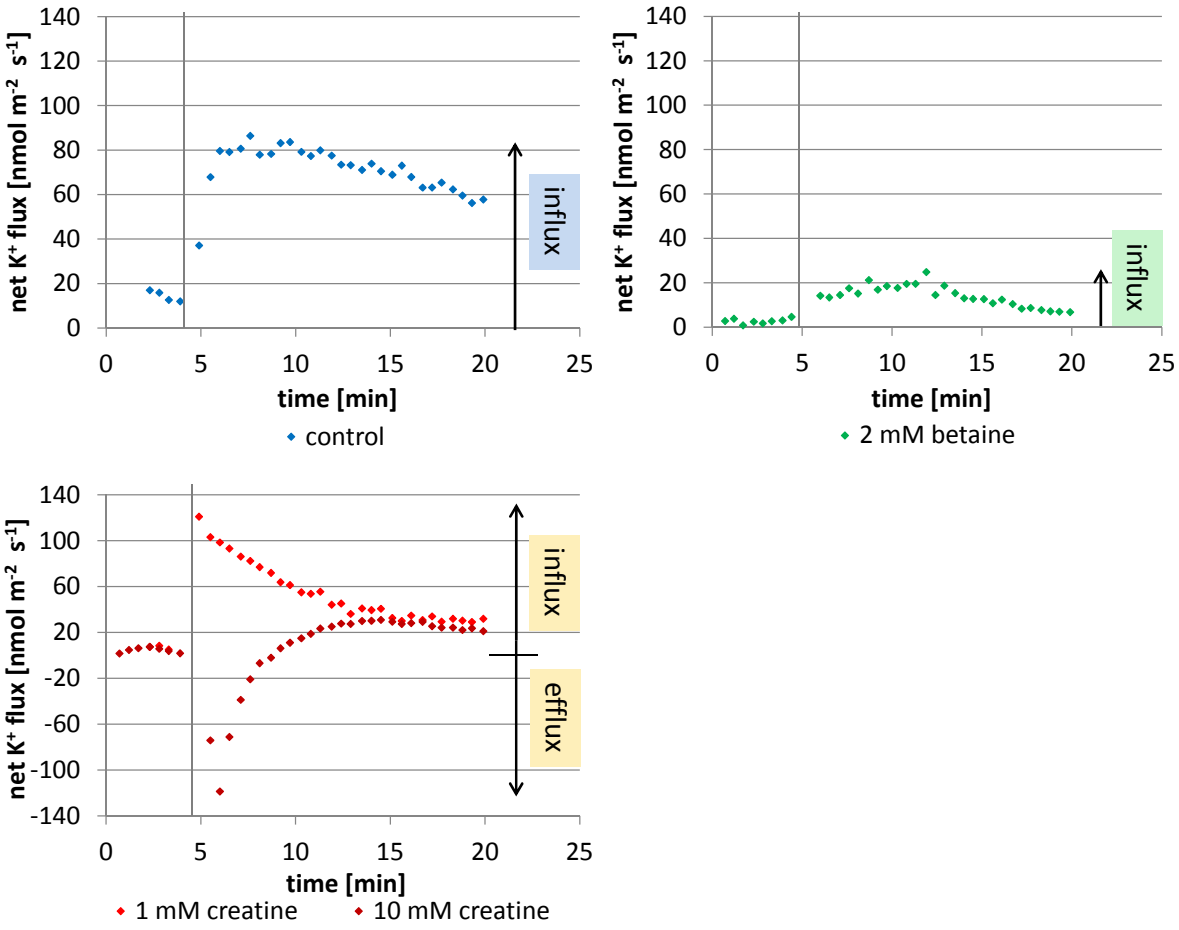

Figure 3.14: K^+ fluxes over membranes of *E. coli* MKH13, observed by using MIFE-technique. Cells were adhered to a glass cover slip as a monolayer and were adapted to conditions in measuring solution containing 1 %NaCl (w/v) for several minutes prior to flux measurements. 2 - 5 minutes after start of measurements, cells were shocked with sucrose (grey line) to a final osmolarity of 1.03 osmol/L.

Potassium transport after sucrose shock was also determined using FLISE technique. In figure 3.15 changes of extracellular K^+ concentrations following osmotic up-shock with sucrose are displayed. Serving as a measure for altered fluxes, decreasing potassium concentrations in the cuvette reflect net uptake by the cells.
Influx of K^+ was observed when control cells were subjected to osmotic up-shock with sucrose. Creatine and guanidino-ectoine strongly reduced net K^+ transport after hyper-osmotic shock, which can be interpreted as either reduced uptake or increased efflux.
With both MIFE and FLISE technique, the problem of determining only net fluxes arises. Hence, it cannot be concluded definitely if influx or efflux systems are affected by

betaine and creatine. Furthermore FLISE and MIFE results are in parts contradictory. Possible reasons will be discussed in chapter 4.1.3

Before changes in H^+ concentrations, which have also been determined using FLISE, will be considered, the phenotype resulting in altered K^+ transport will be described.

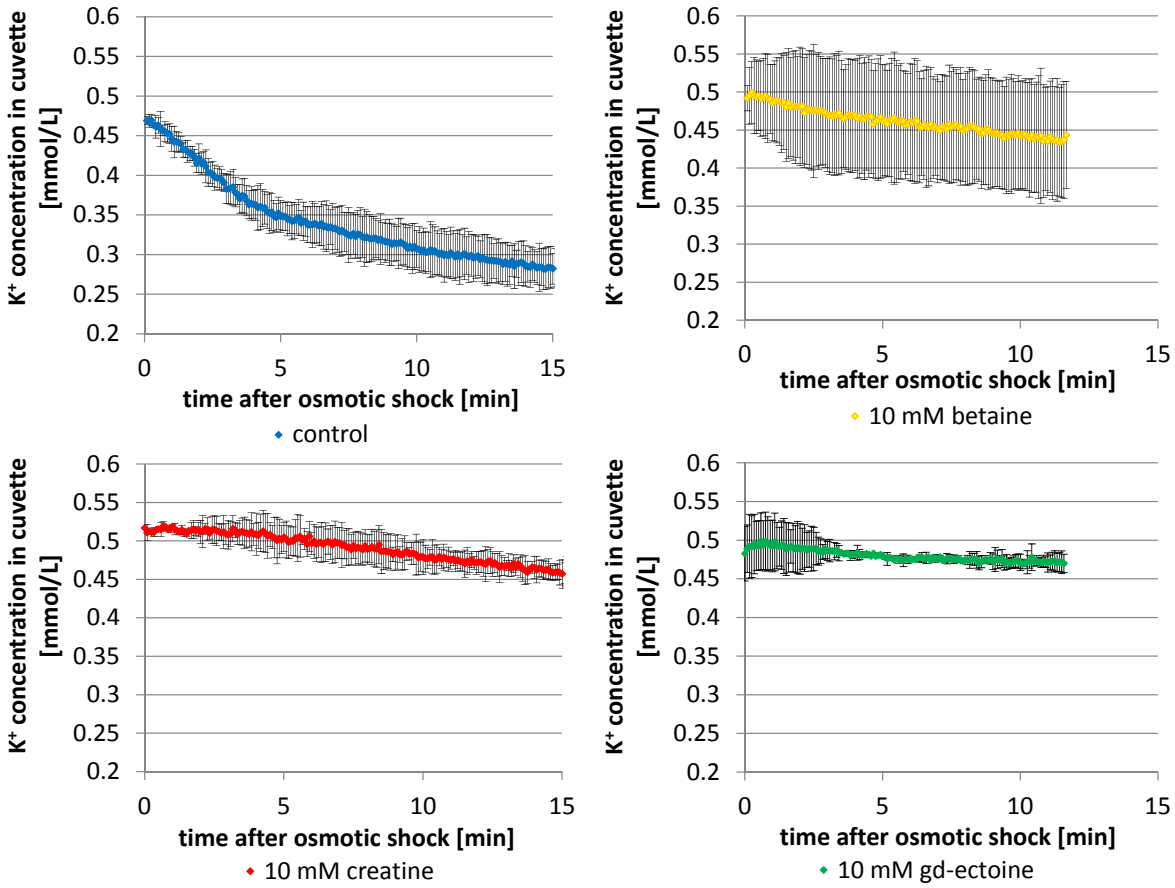

Figure 3.15: K^+ concentration of measuring solution (containing comparable numbers of exponential *E. coli* MC4100 cells ($OD_{600} = 6$)), after hyperosmotic shock with sucrose to a final osmolarity of 1.03 osmol/L. Changes of concentrations were determined using flux measurements with ion selective electrodes (FLISE). Each measuring point, reflects the arithmetic mean of measurements on 2 independent cell cultures with error bars providing the highest and the lowest values.

Significance of change in K^+ transport for growth of *E. coli*

In the following, consequences of K^+ homoeostasis disruption for growth of *E. coli* under different conditions in terms of K^+ concentrations in the medium and point in time of osmotic stress will be considered.

Osmotic up-shock in exponential growth phase Potassium homoeostasis is not only crucial during growth at high osmolarity from the beginning but gains in importance in osmotic shock situations. Therefore, growth behaviour of *E. coli* MC4100 was observed in media reflecting different potassium availability situations: KMM63 medium representing highly exceeding K^+ concentrations, MM63 medium, which is rich in potassium but not immoderately, and K5 medium with only 5 mM K^+ reflecting a potassium limitation situation. In the beginning media contained only 1 % NaCl or KCl, respectively. 2 % of the particular salt was added in the middle of exponential growth phase at optical densities of 0.3 - 0.4. Results are combined in figure 3.16.

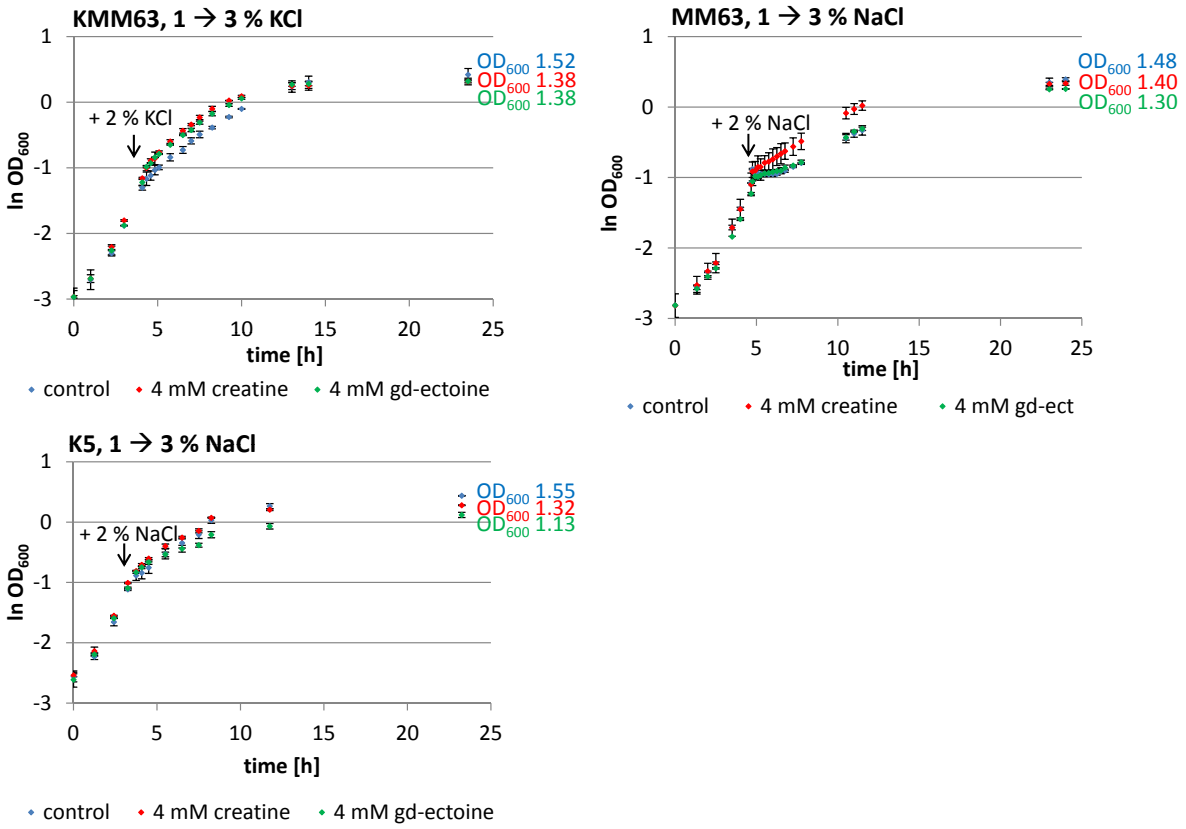

Figure 3.16: Growth of *E. coli* MC4100 in KMM63, MM63 and K5 medium with an initial salinity of 1 % (w/v). In the middle of exponential growth phase an osmotic shock was set by adding 2 % of the respective salt. Cultures were supplemented with 4 mM creatine or guanidino-ectoine. Unsupplemented cultures served as control. Each data point reflects the aritmethic mean of 2 measurements and error bars provide the highest and the lowest values.

Independent on supplementation, all cultures showed the same growth pattern prior to

osmotic up-shock in their respective growth medium. This behaviour changes after addition of KCl to KMM63 or NaCl to MM63 and K5 to a final osmolarity of 1.03 osmol/L. Control cultures continue to grow slightly more slowly but over a longer time periode than creatine and guanidino-ectoine supplemented cultures in **KMM63** medium. This resulted in the highest final optical density of 1.5 whereas optical densities of creatine and guanidino-ectoine supplemented cultures were 1.4.
Contrary to these results, NaCl up-shock led to a short lag phase in control and guanidino-ectoine cultures when grown in **MM63** medium whereas cultures supplemented with creatine continued to grow without a lag phase but naturally more slowly than before salt stress was given. Again control cultures reached the highest OD_{600} of 1.5 followed by creatine cultures with 1.4 and guanidino-ectoine cultures with 1.3.
When potassium was present in only low concentrations in **K5** medium, guanidino-ectoine cultures halted growth soon whereas creatine and control cultures continued to grow equally, but again growth of control cultures lasted longer. Final optical densities were 1.6 in case of the control culture and 1.3 in the creatine supplemented culture.

Osmotic stress from the time of inoculation Comparable to the aforementioned growth experiments where *E. coli* MC4100 was grown in potassium-free medium (figure 3.11) growth experiments were performed in sodium-free medium (**KMM63**) as well. Osmolarity was increased with KCl rather than with NaCl so that K^+ was present excessively and Na^+ only in traces. Results in terms of growth rates are displayed in figure 3.17. Surprisingly, slowest growth was observed for control cultures, which were not supplemented with solutes followed by creatine. Cultures supplemented with guanidino-ectoine grew fastest under the conditions of the experiment.
HPLC-analysis proved creatine and guanidino-ectoine to be accumulated in the cell to slightly increased concentrations compared to cells grown in usual MM63 medium (results not shown). In the absence of Na^+, Nhas are irrelevant so that the fact of a weaker creatine effect is not surprising. Furthermore, extremely high K^+ concentrations are present in KMM63, which might be too high for control cells to compensate. Cultures grown with creatine or guanidino-ectoine, which influence K^+ transport, seem to benefit from supplementation.

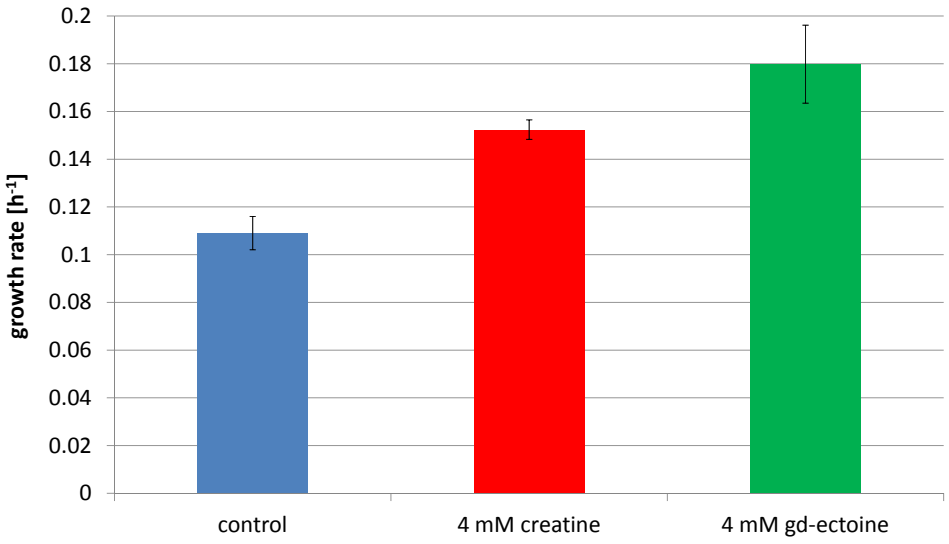

Figure 3.17: Growth rates of *E. coli* MC4100 grown in Na^+-free KMM63 medium containing 3 % KCl (w/v). Cultures were supplemented with 4 mM creatine or guanidino-ectoine. Unsupplemented cultures served as control. Displayed growth rates are mean values of 4 cultures in the case of control cells and creatine cultures with error bars providing the standard deviation. Growth rates of guanidino-ectoine supplemented cultures derive from double determinations with errorbars giving the highest and the lowest measuring points.

To investigate how the situation changes if only a low K^+ concentration is present in the growth medium, growth experiments were performed in **K5** medium, which consists of similar compounds as MM63 but only 5 mM potassium. Growth patterns are shown in figure 3.18.
None of the cultures revealed high growth rates or cell mass at the end of the experiment. Growth of creatine and guanidino-ectoine cultures was inhibited, at which guanidino-ectoine had a stronger effect. In addition to that, supplemented cultures showed a by 10 hours prolonged lag-phase and did not reach stationary phase until measurements were stopped after 34 hours. 5 mM potassium seem to be growth limiting. This effect is enhanced by incompatible solutes which again indicates interaction with K^+ homoeostasis. None of the described results reveal if K^+ uptake or efflux systems are targeted. To answer this question *E. coli* TK2691, which does not feature active K^+ uptake, was grown in MM63 medium containing 3 % NaCl in presence and absence of 4 mM creatine or guanidino-ectoine.

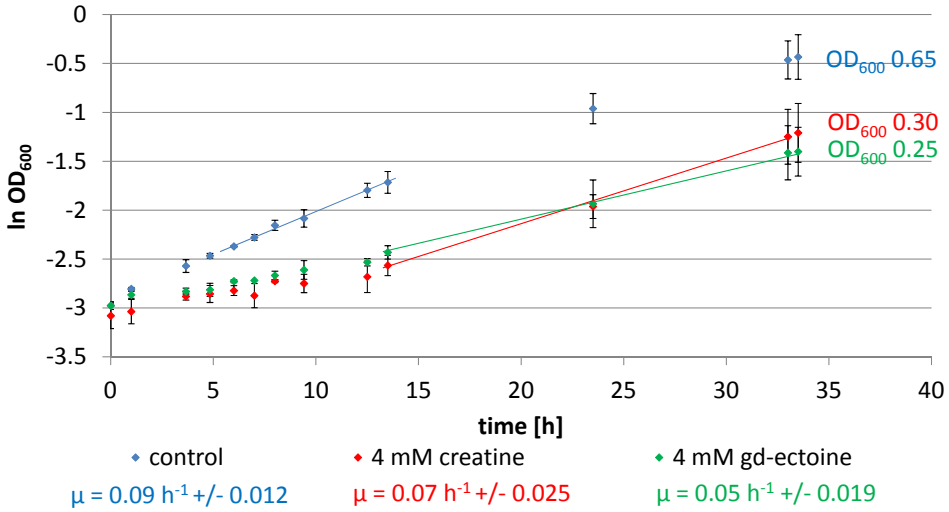

Figure 3.18: Growth of *E. coli* MC4100 in K5 containing 3 % NaCl (*w*/*v*). Cultures were supplemented with 4 mM creatine or guanidino-ectoine. Unsupplemented cultures served as control. Growth rates (μ) are given in corresponding colours and the range of values from which μ was calculated is indicated by lines in the graphs. Displayed measuring points are mean values of 4 cultures in the case of control cells and creatine cultures with error bars providing the standard deviation. Measuring points of guanidino-ectoine supplemented cultures derive from double determinations with errorbars providing the highest and the lowest measuring points.

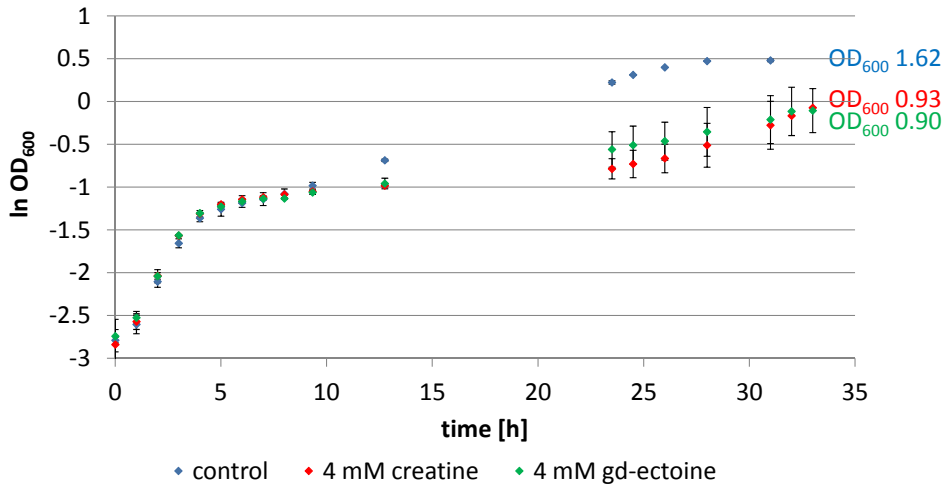

Figure 3.19: Growth of *E. coli* TK2691 at 37 °C in MM63, containing 3 % NaCl (*w*/*v*). Cultures were supplemented with 4 mM creatine or guanidino-ectoine. Unsupplemented cultures served as control.

The first strong increase in optical density during the 2-phase growth which was observed in these growth experiments probably derived from remainder of complex medium which was used to grow-pre cultures.
The results of these growth experiments indicate an interaction with efflux systems: Although all K^+ uptake systems are absent in *E. coli* TK2691, growth was inhibited severely by creatine and guanidino-ectoine (figure 3.19).

Influence on transport activity

To receive further evidence for interaction of creatine and guanidino-ectoine with potassium efflux systems, transport activity measurements with inverted membrane vesicles were performed as above, but KCl instead of NaCl was used to induce ion transport. Inverted vesicles were supplemented with creatine or guanidino-ectoine and activity was determined dependent on the change of emission intensity deriving from pH changes after addition of KCl. Results are shown in figure 3.20.
Compared to not supplemented vesicles, pH changes 20 % faster in the presence of 10 µM creatine. Guanidino-ectoine in the same concentration even increases H^+ transport by nearly 50 %. The compatible solute betaine enhances transport activity by 100 %.

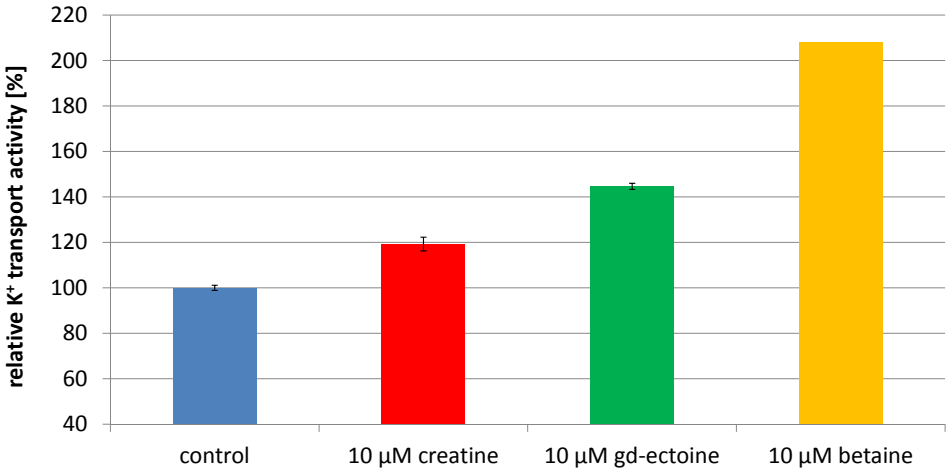

Figure 3.20: Comparison of K^+ transport activities in inverted membrane vesicles of *E. coli* in the absence and presence of the incompatible solutes guanidino-ectoine and creatine and the compatible solute betaine. The slopes of the emission intensities after addition of KCl served as a measure of K^+ transporter activity. The activity in absence of solutes was set to 100 %. Values for control, creatine treated and guanidino-ectoine treated vesicles reflect the mean value of 3 measurements, that of betaine derives from a single measurement. Error bars provide the standard deviations.

All results of this chapter indicate that potassium transport systems are targeted by both guanidino-compounds, of which guanidino-ectoine plays a more prominent role. Moreover FLISE results signified that creatine has an impact on proton homoeostasis, at least in osmotic up-shock situations, which will be shown and further analysed in the following paragraph.

3.3.3 Influence of (in)compatible solutes on pH homoeostasis

Regulation of intracellular proton concentrations can certainly be considered just as important as regulation of cytoplasmic potassium or sodium concentrations. Accordingly, experiments regarding transport of protons after a hyperosmotic shock and changes in intracellular pH during growth were performed.

Influence of (in)compatible solutes on proton transport after osmotic up-shock

Changes in external H^+ concentrations were determined simultaneously with K^+ flux measurements shown in the previous chapter using FLISE. Representative patterns of change in H^+ concentration in correlation with K^+ transport are shown in figure 3.21. H^+ concentrations are displayed by means of pH values.
Decline of pH after osmotic up-shock reflects extrusion of H^+ from the cells and was observed for all cells except creatine treated ones. Interestingly, pH did not decrease immediately after sucrose shock but with a delay of approx. 5 - 6 minutes in the case of control cells. This delay can probably be attributed to the weak buffer capacities of the measuring solution which is exceeded at specific H^+ concentrations. If H^+ extrusion is increased, the limit of buffer capacity is exceeded earlier and the delay is shorter as observed for guanidino-ectoine and betaine treated cells. Change in pH in presence of betaine was comparable to that observed for guanidino-ectoine. Supplementation with creatine, on the other hand, disrupted pH change completely. This result indicates that creatine does not only disrupt sodium and potassium homoeostasis but also transport of protons and hence might influence intracellular pH, which is crucial for a functional metabolism.

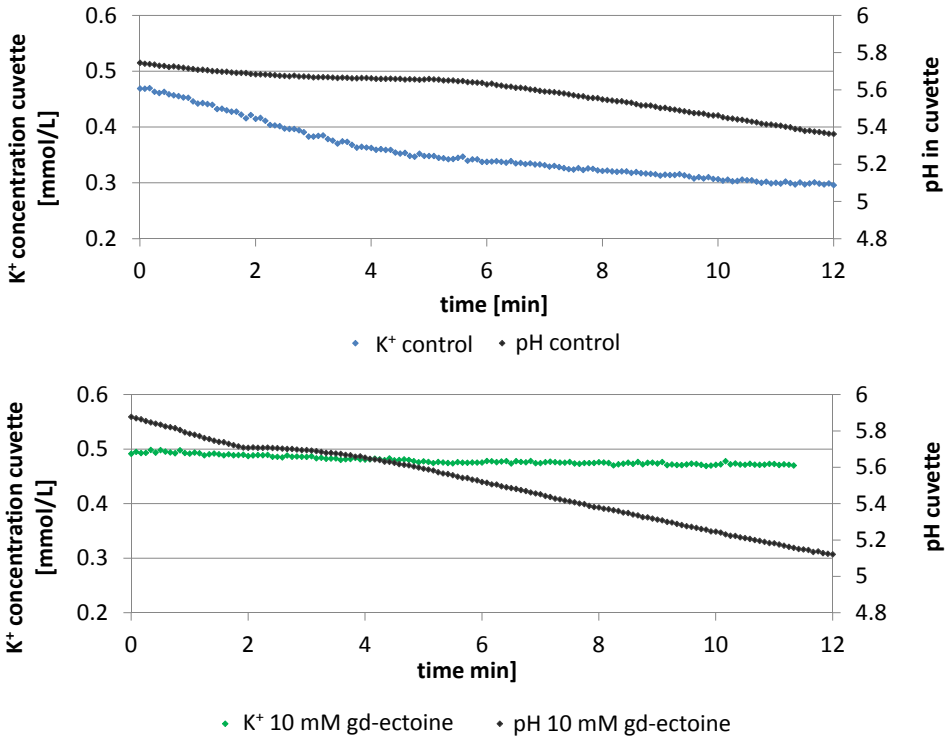

Figure 3.21: K^+ concentration of measuring solution (containing comparable numbers of exponential *E. coli* MC4100 cells (OD_{600} = 6)) and pH of measuring solution after hyperosmotic shock with sucrose to a final osmolarity of 1.03 osmol/L. Changes of concentrations were determined using flux measurements with ion selective electrodes (FLISE).

Influence of creatine on intracellular pH during growth

pH-sensitive GFPs provide a convenient possibility to observe intracellular pH values *in vivo* and therefore to investigate H^+ homoeostasis. deGFP1 is such a GFP-derivative, wich was cloned into *E. coli* DH5α as described in chapter 2.2.12. The resulting strain *E. coli* DH5α-pUC-deGFP1 (in the following termed as *E. coli*-deGFP1) was grown in MM63-3 in mini fermentation units with and without 4 mM creatine. pH value of medium was maintained at 7.0. At different points in time, samples were taken, fluorescence measurements were performed and pH values were calculated (chapter 2.2.8).

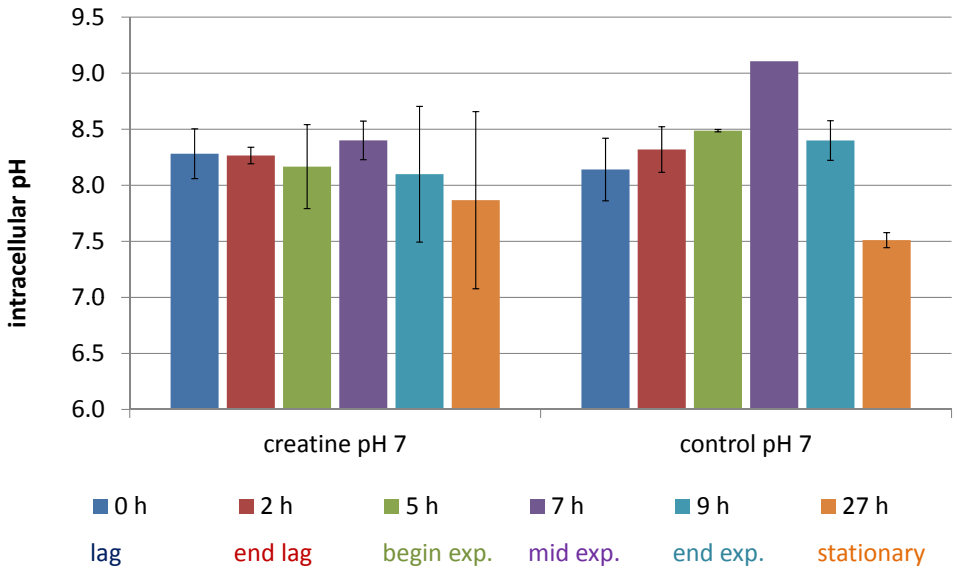

Figure 3.22: Intracellular pH values of *E. coli*-deGFP1 during growth in MM63 containing 3 % NaCl in minifermentation units. Times of cultivation are given in hours and respective growth phases are specified in corresponding colours. Each measuring point reflects the arithmetic mean of 4 cultures with error bars giving standard deviations (except control 7 h: only two measurements).

One has to note that calculation was performed using the calibration curve of the preculture of this experiment one day in advance. Therefore, calculated values might not reflect the actual values accurately. Nevertheless, values between creatine and control cultures are comparable.

Resulting pH values as well as times of sampling and corresponding growth phases are given in figure 3.22. Contrary to control cells, creatine supplemented cells seem to maintain internal pH at an equal level. pH values of control cultures rise until middle of exponential phase by 1 unit and subsequently decrease until late stationary phase to a value 0.5 units lower than the initial value.

Here again evidence is given that creatine interacts with systems responsible for H^+ homoeostasis in *E. coli*.

Based on the experiments of this chapter it becomes clear that creatine and guanidinoectoine influence ion-homoeostasis in different ways and with different strengths. This disruption does surely participate in growth inhibition, but it cannot be concluded that no other cell machineries are involved. Therefore, interaction with ribosomes as a further possible target already known for guanidino-function carrying antibiotics was investi-

gated.

3.4 The effect of incompatible solutes on thermal stability of ribosomes

Previous experiments indicated an interaction between creatine and nucleic acids, first of all RNA (Mann, 2008; Sell, 2009). To check whether there is an interaction between incompatible solutes and ribosomes, which comprise approx. 66 % RNA, calorimetric measurements on purified ribosomes of *E. coli* K-12 were performed in the absence and presence of creatine and guanidino-ectoine (see chapter 2.2.10). For all measurements 1 µM ribosomes were applied and temperature was increased by 60 °C in the period of one hour from 25 - 85 °C. Calorimetric measurements of purified ribosomes showed a typical pattern for *E. coli* ribosomes (Mackey *et al.*, 1991) with a melting point at 69 °C (figure 3.23).

In figure 3.24 melting points of ribosomes treated with 0.10 M and 0.13 M creatine or 0.1 M guanidino-ectoine are displayed and compared to that of ribosomes without any solute and ribosomes with compatible solutes. Measurements for values with compatible solutes were performed by Britta Seip. One has to consider that higher concentrations compared to incompatible solutes were applied here. Addition of 0.1 M creatine resulted in a 0.4 °C lower melting point (68.5 °C) compared to ribosomes without solutes, and increase of creatine concentration to 0.13 M led to a further decrease of ribosome stability by nearly 1 °C. As discovered in later experiments (see chapter 3.5), creatine is converted to creatinine in aqueous solutions at high temperatures. Therefore, the assumed effect of creatine on ribosomes might in practice derive from creatinine.

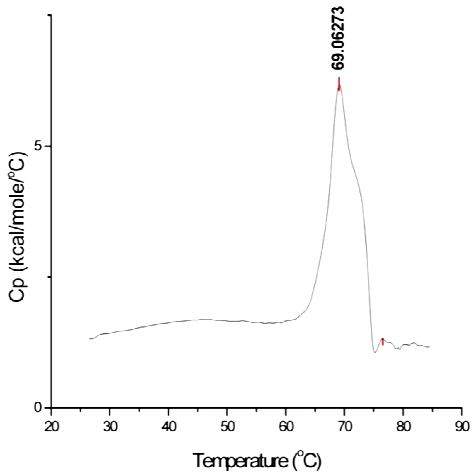

Figure 3.23: Melting profile of purified crude ribosomes of *E. coli* K-12 generated with differential scanning calorimetry. The highest peak at 69 °C is supposed to derive from denaturation of the 50S subunit.

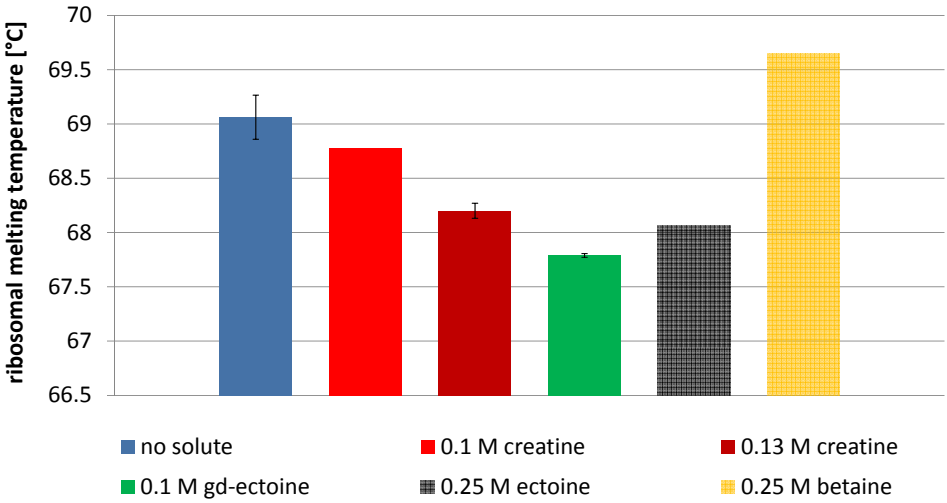

Figure 3.24: Melting points of *E. coli* K-12 ribosomes in presence and absence of 0.1 M and 0.13 M creatine or 0.1 M guanidino-ectoine compared to 0.25 M ectoine or betaine, respectively. Displayed are temperatures of the biggest peak in each melting profile, which supposably represents denaturation of 50S ribosomes. Values for thermal melting temperature with betaine and ectoine were kindly provided by Britta Seip. Measurement with betaine, ectoine and 0.1 M creatine were performed once, measurements without solutes, with guanidino-ectoine and 0.13 M creatine were performed twice with ribosomes of independent purification charges. Error bars reflect the highest and lowest values.

An even greater decrease of melting temperature was observed when 0.1 M guanidino-ectoine was supplied. Presence of guanidino-ectoine during the measurement led to a 1.4 °C lower melting point compared to that of ribosomes without incompatible solutes. Both, creatine/creatinine and guanidino-ectoine destabilise the ribosomal complex of *E. coli in vitro*. Furthermore, an increase of the creatine concentration from 0.1 M to 0.13 M led to a decline of melting temperature from 68.8 °C to 68.2 °C. This indicates that higher concentrations would result in higher degrees of destabilisation of the ribosomal complexes. With the unavoidable problem of creatine being poorly water soluble (max. 0.13 M) (and nearly not soluble in solvents like ethanol and diethyl ether), higher concentrations could not be tested. Solubility of guanidino-ectoine is even lower ($\leq$ 100 mM). Comparison to melting temperatures of ribosomes in presence of compatible solutes revealed that betaine has an opposite effect. It increases thermal stability and ectoine effects destabilisation but to a lower degree than the incompatible solutes do.

To check whether the above described influence of incompatible solutes on ribosomes is due to a direct interaction, such as binding, gel shift experiments were performed: Ribosomes in storage buffer (see chapter 2.1.3) were incubated with different concentrations of creatine or guanidino-ectoine for 1 hour at room temperature and subsequently loaded onto an agarose-gel (0.8 % agarose) to perform an electrophoresis at 50 V for 4 hours. The gel was dyed with GelRed^{TM} for 25 minutes and examined in UV-light. Results are shown in figure 3.25. The first two lines contain ribosomes together with 130 mM and 65 mM creatine whereas line 3 and 6 show the run of ribosomes without any solute. Samples containing creatine run more slowly than those without solutes, but creatine concentration does not seem to have any effect. Contrary to that, running time of ribosomes are obviously dependent on guanidino-ectoine concentration; the higher the concentration, the slower the sample runs in the agarose gel.

With these results a binding of creatine/guanidino-ectoine and ribosomes becomes more likely. But still, the question of whether the interaction occurs between the rRNA and incompatible solutes or ribosomal proteins and incompatible solutes remains unanswered. Furthermore, the changed running time in the agarose gel can as well derive from changes in conformation instead of a direct interaction (binding) of incompatible solutes with ribosomes.

If the interaction of incompatible solutes with ribosomes is based rather on an interaction with rRNA than with ribosomal proteins, interactions with DNA should also be considered.

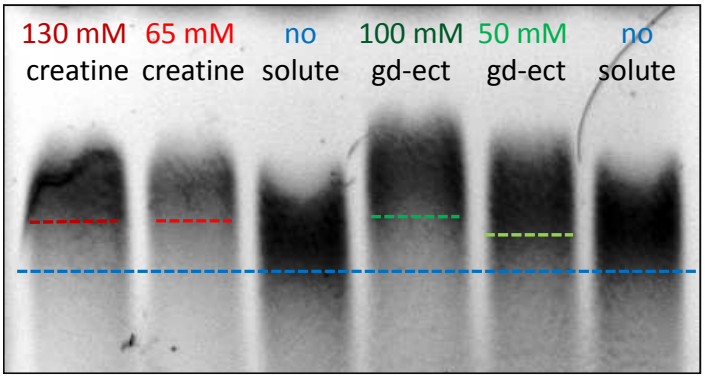

Figure 3.25: Agarose gel electrophoresis of purified ribosomes of *E. coli* K-12 in storage buffer with 130 mM and 65 mM creatine without incompatible solutes and with 100 mM and 50 mM guanidino-ectoine. Lines for endpoints of bands were drawn in each lane for clarification.

3.5 The effect of (in)compatible solutes on thermal stability of DNA

To receive first indications for interaction of incompatible solutes with nucleic acids, thermal melting curve analysis was performed. Absorption of 20 µg calf thymus DNA, supplemented with either compatible or incompatible solutes and without solutes for control, was measured spectrophotometrically at 260 nm with a heating profile of 10 °C per hour from 40 °C - 90 °C. As already mentioned in chapter 2.2.11, creatine is transformed to creatinine in hot water solutions so that measurements with creatine were not meaningful. Nevertheless, measurements with guanidino-ectoine showed significant differences compared to measurements without any solutes (see figure 3.26). The effect of guanidino-ectoine on calf thymus DNA is contrary to that of betaine and severalfold stronger. While 1 M betaine decreases the melting point by 3 - 4 °C to 59 °C, guanidino-ectoine with a concentration of 50 mM stabilises DNA resulting in a 9 °C higher melting point of 71 °C compared to a melting temperature of 62 °C for untreated DNA.
The phenomenon of guanidino-ectoine (as a representative for incompatible solutes with a guanidino-function) revealing a very strong effect on shift of thermal melting point of calf thymus DNA cannot be explained up to now. Further experiments with synthetic poly(deoxyadenylic - deoxythymidylic) acid (poly(dA - dT)) were performed to understand the interaction.

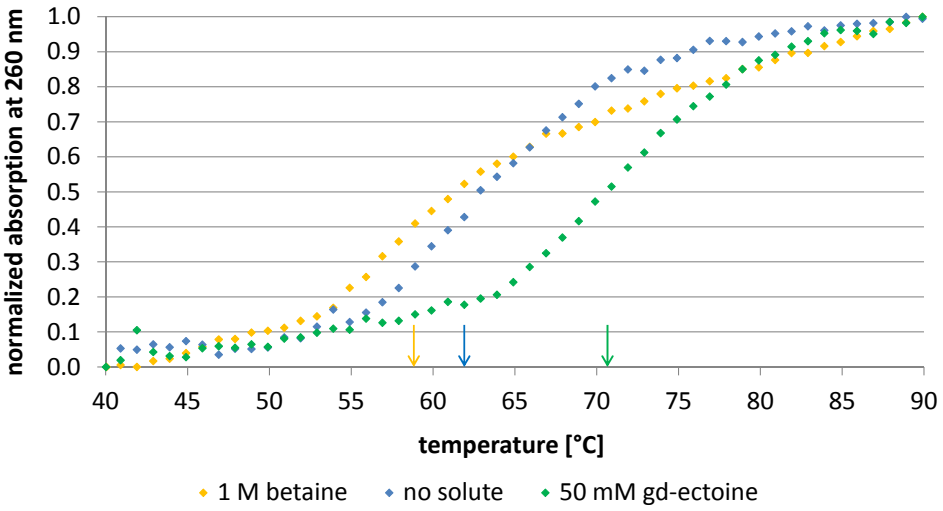

Figure 3.26: Normalised melting curves of 20 µg calf thymus DNA in potassium acetate buffer. A temperature profile of 10 °C h^{-1} was used. DNA was applied without solutes, with 1 M betaine or with 50 mM guanidino-ectoine. Melting temperatures are indicated by arrows in corresponding colours.

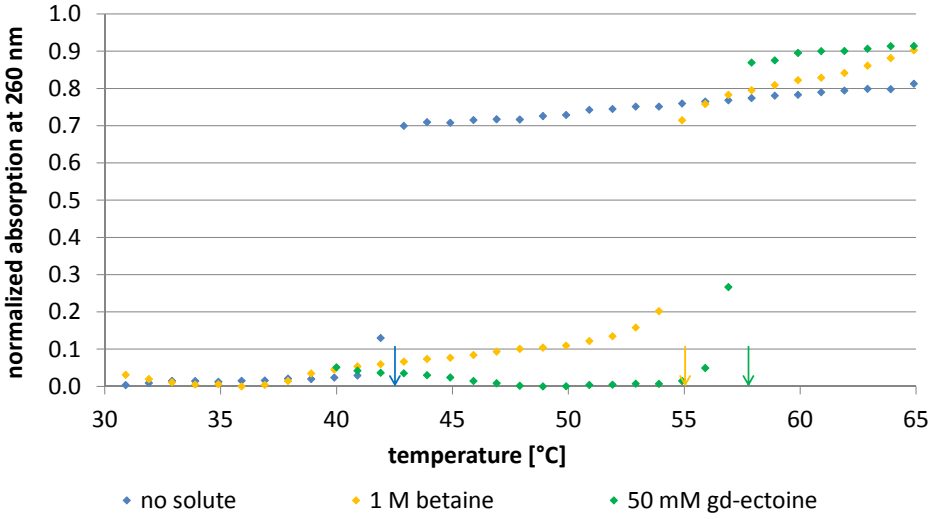

Figure 3.27: Normalised melting curve of 20 µg synthetic poly(dA - dT) in potassium acetate buffer. A temperature profile of 10 °C h^{-1} was used. Synthetic poly(dA - dT) was applied without solutes, with 1 M betaine or with 50 mM guanidino-ectoine. Melting temperatures are indicated by arrows in corresponding colours.

If no changes in the shift are exhibited, interaction with guanine or cytosine becomes

more likely whereas changes in shift of melting points would indicate interactions with the phosphate backbone of the DNA. Results of melting profiles of the guanine and cytosine-free DNA are displayed in figure 3.27.
Since its melting point is much lower compared to that of calf thymus DNA, absorption was monitored from 30 - 65 °C.
Melting temperature without solutes was 44 °C. Surprisingly, both, betaine and guanidino-ectoine stabilise DNA. 1 M betaine, however, increases melting point by 9 °C whereas 50 mM guanidino-ectoine again reveals a stronger effect. Melting temperature is shifted by nearly 15 °C and is 57 °C.
All results of thermal melting curve analyses demonstrate that guanidino-ectoine interacts with DNA, regardless of nucleobase composition. The effect is opposed to that of betaine in the case of calf thymus DNA and much stronger than that of betaine in all cases tested. Additional to that, the stabilising effect of guanidino-ectoine is even greater on synthetic poly(dA - dT) than on calf thymus DNA.

3.6 Growth of bacteria in presence of creatinine

In 2012 McDonald *et al.* reported creatinine-HCl to inhibit bacterial growth (McDonald *et al.*, 2012). Surprisingly, inhibition was much stronger than that observed with creatine, and increased osmolarity (which induces activity of (in)compatible solute uptake systems ProU and ProP) does not seem to be necessary. Furthermore, Gram-positive as well as Gram-negative bacteria are affected while only Gram-negative ones are inhibited by creatine. Since the incompatible solute creatine is in equilibrium with creatinine under certain conditions, it is possible that the mode of action of both substances is similar. To characterise the creatinine-effect more precisely, a range of growth experiments was performed. Results are described in the following paragraphs.

Growth of *E. coli* MC4100 in the presence of creatinine

When *E. coli* is grown in complex medium with only very low amounts of NaCl (0.5 %, (w/v)), 4 mM creatinine does not have any effect on growth (not shown). The same can be expected for growth in presence of 4 mM creatine in place of creatinine. HPLC-analysis revealed that only very low amounts of creatinine are taken up under these conditions ($\leq$ 0.01 mmol/g dw. Results not shown).
Similar results were observed when *E. coli* was grown in MM63-1 (data not shown). Growth patterns of supplemented and not supplemented cultures were comparable.

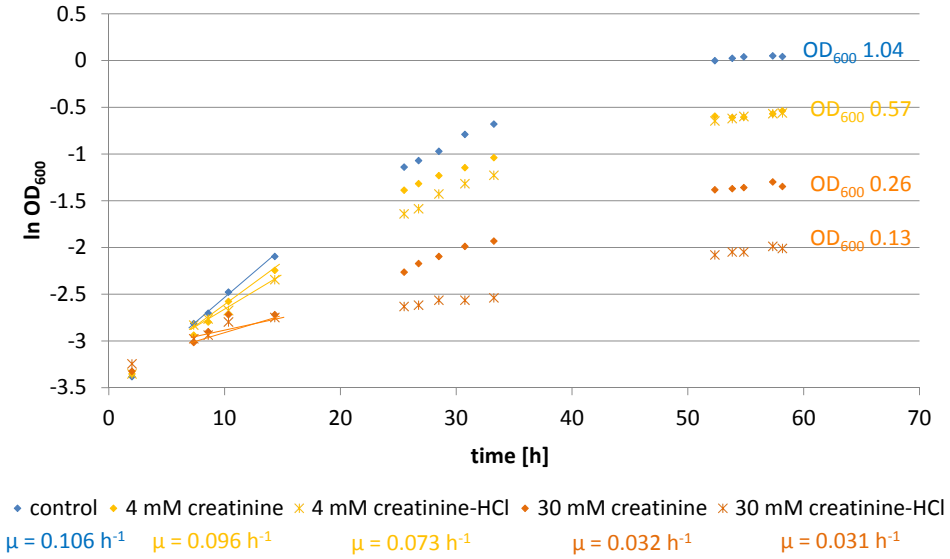

Figure 3.28: Growth of *E. coli* MC4100 in MM63 containing 3 % NaCl (*w*/*v*). Cultures were supplemented with 4 mM and 30 mM creatinine or creatinine-HCl, respectively. Control cultures were not supplemented. Growth rates (μ) are given in corresponding colours and the range of values from which μ was calculated is indicated by lines in the graphs.

Again, low amounts of creatinine were taken up. Interestingly, creatinine was partially converted to creatine. Under these conditions creatine would not have an effect on growth either, and uptake would appear to a similar level as observed for creatinine here.

If osmotic stress is given in terms of 3 % NaCl (*w*/*v*), creatinine reduces growth of *E. coli* in minimal medium. As demonstrated in figure 3.28, higher concentration (30 mM compared to 4 mM) led to a stronger effect. Additionally, supplementation with creatinine-HCl rather than creatinine decreased growth rates further. In presence of 30 mM creatinine-HCl no growth was detectable.

Similar to the effect of creatine (see chapter 3.2), creatinine reduces glutamate levels in the cytoplasm at high salinities (figure 3.29).

This can be caused by intracellular conversion of creatinine to creatine or due to effects of creatinine itself, such as disruption of K^+ homoeostasis. Under the conditions of the growth experiment trehalose is synthesised. Surprisingly, the amount of accumulated trehalose is not reduced with creatinine, although creatinine is again converted to creatine (figure 3.29).

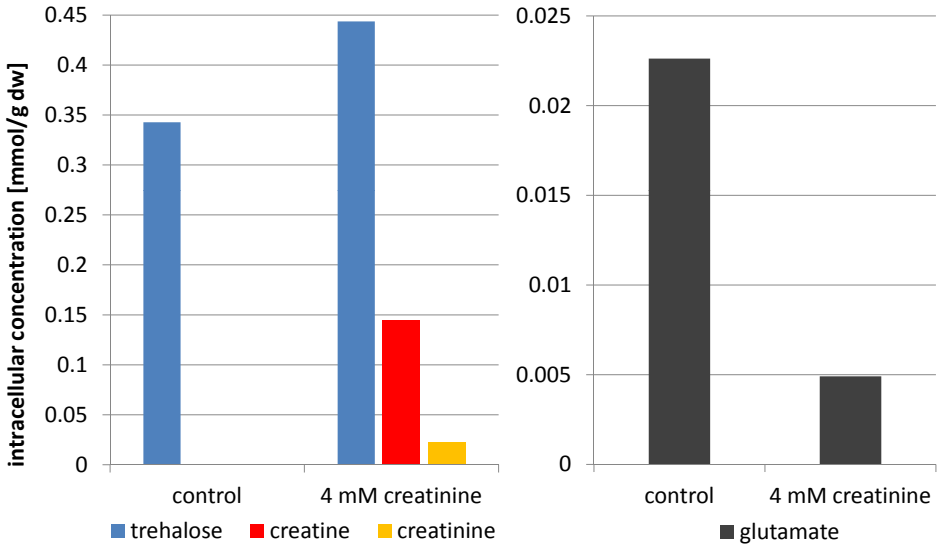

Figure 3.29: Solute and glutamate concentrations of *E. coli* MC4100 revealed by HPLC. *E. coli* was grown in MM63 containing 3 % NaCl (*w*/*v*) and 4 mM creatinine. Control cultures were not supplemented. Depicted bars reflect values of single determinations.

Usually, creatine inhibits trehalose synthesis in a similar manner to that known for compatible solutes even though to a lower degree (half trehalose concentration with creatine compared to unsupplemented cultures and nearly no trehalose in presence of betaine (see figure 3.4)). One possible explanation for this is that there exists a feed back regulation between the active uptake systems for compatible solutes and trehalose synthesis, but creatinine is taken up via different and trehalose-independent systems. This was checked with different mutant strains of *E. coli*.

Determination of creatinine uptake systems in *E. coli*

Mutants of *E. coli*, which are deficient either in both uptake systems *pro*U and *pro*P (*E. coli* MKH13) or only in *pro*U (*E. coli* MKH17), were grown in MM63-3 and 4 mM creatinine. It has already been shown that creatine is not taken up by *E. coli* MKH13 and only to low concentrations in *E. coli* MKH17 and therefore does not reveal any growth inhibitory features on these strains.
None of the announced mutant strains was inhibited by 4 mM creatinine or creatinine-HCl (not shown). Thus, it was surprising to prove creatinine and creatinine-HCl being taken up by *E. coli* MKH17 but not by *E. coli* MKH13 (≤ 0.01 mmol/g dw, see figure 3.30).

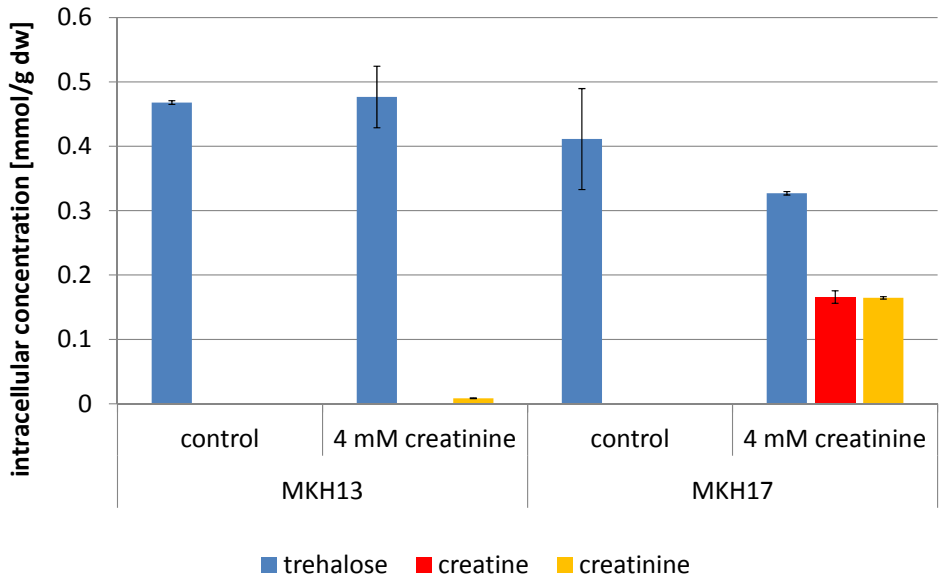

Figure 3.30: Solute concentrations in *E. coli* MKH13 (Δ*pro*P Δ*pro*U) and *E. coli* MKH17 (Δ*pro*U) revealed by HPLC. *E. coli* strains were grown in MM63 containing 3 % NaCl (*w*/*v*) and 4 mM creatinine. Control cultures were not supplemented. Each bar reflects the mean value of 2 measurements with error bars providing the highest and the lowest values.

Again, creatinine was partially converted to creatine, and in contrast to wild type, trehalose level was decreased slightly. Moreover, it is conspicuous that the sum of accumulated creatine and creatinine is 2.5 times higher than in the wild type strain, which makes results of growth experiments where no inhibition was detected all the more interesting.

Influence of creatinine on potassium transport

Since guanidino-ectoine and creatine have been shown to interfere with potassium transport systems, it was of interest to see if creatinine has the same effect. Therefore, activity measurements after osmotic shock with KCl were performed with inverted membrane vesicles of *E. coli* K-12 as described in chapter 2.2.7 and chapter 3.3.2.
While control measurements without creatinine revealed a decrease of fluorescence intensity and therefore acidification of the medium, no change was observed when creatinine in a concentration of 10 µM was present. Since an acidification of the vesicle surrounding medium under the conditions of the experiment implicates potassium efflux via K^+ H^+ antiport systems, it seems that particularly potassium efflux is abolished in the presence of 10 µM creatinine.

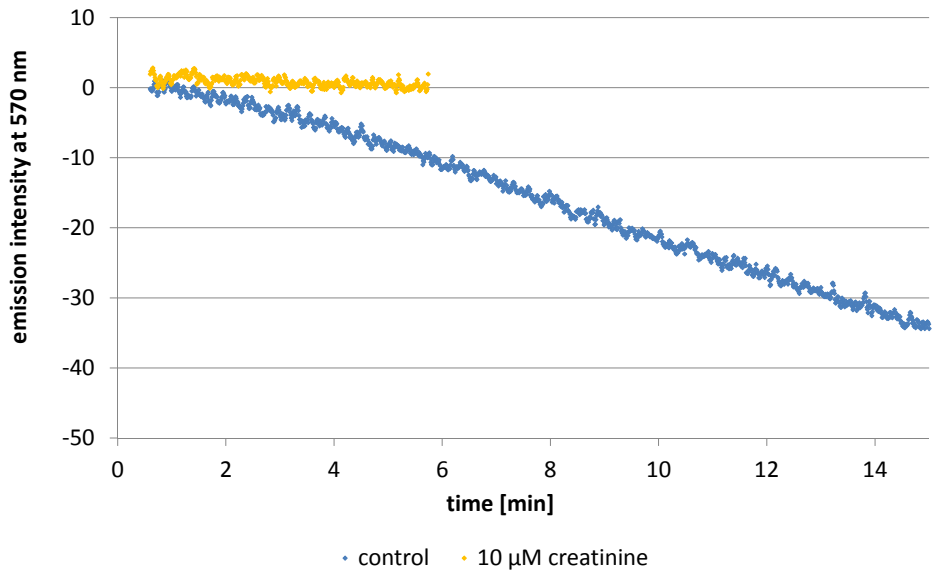

Figure 3.31: Comparison of K^+/H^+ antiport activities in inverted membrane vesicles of *E. coli* K-12 in the absence and presence of creatinine. Changes in emission intensities after osmotic up-shock with 10 mM KCl are depicted.

Comparison with results of McDonald *et al.* (2012)

Within further growth experiments, the effect of creatinine-HCl on Gram-positive strains, which had been proven to be insensitive to creatine (Mann, 2008), was investigated. Hence, the same conditions as described in the paper of McDonald (McDonald *et al.*, 2012) were chosen: Complex growth medium without NaCl (LBG containing 1 % glucose) and supplementation of growth medium with 30 mM creatinine-HCL. The experiment was performed with *E. coli* MC4100 as representative for Gram-negative organisms and *Staphylococcus carnosus* and *Bacillus subtilis* as Gram-positive test organisms. Results of these experiments are combined in figure 3.32. The rhombi reflect unsupplemented cultures and the dashes show growth of cultures supplemented with 30 mM creatinine-HCl.

It becomes obvious that all cultures supplemented with creatinine-HCl grew slower than control cultures. While creatinine cultures of *E. coli* (blue) and *S. carnosus* (red) revealed extended lag-phases and reduced final optical densities, *B. subtilis* (green) was not able to grow with creatinine under these conditions at all.

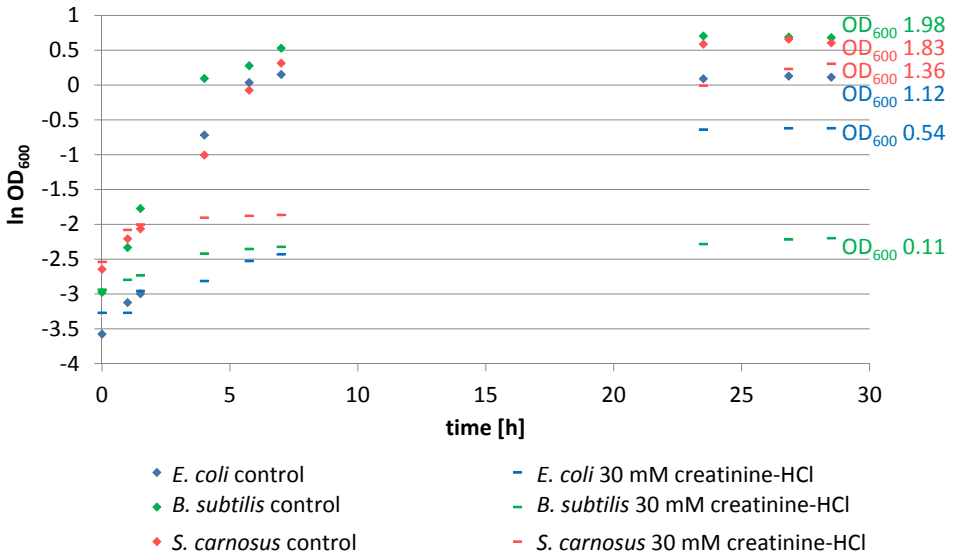

Figure 3.32: Growth of the Gram-negative *E. coli* MC4100 and the Gram-positive strains *S. carnosus* and *B. subtilis* in LBG- 1 % glucose and 30 mM creatinine-HCl (lines). Control cultures were not supplemented with creatinine (rhombi).

From these results it can be concluded that creatinine-HCl inhibits growth of bacteria independently of the classification of the tested species into Gram-positive or Gram-negative bacteria. 4 mM creatinine (without HCl) reveal similar characteristics to creatine: No inhibitory effect at low salt concentrations or in complex medium but uptake at elevated osmolarity, similar growth inhibition and reduction of glutamate level. But interestingly, it is converted to creatine and does not reduce the amount of accumulated trehalose. Creatinine-HCl leads to slightly stronger growth inhibition than creatinine, and supplementation with 30 mM of this substance results in intense reduction or even complete halt of growth, independent on osmolarity or presence of complex media compounds. Furthermore, ProP was identified as one uptake system for creatinine but it cannot be stated from these results if uptake is also performed via ProU in wild type cells.

4 Discussion

Creatine has first been discovered as an incompatible solute in 2004 in the course of the SESCOWA project (see chapter 1.2.2). During several diploma theses (Fassbender, 2004; Mann, 2008; Sell, 2009) its impact on bacterial growth has been investigated, but the mode of action of creatine remained unclear. To prove that the guanidino-function in creatine is responsible for the contrary effect to the structural similar compatible solute betaine, a further guanidino compound was synthesized: Guanidino-ectoine, which resembles the compatible solute ectoine (see chapter 1.2.2). Both, creatine and guanidino-ectoine inhibited growth of Gram-negative but not Gram-positive bacteria and a similar mode of action was predicted for the two guanidino-compounds (Sell, 2009). This work revealed two main conclusions:

1. Although the guanidino group is believed to be the critical function for the inhibitory effect, it must be concluded that creatine and guanidino-ectoine bear different modes of action.
2. Both, creatine and guanidino-ectoine hamper cell function in various respects; the cause of growth inhibition is not limited to one target.

In the following chapters, results of this work will be discussed with regard to the different targets of creatine and guanidino-ectoine and consequences for bacterial growth.

4.1 Creatine and guanidino-ectoine disrupt ion homoeostasis of *E. coli*

In chapter 3.3 it has been shown that creatine and guanidino-ectoine disrupt ion homoeostasis in *E. coli* severely. While creatine influences transport of all three examined ions (Na^+, K^+ and H^+), guanidino-ectoine only seems to influence K^+ transport but to a higher extent compared to creatine.

4.1.1 Creatine inhibits sodium-proton antiporter activity

Already in 1969 Paolini discovered that structure, size and charge density of trihydrated sodium ions in aqueous solution resemble the guanidine group, which exists in its protonated form at physiological pH as the guanidinium ion (Paolini, 1969). These findings are demonstrated in figure 4.1.

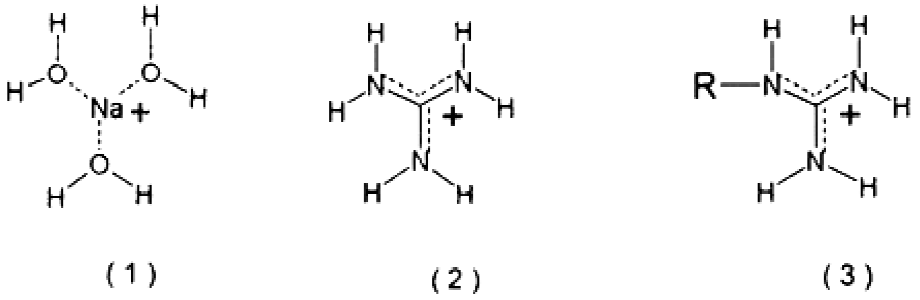

Figure 4.1: The figure is taken from Lang, 2003 and displays findings of Paolini, 1969. Structures of the trihydrated sodium ion (1), the guanidinium ion (2) and the substituted (R) guanidinium ion (3) are displayed.

In 1982 this phenomenon was rediscovered by Natochin (Natochin, 1982). At this time, first fundamental studies on the inhibitory effect of amiloride and its derivatives on sodium proton antiporter had been performed and could be explained with a competition between the guanidinium moiety and the trihydrated sodium ions for the alkali cation-binding site of the antiporter (Natochin, 1982; Lang, 2003).
For a long time, studies were limited to effects on mammalian antiporters, until 1985 Schönheit demonstrated inhibition of a sodium proton antiporter in the methanogenic bacterium *Methanobacterium thermoautotrophicum* by amiloride (Schönheit & Beimborn, 1985). 10 years after that, Pinner and colleagues found that amiloride also inhibits NhaB in *E. coli* (Pinner *et al.*, 1995). Yet another 10 years later, the first specific inhibitor for NhaA type antiporters in *E. coli* has also been discovered: 2-aminoperimidine, which is an amiloride analogue. In the meantime it has been proven to inhibit sodium proton antiport via NhaA with a half maximal inhibitory concentration (IC_{50}) of only 0.9 µM (Dibrov *et al.*, 2005). Structures of 2-aminoperimidine and amiloride are displayed in figure 4.2.
Results of chapter 3.3.1 exhibit that creatine but not guanidino-ectoine is another inhibitor for bacterial Nhas. Whether NhaA or NhaB is affected, could not be clarified. The effect of the above incompatible solutes on the activity of Nhas was determined

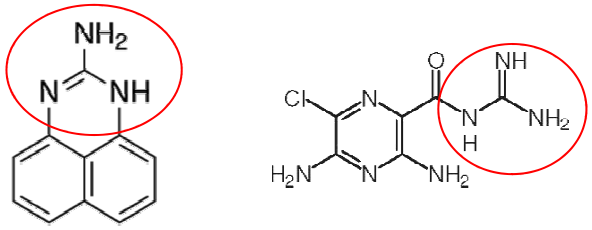

Figure 4.2: Structures of 2-aminopyrimidine (2-perimidinylammonium ion) and amiloride. The guanidino moietes (red circle) mimic trihydrated Na^+ ions and compete for binding sides on sodium proton antiporters, which leads to inhibited ion transport.

on inside-out membrane vesicles with the help of acridine orange, a fluorescent probe for pH difference across the membrane. Creatine clearly inhibited Nha activity at µM concentrations while neither its corresponding compatible solutes betaine nor guanidino-ectoine affected antiport activity. With an IC_{50} of 10 µM in presence of 10 mM NaCl, the effect of creatine seems weaker than that observed for 2-aminoperimidine (IC_{50} of 0.9 µM) (Dibrov *et al.*, 2005) and amiloride (IC_{50} of 0.9 µM) (Pinner *et al.*, 1995) at first glance. But one has to consider that vesicles from *E. coli* wild type were used in activity experiments of this work. This means if only one antiporter is targeted by creatine, the other one would still be functioning and is likely to compensate the inhibitory effect partially. In experiments described in the above cited publications, vesicles of NhaA and/or NhaB-deletion mutants were used, which results in inhibitory effects exclusively on one of the antiporters. It would be interesting to observe which antiporter is affected by creatine but in the course of this work purification of intact and stable inverted membrane vesicles of Nha mutants has not been successful.

The fact that creatine is actively accumulated in the cytoplasm distinguishes it from other inhibitors of bacterial Na^+ H^+ antiporters, which have only been investigated on inverted vesicles. This advantage can be helpful in respect to further investigation of the physiological role of sodium proton antiporters in *Enterobacteriaceae*.

Despite of extensive screening (Pinner *et al.*, 1995), the only discovered inhibitors for bacterial Nhas have been amiloride and 2-aminoperimidine until now. In view of this fact, it was not surprising to find that guanidino-ectoine, in spite of its guanidino moiety, does not inhibit activity of the sodium proton antiport systems. Although the Nha inhibitor 2-aminoperimidine and guanidino-ectoine both exhibit their guanidino-function in a ring system, they are structurally different with regard to an additional ring-bound

carboxylgroup in guanidino-ectoine. Therefore it is possible, that the Na^+ binding sites are simply not accessible to the guanidino-group of guanidino-ectoine due to its steric configuration.

Apart from that, guanidino-ectoine is not commercially available and therefore self-synthesised. The product has not been analysed with respect to its purity by NMR after every synthesis. Hence, it is possible that incomplete synthesis reactions or impurities due to insufficient washing of the product changed guanidino-ectoine properties during measurements.

Nhas can be found in nearly all species on earth, which illustrates their importance and efficiency. Nhas do not only fulfil extrusion of Na^+, being important to maintain an inwardly directed gradient for several transport processes as well as to keep otherwise toxic concentrations low. Due to the electrogenic stoichiometry of two H^+ transported into the cytoplasm for every Na^+ which is extruded, Nhas can also function as pH regulators. With regard to these two fundamental functions of Nhas, growth inhibition as a result of decreased activity is conceivable. In presence of high Na^+ concentrations, this effect is extremely severe. Na^+ enters the cytoplasm via sodium symport systems and uptake systems, which have not been characterized satisfactorily yet. If Nhas are blocked, sodium will be accumulated in the cytoplasm where it competes with various tasks of potassium.

The fact of Nhas being the target for creatine but not for guanidino-ectoine is also reflected in growth experiments with *E. coli* EP432 which does not contain any of the Nha type antiporters. In absence of these antiporters, growth is only inhibited slightly by creatine whereas guanidino-ectoine nearly completely abolishes growth. Low inhibition by creatine can be attributed to two facts: First of all, Nhas, which have been shown to be one target for creatine, were absent. Additionally, one has to consider the conditions of the experiment. Since *E. coli* EP432 is naturally sensitive to high sodium concentrations, only 0.34 M NaCl were applied (whereas 0.5 M NaCl were used for most other experiments of this work). Already in 2008 Tobias Mann demonstrated that increasing salt concentrations in the growth medium result in intensified growth inhibition (Mann, 2008). Hence, reasons for the low rate of inhibition observed here are probably a combination of absence of one target for creatine and lowered salt concentrations compared to other experiments.

Contrary to the weak creatine effect, the extent of inhibition by guanidino-ectoine is surprising at first glance. Looking into the cells, however, reveals that *E. coli* EP432 does not accumulate trehalose under the conditions of the experiments. *E. coli* K-12, from

which EP432 evolved, would have accumulated approximately 0.15 µmol trehalose/mg cell protein (Styrvold & Strøm, 1991). Extended uptake of potassium and accumulation of glutamate provides one alternative for this mutant to adapt to the elevated salinity despite the absence of the compatible solute trehalose. As discussed in the following paragraphs, guanidino-ectoine most likely accelerates extrusion of potassium which probably results in limitation of cytoplasmic potassium concentrations in absence of trehalose. First evidence that creatine also affects potassium homoeostasis was obtained during growth experiments where osmolarity was increased with sucrose rather than with NaCl (see figure 6.1). If extrusion of sodium was the only disruption generated by creatine, only low rates of inhibition would have occurred in this growth medium with low sodium concentrations, but creatine led to a reduction of growth rate, even though weaker than in medium containing high Na^+ concentrations.

4.1.2 Incompatible solutes disrupt K^+ homoeostasis

In living cells K^+ is transported into the cell during distinctive stress situations via different transport systems. Function of some K^+ transporters is energy dependent while others are K^+ H^+ symporters. Not only uptake of K^+ is critical for survival under certain conditions, a well-balanced ion homoeostasis to keep turgor pressure and membrane potential at a perfect level (where K^+ certainly plays a major role) is also essential for optimal growth of bacteria. Therefore, besides K^+ uptake, K^+ efflux is equally important. Three different efflux systems of *E. coli* haven been characterized during the last decades: KefB and KefC extrude K^+ while taking up H^+, and KefA as a mechanosensitive channel seems to work independently of the proton motive force. Early experiments on these efflux systems have revealed that the K^+ H^+ antiporters KefB and KefC are not essential for growth. Deletion of the corresponding genes did not lead to phenotypes (Booth *et al.*, 1985) whereas deletion of KefA decreased growth of *E. coli* strongly (Levina *et al.*, 1999).
In figure 4.3 K^+ transport systems of *E. coli* and direction of ion transport in living cells and inverted membrane vesicles are outlined.

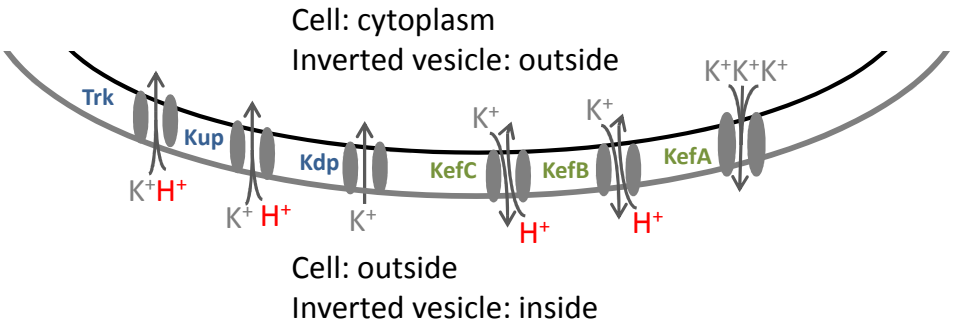

Figure 4.3: Overview of K^+ transport systems in *E. coli* and direction of ion transport in living cells and inverted membrane vesicles. Corresponding names of uptake systems are written in blue, those of efflux systems in green.

With these findings it becomes clear that interpretation of results concerning interaction of incompatible solutes with K^+ homoeostasis (see chapter 3.3.2) is problematic. Obviously, the function of at least one of those systems is changed by creatine and guanidino-ectoine.

MIFE and FLISE techniques revealed altered potassium fluxes following osmotic upshock in presence of (in)compatible solutes. Definite conclusions whether influx or efflux systems are affected can not be drawn due to the facts that only net fluxes are determined with these methods and that inconsistent results were obtained with the two techniques. Advantages and disadvantages of MIFE and FLISE will be discussed in chapter 4.1.3.

Despite those discrepancies, it could be demonstrated by MIFE experiments that betaine and creatine alter potassium flux although they are not taken up. This interesting finding indicates that (in)compatible solutes trigger potassium efflux extracellularly and not by increasing cell turgor due to cytoplasmic accumulation.

Growth experiments with *E. coli* TK2691, which is deficient in genes for all three known K^+ uptake systems, have demonstrated that creatine as well as guanidino-ectoine inhibits growth of this mutant strain severely. This indicates an interaction with K^+ efflux systems rather than uptake systems.

This suspicion is further encouraged by results of K^+ transport activity measurements on inverted membrane vesicles. Creatine and guanidino-ectoine enhanced activity of at least one H^+ dependent K^+ transport system, which can be both, uptake or efflux systems. Since the experimental conditions mimic a situation of increased intracellular K^+ concentration, it is more likely that the effects of increased activity derive from interactions with efflux systems.

In 1987 Bakker *et al.* showed that compatible solutes such as betaine evoke K^+ efflux via KefA, either caused by the molecule itself or by increased turgor pressure due to accumulation of those osmotically active compounds to high cytoplasmic concentrations (Bakker *et al.*, 1987). If the presence of compatible solutes themselves reveal that phenomenon, it is likely that incompatible solutes provoke the same. Since KefA works independently on H^+, however, the acridine orange method used in this work does not reveal interaction with this efflux system. Despite of that, betaine increased activity of H^+ dependent K^+ transport systems more than the incompatible solutes did (see figure 3.20). Therefore, it can be concluded that at least one further system is affected by betaine as well as by creatine and guanidino-ectoine. ChaA constitutes a possible candidate here. First described as a Na^+- and Ca^{2+}- proton antiporter, ChaA has been shown to accomplish K^+ efflux, as well (Radchenko *et al.*, 2006). In addition to that, Radchenko and co-workers demonstrated that antiporter activation is provoked by pH values above 8.0 and simultaneously high KCl concentrations. If this is referred to cytoplasmic or medium potassium concentration, however, does not become clear. MdfA is another potential K^+- and Na^+- H^+ antiporter, but it had been shown to reveal only a low affinity of 50 mM for these monovalent cations (Lewinson *et al.*, 2004). When the correlation with Na^+ and K^+ was discovered, MdfA had been studied with regard to its ability to regulate cytoplasmic pH homoeostasis. The antiporter has been shown to require either K^+ or Na^+ but it seems that it does not function with regard to sodium or potassium toxicity, meaning that it deals with the pH problem in principle (Lewinson *et al.*, 2004).

The finding of creatine and guanidino-ectoine affecting potassium transport is also reflected in growth experiments with *E. coli*. Depending on potassium concentration of the growth media, different effects of creatine and guanidino-ectoine on the growth patterns were observed. To define these effects more precisely, experiments with mutants with deletions of genes coding for single potassium uptake and efflux systems will be necessary.

Besides change in potassium flux, FLISE measurements have demonstrated that the typically observed extrusion of H^+ following osmotic up-shock does not take place when creatine is present. Guanidino-ectoine and betaine on the other hand do not disrupt this mechanism, the pH even changes faster with these compounds compared to measurements with control cells, indicating that not only K^+ H^+ antiport systems are affected by guanidino-ectoine as proposed after transport activity measurements with inverted membrane vesicle but also activity of a H^+ independent export systems such as KefA is

influenced by guanidino-ectoine. To investigate changes in intracellular pH following an osmotic up-shock, measurements with *E. coli* deGFP1 have been performed but unfortunately the poor time resolution of the old software available for this work did not allow reproducible results (data not shown). Measuring pH dependent fluorescent with the GFP derivative deGFP1, however, would be promising with proper technical equipment on hand.

4.1.3 Advantages and disadvantages of the MIFE and FLISE technique

Potassium flux measurements after osmotic up-shock were performed using the MIFE and FLISE system. As described in chapter 2.2.9, preparation of each MIFE measurement is complicated and turned out to be hardly reproducible. Amongst other factors, which are discussed in the following, this probably constitutes inconsistent results obtained using MIFE and FLISE. While net K^+ transport was decreased with creatine according to FLISE measurements, increased influx of K^+ was observed using MIFE. This can be ascribed to methodical discrepancies. During MIFE measurements cells are immobilised on glass cover slips, whereas a stirred dense cell solution is used for FLISE-measurements. In addition to that, fluxes of only very few cells are measured with MIFE, which increases the likelihood to receive false data from damaged cells. Also density of the cells in the often inhomogeneous monolayer is variable which inevitably results in the measurement of fluxes of varying numbers of cells and therefore hardly reproducible results. FLISE, on the other hand, is not as sensitive as MIFE, but the variability is much greater. The ion selective electrodes are positioned in the cell suspension and changes in electric tension arising from fluxes over membranes of billions of cells are detected. As described in chapter 2.2.9, preparation of ion selective electrodes is a crucial step for successful MIFE measurements. Amongst other things, diameter of the electrode tip, amount of liquid ion exchanger and quality of silver wires are factors which are estimated only by visual judgement, and new electrodes have to be prepared at least once a day. Contrary to this, FLISE operates with long-living manufactured electrodes.

Apart from these methodical differences it became apparent that growth phase and environmental conditions are critical for a certain stress response. Cells in late exponential phase behaved differently to cells in early stationary phase for example (data not shown). The availability of oxygen, which is relatively high in MIFE measurements compared to

high cell density FLISE measurements, might therefore be a further factor which leads to contradictory results of MIFE and FLISE measurements.

4.2 Accumulation of (in)compatible solutes leads to changes in metabolome

In the course of metabolome studies during this work it became obvious that incompatible solutes affect the cytoplasmic composition in a similar manner than compatible solutes do in various respects.

4.2.1 γ-aminobutyrate

Comparison of the cytoplasmic composition of *Escherichia coli* grown at different conditions analysed by GC/TOF-MS have led to the conclusion that considering the role of 4-aminobutyrate (GABA) more closely could be worthwhile. Besides the long known effect of increasing cytoplasmic glutamate concentration as response to rising salt concentration a similar behaviour was revealed for GABA (see figure 3.6). While glutamate concentrations decreased in presence of betaine, creatine and guanidino-ectoine, GABA could not be detected at all when these solutes were accumulated. GABA is the decarboxylation product of glutamate, which has been studied elaborately in respect to acid resistance in *Escherichia coli* and other organisms. Its role in osmoprotection is not clear up to now and an increase in accumulation under salt stress conditions had only been detected when GABA was applied to the growth medium. Although Na^+ (but not K^+) seems to play a role in GABA production at least in acidic milieu (Richard & Foster, 2007) cell own synthesis of GABA in non acidic milieu caused by increased osmotic potential of the environment has not been shown to date.
Conversion of glutamate to GABA is known to be achieved with the help of the GAD system, comprising two decarboxylases and an antiporter, which imports glutamate and exports GABA. With this process cells reduce cytoplasmic H^+ concentration (the released carboxylgroup is exchanged with a proton) (O'Byrne & Karatzas, 2008). As observed in this work, GABA is accumulated in the cytoplasm an therefore probably not extruded from the cells. GABA is the decarboxylation product of the negatively charged glutamate which is accumulated during salt stress situations anyway. As a small zwitterionic compound it probably features characteristics typical for compatible solutes. Different to the acid stress response (Richard & Foster, 2007), cytoplasmic potassium

concentrations might be the signal for GABA production during osmotic stress which would be consistent with the observation of total reduction in presence of (in)compatible solutes.

4.2.2 Glutamate and trehalose

In 1986 Sutherland *et al.* found that accumulation of betaine decreases intracellular concentrations of K^+, probably to reduce disadvantageous effects of high cytoplasmic cation concentrations on macromolecules (Sutherland *et al.*, 1986). One year after that, it was discovered that betaine elicits K^+ efflux via KefA (Bakker *et al.*, 1987), which was later on shown to be a cation-specific mechanosensitive channel with significant importance in osmotic adaptation of *E. coli* (Levina *et al.*, 1999; McLaggan *et al.*, 2002). This change in intracellular K^+ concentration entails alteration of several other adaptation mechanisms of *E. coli* in response to increased medium osmolarity. Glutamate dehydrogenase, which catalyses the formation of α-ketoglutarate to glutamate and vice versa, is stimulated by K^+ (Measures, 1975). Therefore, glutamate is accumulated when intracellular K^+ concentration increases and serves as a counter-ion for K^+. Since the intracellular K^+ concentration is significantly lower when betaine is available, the amount of accumulated glutamate is also reduced.
Besides accumulation of glutamate, synthesis of trehalose is strictly regulated by intracellular K^+ concentrations (Giaever *et al.*, 1988). Trehalose, a non-reducing disaccharide of glucose, has been shown to play a dominant role when it comes to environmental stresses such as desiccation, temperature stress or high osmolarity (Crowe *et al.*, 1992; Crowe *et al.*, 1990; Kaasen *et al.*, 1992; Giaever *et al.*, 1988). Similar to what has been observed for glutamate, synthesis of the compatible solute trehalose is reduced in presence of betaines (Rod *et al.*, 1988; Cayley *et al.*, 1989) or proline (Dinnbier *et al.*, 1988).
As discussed in the previous chapter, K^+ homoeostasis is disrupted by creatine and guanidino-ectoine. With the knowledge of betaine reducing intracellular concentration of glutamate and trehalose due to inhibited K^+ accumulation, it is not surprising to find similar features for the incompatible solutes. Creatine reduces trehalose accumulation to a greater extent than guanidino-ectoine but not completely as observed with betaine (see figure 3.4). The glutamate level in cells grown with creatine or guanidino-ectoine, on the other hand, is reduced comparably to that in cells grown with betaine.

Growth experiments of *E. coli* in media containing sucrose instead of NaCl to increase osmolarity revealed that osmotic pressure but not NaCl stress *per se* is responsible

for the growth inhibitory effect of the incompatible solutes. In addition to that, it has been observed that intracellular creatine and guanidino-ectoine concentrations are significantly higher when osmotic stress is applied with sucrose rather than NaCl (see figure 6.1) but an explanation can hardly be given at the actual status of research.
Overall it can be concluded that cells treated with the incompatible solutes creatine and guanidino-ectoine behave similarly to cells treated with the compatible solute betaine with respect to various aspects such as their active uptake and cytoplasmic accumulation and the reduced amount of trehalose, glutamate, 4-aminobutyrate and other amino compounds.
All the more surprising is the finding that betaine compensates the creatine effect although both solutes are taken up (see figure 6.2 and figure 3.9) so that a competition at the level of the transport systems can be excluded. Definite explanations cannot be given at the present status of the research. Nevertheless, it is conceivable that contrariwise interaction of compatible and incompatible solutes with ribsomes and/or DNA, which will be discussed in the following, play a role in this.

4.3 Incompatible solutes interact with ribosomes

In chapter 3.4 it was shown that purified ribosomes from *E. coli* K-12 are less temperature stable when treated with creatine and guanidino-ectoine than untreated ribosomes. In 1967 Leon *et al.* already discovered during spectroscopic determinations that thermal stability of ribosomal subunits and complexes increases in the succession 30S - 50S - 70S (Leon & Brock, 1967). This was confirmed several years later by Mackey and colleagues using calorimetric measurements (Mackey *et al.*, 1991). Depending on buffer composition and dilution factor of ribosomes, the denaturation peak of the 30S subunit was more or less dominant. Description of results obtained in the work on hand are restricted to changes of the most dominant peak, probably reflecting denaturation of the 50S subunit, which shifted depending on solute supplementation. At first glance, 1 °C reduction of melting temperature reached with incompatible solutes might not seem very prominent, but considering that very low concentrations of the solutes were applied, the results gain in importance. Since only 0.1 - 0.13 M creatine and guanidino-ectoine are soluble in water, higher concentrations have not been tested. As shown by Britta Seip, effects of compatible solutes on ribosomal stability can be diverse (Seip, unpublished). She has demonstrated ectoine to be an example for compatible solutes, which destabilise ribosomal complexes at high temperatures, whereas betaine and several more tested

solutes reveal the contrary effect of thermal stabilisation. While 0.25 M ectoine decreases melting temperature by 1 °C, the same concentration of betaine increases the melting point by only 0.4 °C. Up to a certain concentration, increasing amounts of compatible solute lead to an enhancement of the (de)stabilising effect, e.g. in presence of 0.75 M betaine, melting temperature is already shifted by nearly 2 °C. As indicated in figure 3.24, an increase of the creatine concentration from 100 mM to 130 mM led to a decrease of melting temperature from 68.8 °C to 68.2 °C. This indicates that higher concentrations would result in a higher degree of destabilisation of the ribosomal complexes, possibly comparable to that of the compatible solutes betaine and ectoine, if not yet higher. As revealed in later experiments, creatine is at least partially converted to creatinine in hot aqueous solutions. Shifts of melting temperatures of ribosomes treated with creatine have therefore to be considered to derive from creatinine rather than from creatine. Nevertheless, creatine/creatinine and guanidino-ectoine destabilise ribosomal complexes of *E. coli* at high temperatures at least *in vitro*. A disadvantageous interaction with ribosomes could disrupt essential mechanisms of protein biosynthesis which again could explain the growth inhibitory effect of creatine and guanidino-ectoine.

Apart from compatible solutes, which are known to protect macromolecules from different stresses, a range of commonly used antibiotics is known to exert influence on ribosomes. Streptomycin e.g. is an antibiotic from the class of aminoglycosides exhibiting two guanidino moieties and is known to reveal its antimicrobial effect due to interactions with ribosomes. More precisely, streptomycin is known to influence conformational changes of ribosomal subunits, which have been shown to be critical for protein-biosynthesis (Heintz *et al.*, 1966; Page *et al.*, 1967; Mangiarotti & Schlessinger, 1966; Kaempfer, 1968). In 1969 it was proposed that this change in the three-dimensional structure of ribosomes results in an inhibition of the polypeptide synthesis and the stimulation of misreading of the genetic code (Sherman & Simpson, 1969). In addition to that, it was shown that streptomycin binds reversibly to ribosomes, which probably loosens cohesion of the subunits in the 70S complex (Sherman & Simpson, 1969). Two years before this investigation, Leon *et al.* (Leon & Brock, 1967) had pointed out, that streptomycin replaces magnesium ions, at least partially. Mg^{2+} concentrations are crucial to maintain the native state of the 70S complex. A replacement of these ions by streptomycin is therefore likely to alter the stability of ribosomes. Not until one decade later, the binding site of streptomycin was detected to be located within the 30S subunit (Brakier-Ginggras *et al.*, 1978) in a region with sulfhydryl groups of the proteins S1 and S18. In addition to that, Brakier-Ginggras reported that streptomycin reduces the de-

gree of regularity within ribosomal RNA or rather the quantity of base-paired regions, simultaneously increasing the number of unpaired guanine residues.
Interestingly, it has been demonstrated that within the aminoglycosides, compounds carrying a guanidino-function like streptomycin (e.g. dihydro-streptomycin or bluensomycin) have a different mode of action compared to other antibiotics of this class (e.g. kanamycin) (Davies & Davis, 1968; Zierhut *et al.*, 1979). This indicates that the guanidino function is crucial for the particular effects described above and the suspicion of a direct interaction of the guanidino-compounds of this work with ribosomes appears to be obvious.
A disruption of ribosome functions, as observed for streptomycin, becomes more likely if the interaction of the incompatible solutes also originates from a binding to ribosomal structures, which would not only occur at high temperatures but also at physiological conditions. To support the synthesis of such an interaction, agarose gel shift experiments were performed (see figure 3.25). Indeed, a slower movement of ribosomes incubated with incompatible solutes compared to pure ribosomes does not prove a direct binding, but an interaction at room temperature is obvious. Changes in band level might be caused by binding of solutes to ribosomes which would result in an enlarged mass. On the other hand, a change in conformation of the ribosomal complex in presence of the zwitterionic solutes is supposable. Further evidence for a direct binding is given by results obtained by pure chance. Compatible solutes in concentrations above 150 mM were incubated with 1 µM ribosomes and without ribosomes but in the same buffer solution. Surprisingly, solutes were completely soluble in presence of ribosomes whereas precipitates remained without ribosomes (data not shown). This phenomenon verifies the possibility of a binding of incompatible solutes to structures within ribosomal complexes. It also provides an explanation for an observation already made by Tobias Mann in 2008 (Mann, 2008): The concentration of accumulated creatine in the cytoplasm of *E. coli* was 3.5 times higher than solubility in water allows, but no crystalline deposits were visible by microscopic analysis. This indicates a direct interaction of creatine with cytoplasmic compounds and can now be referred to structures within ribosomes.
In 1959 Trissières and co-workers found that *E. coli* ribosomes consist of the 30S and 50S subunits, which form 70S or 100S complexes, depending on the surrounding magnesium concentration (Tissières *et al.*, 1959). In addition to that, they observed that during exponential growth phase 30 % of the bacterial dry weight is constituted by ribosomal subunits or complexes which consist of about 63 % nucleic acids (RNA) and 37 % protein. The implication of guanidino-ectoine on the major constituent of ribosomes, namely

nucleic acids, will be discussed in the following paragraphs, mainly with regard to the following questions:

1. Do incompatible solutes reveal a similar mode of action like guanidino function carrying aminoglycoside antibiotics?
2. Can differences in the effect of compatible and incompatible solutes on ribosomal stability be ascribed to diverse interaction with nucleic acids?

4.4 Guanidino-ectoine stabilises DNA

DNA melting curve analysis revealed surprising results with guanidino-ectoine. Meaningful measurements could not be performed with creatine since it is converted to creatinine in hot water solutions which leads to changes in absorbance during the measurement. Absorbance patterns can therefore hardly be correlated with either conversion of double stranded to single stranded DNA or conversion from creatine to creatinine.
Nevertheless, thermal melting curve analysis proved a strong stabilisation of dsDNA by guanidino-ectoine. Only 50 mM of the incompatible solute increased the melting temperature of calf-thymus DNA by 10 °C. The compatible solute betaine, on the contrary, decreased stability, but higher concentrations were necessary to detect any effect. 1 M betaine decreased the melting temperature by 3 - 4 °C. Calf thymus DNA is known to possess a GC-content of approx. 42 % and is often subject of investigation when it comes to questions about thermal stability of DNA under certain conditions. Rees and colleagues (Rees *et al.*, 1993) tested the effect of betaine on DNA with different GC-contents using a similar temperature profile and a similar buffer as used in experiments of this work and achieved comparable results: Without addition of solutes the melting temperature was 62 °C and betaine decreased thermal stability of this DNA. Effects of different additives on the stability of DNA were precisely reviewed by M. Kurz in 2008 (Kurz, 2008) and are displayed in figure 4.4.
It is obvious that compatible solutes destabilise double stranded DNA. 1 M betaine, e.g., decreases the melting temperature by 2 °C, which is consistent with results of this work. Interestingly, according to Kurz, 0.1 M NaCl stabilise DNA by 9 °C. In 2004 the group of Felitsky proved that betaine is strongly excluded from anionic surfaces, such as the negatively charged phosphate backbone of nucleic acids or negatively charged amino acids in proteins, while urea is considered an inert solute, occurring in similar concentrations at the negatively charged surface or in the surrounding solution (Felitsky

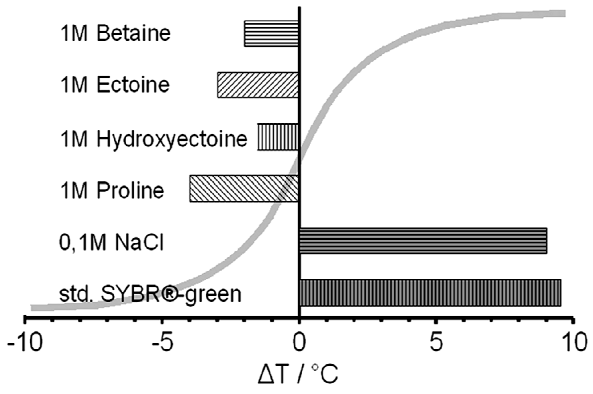

Figure 4.4: The figure as well as the following description are taken from Kurz, 2008: "**Solute effects on melting temperature T_M**. The melting temperature T_M of double stranded DNA is shifted by solutes. Compatible solutes like betaine, tetrahydropyrimidines and proline lower T_M. Sodium chloride shows the same shift in opposite direction at concentrations tenfold lower. Dyes interacting with dsDNA like SYBR®-green also increase T_M at those very low concentrations which are used in realtime applications. The applied standard concentrations are not disclosed by the manufacturer. (Kurz and co-workers, unpublished data for 50 % GC-content.)."

et al., 2004). Further they proposed that this extensive exclusion from cytoplasmic nucleic acids, and within those especially rRNA, is the reason of betaine being an effective osmoprotectant and at the same time a compatible solute.

Considering these explanations of compatible solutes being compatible with the metabolism because they are excluded from macromolecular surfaces could lead to the conclusion that the incompatibility of creatine and guanidino-ectoine with the bacterial metabolism is constituted to an opposed effect: Instead of being excluded, they bind to nucleic acids and therefore also to ribosomes. This again leads, as shown in results of this work, to stabilisation in the case of double stranded DNA or destabilisation in the case of ribosomes, both fundamental compounds of the cell machinery. Binding of incompatible solutes to DNA and ribosomes is also consistent with the finding of much higher compatible solute concentrations in the cytoplasm compared to incompatible solutes. As demonstrated in figure 3.4, 1.4 mmol/g dw betaine and 1.1 mmol/g dw ectoine have been accumulated by *E. coli* by the end of exponential growth phase while only 0.1 - 0.4 mmol/g dw of the incompatible solutes were detected. The phenomenon of betaine being found in higher concentrations in the free cytoplasmic water compared to other solutes was suggested to derive from the strong exclusion of betaine from anionic surface by Felitsky *et al.* (2004). According to them, this again might explain why betaine is

the most striking among osmoprotectants in *E. coli*. If lowered detected concentrations do argue for a stronger binding, and a stronger binding results in growth inhibition, the differing effect of guanidino-ectoine and creatine could be explained. Although creatine but not guanidino-ectoine has been shown to inhibit sodium proton antiporter activity and proton efflux after a hyperosmotic shock, guanidino-ectoine has always revealed a stronger growth inhibitory effect. Additionally, detected guanidino-ectoine concentrations are always lower than those of creatine. Furthermore, the destabilising effect of guanidino-ectoine on ribosomes has been shown to be stronger than with creatine (or creatinine, respectively). In addition to that, guanidino-ectoine reveals a stabilising effect on double stranded DNA, which is comparable, if not yet higher, to that of NaCl whose sodium ions most probably interfere with the negatively charged phosphate backbone.
During experiments prior to this work (Mann, 2008; Sell, 2009) an enhanced solubility of creatine in presence of nucleic acids, first of all RNA, compared to solubility in water was proven. Testing single components of nucleic acids revealed a particularly strong increase in solubility in presence of guanosine (guanine + ribose) but not with ribose alone. It was supposed that the incompatible solutes might compete for guanine binding with cytosine and somehow intercalate with double stranded DNA, which might affect thermal stability of DNA. To investigate if this suspicion is founded, thermal melting curve analysis was performed with synthetic poly(dA-dT). An exclusive effect on guanine would have resulted in no shift of melting temperature in the presence of guanidino-ectoine, but the contrary was observable. This GC-free DNA was stabilised even stronger by guanidino-ectoine than calf thymus DNA. 50 mM guanidino-ectoine increased the melting temperature by 15 °C (10 °C with calf thymus DNA). This result indicates that the stabilising effect of guanidino-ectoine does not derive from a binding to guanine but rather from a binding with the phosphate backbone of DNA. Since the effect is stronger in the absence of guanine and cytosine, a destabilising interaction with one of those bases, probably guanine, is likely. Betaine also revealed a stabilising effect on poly(dA-dT) but to a lesser extent than guanidino-ectoine. 1 M betaine enhanced the melting temperature by 12 °C. This result is consistent with suggestions made by e.g. Rees and colleagues, who showed that the correlation between GC content and melting temperature of double stranded DNA can be abolished by betaine or at concentrations high enough even reversed (Rees *et al.*, 1993). Rees *et al.* further proved that betaine binds weakly to AT-base pairs in α-helical DNA of the B-form, which leads to stabilisation of bondings between those bases, while GC base pairing is destabilised. Since concentrations as high as 1 M betaine reveal only a weak effect on thermal stability of

DNA with both GC and AT base pairs, the effect is probably physiologically not relevant in *E. coli*, where approx. 1.3 M betaine are accumulated when initial salinity is 0.5 M NaCl (calculated from data shown in figure 3.4). In contrast to that, guanidino-ectoine concentrations of 50 mM used for thermal melting curve analysis are clearly exceeded in the cytoplasm so that a physiological relevance can be predicted.
During investigations on improvement of PCR-techniques, Weissensteiner and Lanchbury discovered that betaine was able to counteract the stabilising effect of NaCl on DNA in a so far unknown manner (Weissensteiner & Lanchbury, 1996).
The same might apply to betaine and creatine, when supplied simultaneously. As shown in chapter 3.2.1 and discussed in chapter 4.2.2, both solutes are taken up to "normal" concentrations, but regardless of that, 10 times lower betaine concentrations compensate the growth inhibitory creatine effect.
Overall it can be concluded from results obtained by calorimetric measurements with ribosomes and thermal melting curve analysis of calf thymus DNA with a GC content of approx. 42 % and GC-free DNA that at least guanidino-ectoine interacts with nucleic acids or more precisely the phosphate backbone and guanine, which differs from the phenomenon of betaine being excluded from the negatively charged phosphate backbone of nucleic acids but binding weakly to AT base pairs. In addition to that, guanidino-ectoine most probably behaves differently to guanidino-function carrying antibiotics, which have been discussed in chapter 4.3. However, from results of this work, it cannot be precluded that incompatible solutes also effect proteins. Nevertheless, preferential binding of incompatible solutes to nucleic acids might compete directly with protein binding necessary for ribosome formation. The chance can also be taken to draw the conclusion that incompatible solutes are not compatible because they are not excluded from macromolecular surfaces and therefore interfere with the metabolism.

4.5 The equilibrium of creatine and creatinine

The fact that creatine and creatinine are in an equilibrium has already been described a century ago, e.g. by Edgar and Shiver in 1925 (Edgar & Shiver, 1925), and has turned out to be problematic during several experiments of this work. The stability of creatine and derivatives used as nutritional additive and its impact on the human body have been discussed by Ralf Jäger in several publications. In 2011 he demonstrated that creatine monohydrate in its solid form was stable at 40 °C for more than three years, and only low amounts of creatinine were detected after storage at 60 °C for a long period of time

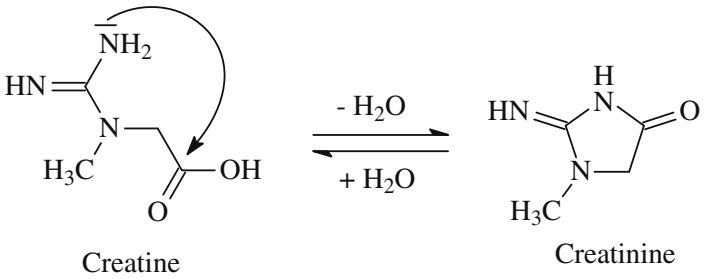

Figure 4.5: The scheme is taken from (Jäger *et al.*, 2011). Equilibrium of creatine and creatinine in aqueous solution.

(nearly four years) (Jäger *et al.*, 2011). In contrast to that, conversion by intramolecular cyclisation (see figure 4.5) takes place in aqueous solution, depending on temperature and pH but independently on creatine concentration.
Edgar and Shiver (Edgar & Shiver, 1925) also demonstrated what Jäger recreated almost a century later. He states that degradation accelerates with increasing temperature and decreasing pH. Earlier researches revealed that creatine in aqueous solution was nearly stable at neutral pH and lowering of pH led to increased conversion to creatinine (Edgar & Shiver, 1925; Dash & Sawhney, 2002). After three days at room temperature, 4 % creatine were degraded at pH 5.5 and even 21 % were degraded at pH 3.5. Storage below room temperature decreased creatinine formation. The effect of temperature has nicely been shown by Edgar and Shiver: After 100 days at 25 °C, the ratio of creatinine/creatine was 0.5, after six days at 50 °C it was 1 and after three days at 70 °C it was 1.5. What does that mean for the experiments of this work? Creatine has always been used in aqueous solutions at moderate temperatures, not exceeding 37 °C and at neutral pH (except in calorimetric measurements with ribosomes and DNA melting curve analysis). Conversion to creatinine will therefore be negligible. During calorimetric measurements, temperature was increased by 1 °C per minute from 25 - 85 °C at pH 7 - 8. Considering the above findings of circumstances for creatinine formation, it can be proposed that only low amounts of creatinine are present in the measuring buffer by the end of the experiment. Hence, the observed effect does presumably derive from creatine. Nevertheless, this knowledge does not help to solve problems occurring during spectrometrically performed thermal melting curve analysis since already low creatinine concentrations change absorption properties.
Although experimental data can most likely be ascribed to creatine, it was of interest to see whether creatinine exhibits similar growth inhibitory features as creatine.

4.5.1 The impact of creatinine on bacterial growth

In dependence on a recent publication of McDonald *et al.* (McDonald *et al.*, 2012), growth experiments with different organisms have been performed with creatinine and creatinine-HCl. McDonald stated that creatinine-HCl but not creatinine acts growth inhibiting on Gram-negative as well as on Gram-positive organisms and that concentrations have to exceed 30 mM to obtain a 50 % decrease of final optical density of bacterial cultures. Results of the work on hand are only partially consistent with findings of McDonald. When creatinine(-HCl) concentrations of only 4 mM were applied, growth inhibition was observable when osmotic stress was given by means of 3 % NaCl in minimal medium. Under the same conditions, 30 mM creatinine(-HCl) led to an almost complete halt of growth (see figure 3.28). With both concentrations, inhibition was greater when creatinine-HCl rather than creatine was applied. Most interestingly, HPLC analysis revealed that creatinine was converted to creatine, but despite that, the amount of accumulated trehalose was not reduced with creatinine (see figure 3.29). Usually creatine inhibits trehalose synthesis in a similar manner as it is known for compatible solutes even though to a lower degree (half trehalose concentration with creatine compared to unsupplemented cultures and nearly no trehalose in presence of betaine). This already indicates that creatinine, other than creatine and guanidino-ectoine, does not enhance potassium efflux so that trehalose synthesis is not limited. Further evidence of this suspicion has been provided by ion transport measurements with inverted membrane vesicles. While creatine, betaine and guanidino-ectoine enhanced flux of potassium as a consequence of KCl up-shock, creatinine and creatinine-HCl halted this effect completely (see figure 3.31). Therefore, it seems that potassium homoeostasis is also disrupted by creatinine but in a contrary manner compared to the other solutes tested in this work. McDonald *et al.* proposed that creatinine overwhelms the ability to pump out protons, which leads to acidification of the cytoplasm and at concentrations high enough to a breakdown of membrane potential. However, results of this work lead to a different conclusion. If potassium efflux, which is mostly accompanied by proton uptake (see chapter 1.3.1), is inhibited, alkalisation of the cytoplasm is more likely than acidification. Disruption of potassium efflux is particularly disadvantageous when uptake of potassium is increased. This situation might occur in acidic milieu where potassium uptake via the Kup system is activated at low osmolarity. These conditions exist in experiments performed by McDonald *et al.*. With this knowledge it is little astonishing to find creatinine to be especially effective in acidic milieu. Both, the potassium efflux system KefB and the uptake system Kup can be found within a wide range of bacteria, Gram-

positives and Gram-negatives. Hence, it is not surprising to discover creatinine inhibit bacteria from both classes. Creatine, on the other hand, has been shown to affect only Gram-negative species and to enhance potassium efflux, which might be mediated by KefC only occurring in Gram-negative bacteria. In addition to that, it had been shown in earlier research (Sell, 2009) that creatine does not inhibit growth in acidic milieu; on the contrary, growth rates were increased with lowered pH. Here again, potassium uptake was probably increased by activation of the Kup system. Simultaneously, the presence of creatine led to efflux of potassium so that intracellular conditions might have been superior to those in cells with "normal" efflux behaviour. Interestingly, glutamate concentrations are decreased in presence of creatinine in a similar manner than with creatine or guanidino-ectoine. This finding implies that either glutamate as the usual counterion for potassium is replaced by another anion in presence of creatinine or, even more likely that conversion to creatine leads to a reduction of the glutamate level. If the latter suspicion is true, one might conclude that accumulation of glutamate is not simply dependent on intracellular potassium concentrations but also on the presence of (in)compatible solutes *per se*.

The surprising finding of creatinine not revealing any inhibitory effect on *E. coli* MKH17, which is deficient in the solute uptake system ProU, may be explained on the one hand by simultaneous presence of similar amounts of creatine and creatinine and on the other hand by features of the uptake system ProP. If the above discussed suspicions are founded, it is conceivable that creatine and creatinine in an intracellular proportion of 1:1 cancel out each other's effects: Creatinine decreases potassium efflux, which is in turn increased by creatine, resulting in a compensation. In addition to that, ProP is a solute proton symporter, which can partially counteract potential alkalisation of the cytoplasm provoked by creatinine which might also decrease its harmfulness. In presence of both solute uptake systems ProP and ProU, creatinine is probably also taken up by ProU which works independently on H^+.

The question about the mode of creatinine conversion to creatine in *E. coli* cannot be answered with the results of this work. Conversion of creatine to creatinine has already been studied in many cases but the reverse reaction is less interesting regarding medical importance and therefore less understood. Nevertheless, Benedict and Edgar (Benedict & Osterberg, 1914; Edgar & Shiver, 1925) have indicated that creatinine is at least partially converted to creatine at alkaline conditions. It is imaginable that creatinine leads to an alkalisation of the cytoplasm, which would surely be disadvantageous for most cell functions and would lead to an inhibition or even halt of growth. Alkalisation

of the cytoplasm would also indicate a disruption of sodium proton antiport activity as observed for creatine. Those antiporters are crucial for pH homoeostasis within cells. Still, it is likely that creatinine is converted to creatine by unknown enzymatic reactions and that it has other features which are incompatible with the metabolism, probably similar to creatine or guanidino-ectoine.

4.6 Outlook

Although various effects of creatine and guanidino-ectoine on cellular mechanisms have been revealed in this work, multiple unresolved issues remain.
γ-aminobutyrate (GABA) was accumulated to concentrations comparable to glutamate at elevated osmolarity by *Escherichia coli*. Growth experiments with supplementation of GABA at different osmolarities and potassium concentrations can give an answer to whether the suspicion of GABA being a compatible solute is founded and if accumulation is triggered by intracellular potassium concentration.
As shown by different methods, potassium flux is altered when creatine or guanidino-ectoine are present. However, none of the employed methods provided definite evidence to prove if potassium efflux or potassium influx are affected. Determination of intracellular potassium concentrations during growth or after osmotic up-shock is a possibility to obtain more detailed insights. This can be achieved by cation-HPLC whereas it has to be ascertained that only cytoplasmic potassium and no extracellular and periplasmic potassium is detected. Silicone oil centrifugation in combination with perchloride provides a convenient method for separation of medium and cells, but still periplasmic potassium will remain. Atomic absorption spectroscopy exhibits another useful method for quantitative determination of potassium and other ions. These methods can also be used to detect sodium concentrations in cells, which is especially interesting when creatine is added where the activity of sodium proton antiporters is decreased and enhanced cytoplasmic sodium concentrations can be predicted. Simultaneous determination of sodium, potassium and proton fluxes by FLISE is also an interesting task that should be expanded to measurements during ionic rather than organic osmotic up-shock. Further knowledge on the effect of incompatible solutes on ion transport can be gained by using mutant strains which are deficient in genes encoding the different potassium uptake systems or sodium proton antiporters.
FLISE measurements and determination of intracellular pH with the pH sensitive GFP derivative deGFP1 indicated that creatine influences pH homoeostasis in *E. coli*. To get a better idea of the actual target, deGFP1 measurements immediately after osmotic up-shock should be performed. If the cytoplasmic pH stays constant in presence of creatine, an interaction with ATPases becomes likely since it has been shown that ATPases are responsible for the extrusion of protons after osmotic up-shock (Akopyan & Trchounian, 2006). This reaction helps to compensate the increase in positive charge caused by extensive potassium accumulation. For reproducible performance of such experiments,

optimal time resolution during measurements is indispensable.
In conjunction with the examination of proton homoeostasis, determining the impact of (in)compatible solutes on the bacterial membrane potential is an important task. Breakdown of the membrane potential due to disadvantageous reduction or enhancement of ion fluxes is conceivable to result in reduced growth.
Ten years ago, Jean Meury stated that the respiration rate of *E. coli* was temporarily decreased after osmotic up-shock (Meury, 1994). This change in respiration rate was shown to be dependent on the intracellular potassium concentration. An *E. coli* mutant strain lacking potassium uptake systems suffered from a constant repression of respiration following osmotic up-shock, but cells were able to recover from inhibition when betaine was supplied. Considering that cytoplasmic potassium concentrations are lowered when betaine is present, respiration rate does not only depend on potassium concentration but also on the presence of solutes, which indicates that the cytoplasmic volume determines respiration rates, at least in osmotic stress situations. Considering these findings, the question arises whether incompatible solutes would reveal the same effect as the compatible solute betaine. However, determination of respiration rates can be performed using a Clark-electrode which virtually detects pressure of oxygen.
In 1987 Ohwada and Sagisaka found that shortly after an osmotic up-shock the ATP level increases significantly, until it decreases again to a normal level after approximately ten minutes (Ohwada & Sagisaka, 1987). The amount of accumulated ATP is thereby dependent on the extent of the up-shock. Up to now, it has not been investigated whether this characteristic changes in presence of compatible solutes and least of all by incompatible solutes. The ATP content probably increases to accomplish synthesis of products needed to counterbalance increased osmolarity (e.g. ion transport systems, compatible solutes). It is imaginable that compatible and maybe also incompatible solutes reduce this effect because *de novo* synthesis of compatible solutes is not necessary and also the need to take up potassium is lowered. The luciferase assay, which takes advantage of the reaction of ATP with luciferin to luciferase and light, is a convenient method to quantify ATP concentrations. The reaction naturally occurs in fireflies, and constituents of the assay are extracted from those. The intensity of bioluminescence which originates from this reaction can be detected spectrometrically and is proportional to the ATP content in the sample (McElroy, 1947; Chappelle & Levin, 1968). To attain ATP concentrations high enough to exceed the sensitivity of the system, a rapid method to concentrate ATP should be adopted. This can e.g. be achieved by filtration of several millilitres of cell culture followed by an immediate transfer of the filter to boiling extraction buffer. A fur-

ther possibility to achieve an enrichment of ATP without falsification of the actual ATP amounts is the freezing of the samples in liquid nitrogen and subsequent evaporation of the water using e.g. a SpeedVac.

As revealed during several experiments of this work, creatine is converted to creatinine in hot aqueous solutions, which made investigation of stability experiments on macromolecules problematic. Problems arising in increased absorption during DNA-melting curve analysis due to creatinine formation can be avoided by using a different method: Calorimetric measurements instead of spectrophotometric measurements for determination of nucleic acid stability in presence of creatine/creatinine, similar to those performed with ribosomes, could provide expedient results. To determine the extent of creatinine formation from creatine under the conditions present during calorimetric measurements, samples should be removed from the calorimeter after measurements to define creatinine contents by HPLC.

The effect of creatinine on bacterial growth is also interesting and needs to be investigated further. It is possible that activity of sodium proton antiporters is inhibited by this compound similar to what has been revealed for creatine. Experiments on inverted membrane vesicles, as have been performed for this work with creatine and guanidinoectoine, would provide evidence on that.

An accurate investigation of changes in solubility of creatine, creatinine and guanidinoectoine in the presence of ribosomes and DNA with different GC contents will lead to interesting findings on binding behaviour and might allow quantification by means of how many molecules of the incompatible solutes bind to the different macro molecules. A reasonable procedure would be the addition of defined concentrations of incompatible solutes to ribosomes or DNA, following incubation and centrifugation or filtration. Concentration of the remaining solutes in the supernatant can be detected by HPLC. In addition to that, higher solubility of incompatible solutes in the presence of nucleic acids and/or ribosomes allows application of higher concentrations to calorimetric measurements which ensures comparability to already performed measurements with compatible solutes.

Under stress situations, one can observe a down regulation of both, rRNA biosynthesis and ribosome production in *E. coli*. This is widely known as the stringent response, which is regulated by the small nucleotide ppGpp (Stent & Brenner, 1961; Cashel, 1975). ppGpp production and therefore stringent response are predicted to be triggered mainly by growth rate (Potrykus *et al.*, 2011). Cells which take up compatible solutes under stress conditions, might not “feel” stressed, thus ppGpp will not be synthesized, and

rRNA and ribosome production will go on. To confirm this hypothesis, comparison of ppGpp levels during growth with and without (in)compatible solutes is essential. If the above hypothesis is correct, one can expect ppGpp levels to be different in stressed cells grown without any solutes and those grown with compatible or incompatible solutes. Cytoplasmic ppGpp levels can be determined by HPLC. Comparing growth patterns of *E. coli* wild type cells and mutants which lack for example the ppGpp synthesis genes, can also exhibit interesting information about the interaction of (in)compatible solutes with ppGpp and ribosomes, respectively.

Apart from these open tasks, investigating the influence of incompatible solutes on cell wall and membrane composition e.g. by HPLC could be worthwhile for a more detailed understanding of the antimicrobial features of incompatible solutes.

5 Summary

Solutes similar in structure to compatible solutes except for a guanidinium group but with the feature of an opposite physiological effect on growth rate are named incompatible solutes. Examples of this class of compounds and main objects of investigation in this work are creatine, which resembles glycine betaine, and the synthetic guanidino-ectoine with structural similarities to ectoine. The major ambition of this work was to reveal why presence of these zwitterionic compounds leads to decelerated growth in osmotic stress situations, which is the opposite effect observed for compatible solutes. Since balance of ion homoeostasis seems particularly challenging in osmotic stress situations, it appeared promising to pay special attention to the effect of incompatible solutes on ion transport. As shown in various experiments, creatine but not guanidino-ectoine inhibits the activity of sodium proton antiporters. Those antiporters implement the two fundamental tasks of maintaining cytoplasmic sodium concentrations on a low level and of regulating cytoplasmic pH. A decreased activity of those antiporters is likely to result in growth inhibition.

Apart from sodium homoeostasis creatine as well as guanidino-ectoine interferes with potassium transport systems. Experiments with an *E. coli* mutant strain, which is deficient in genes for all potassium uptake systems, just as activity measurements on inverted membrane vesicles of *E. coli* wild type implicated that efflux systems rather than uptake systems are affected. This effect somehow seems comparable to the effect of betaine on potassium flux, although the compatible solute increases transport activity more severely. It can therefore be proposed that the incompatible solutes tested here are either weaker messengers to activate efflux compared to betaine or that other efflux systems are targeted.

Nevertheless, compared to concentration in cells which were not supplemented with incompatible solutes, the reduction of cytoplasmic potassium concentrations is well reflected in decreased trehalose and glutamate concentrations. Here again, the effect is more prominent when betaine as a compatible solute is present.

In the course of metabolome studies, γ-aminobutyrate was observed as a potential com-

patible solute, which is accumulated in increasing concentrations when medium osmolarity rises and which is absent when (in)compatible solutes are provided in the growth medium.
In contrast to betaine, which was shown to be excluded from negatively charged surfaces of macromolecules, experiments of this work lead to the conclusion that at least guanidino-ectoine behaves differently. While only high concentrations of betaine (1 M) slightly destabilised double stranded DNA with a GC content of 42 % (by 2 - 3 °C), guanidino-ectoine with a concentration of only 50 mM already increased the melting temperature of the same DNA by 10 °C. This result together with ribosomal melting profiles and gel-shift experiments propose a binding of guanidino-ectoine, and probably also creatine to nucleic acids.

Reactions, such as decreased intracellular potassium concentrations and consequently reduced trehalose and glutamate level, are advantageous for cells as long as compatible solutes are present. These changes in cytoplasmic composition are highly unprofitable as soon as they are provoked by solutes, which are incompatible with the metabolism by means of interferance with essential macromolecules such as DNA or ribosomes. This is probably the critical feature which turns zwitterionic guanidino-compounds into incompatible solutes.

Apart from the incompatible solutes creatine and guanidino-ectoine, the effect of creatinine on bacterial growth was investigated. This was of interest because creatine is converted to creatinine under certain conditions of which some occurred during experiments in this work. Interestingly, creatinine does not only inhibit growth of Gram-negative bacteria, as observed for creatine, but also of Gram-positive ones. In addition to that, it was shown that creatine is taken up by the solute transporter ProP and maybe also by ProU in *E. coli*. Surprisingly, creatinine is at least partially converted to creatine by *E. coli* so that it cannot be distinguished if growth inhibition derives from creatinine itself or from creatine. Nevertheless, activity measurements on inverted membrane vesicles of *E. coli* suggest that potassium efflux is abolished by creatinine.

6 Appendix

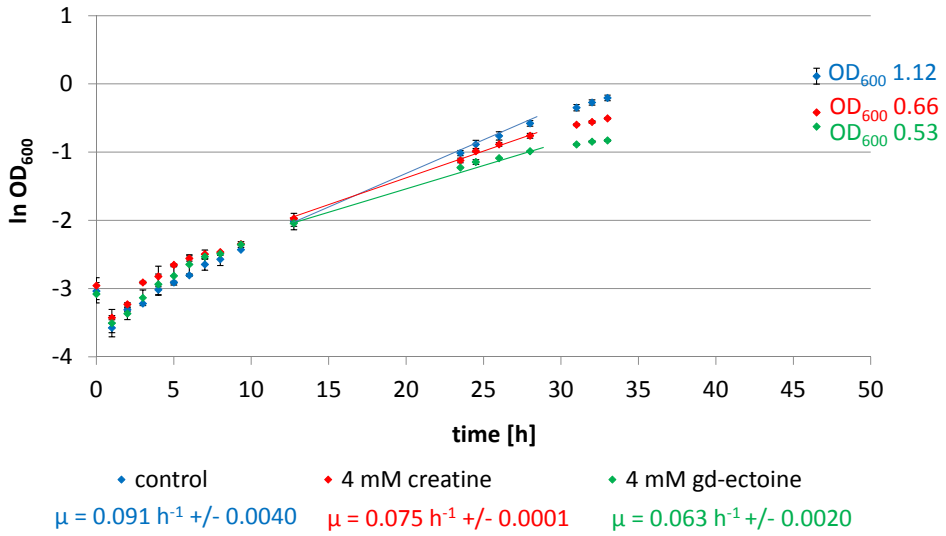

Figure 6.1: Growth of *E. coli* MC4100 at 37 °C in MM63 containing 1 % NaCl and 23 % sucrose (*w*/*v*) (total osmolarity of 1.03 osmol/L). Cultures were supplemented with 4 mM creatine or guanidino-ectoine. Control cultures were not supplemented with any solute. Growth rates (μ) are marked in corresponding colours, and the range of values from which μ was calculated is indicated by lines in the graphs. Each measuring point reflects the arithmetic mean of 2 cultures with error bars providing the highest and lowest value.

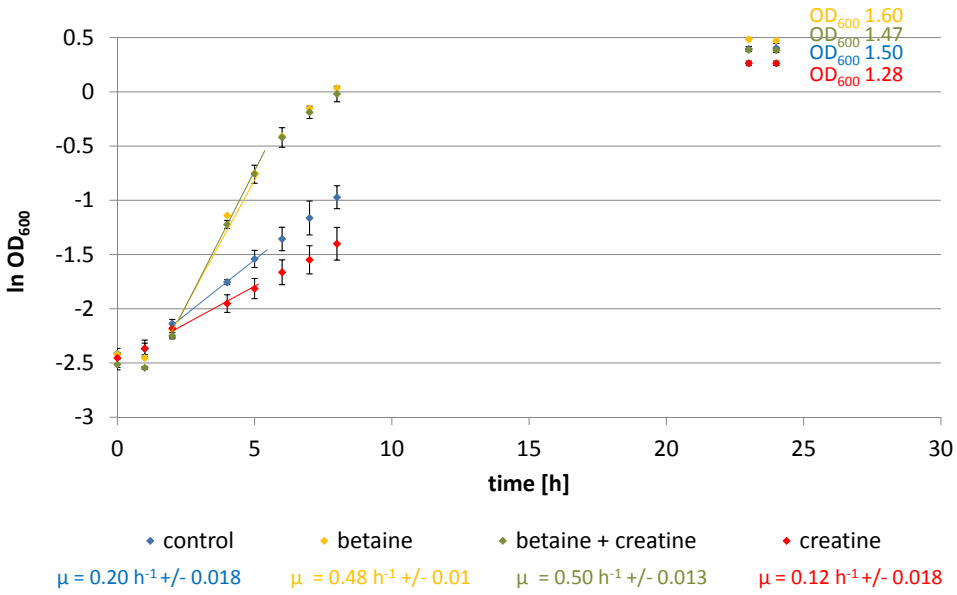

Figure 6.2: Growth of *E. coli* MC4100 in MM63 containing 3 % NaCl. Control: no solutes added, betaine: growth medium supplemented with 0.1 mM betaine, betaine + creatine: growth medium supplemented with 0.1 mM betaine and 2 mM creatine, creatine: growth medium supplemented with 2 mM creatine. Each measuring point reflects the arithmetic mean of 2 cultures with error bars providing the highest and lowest value.

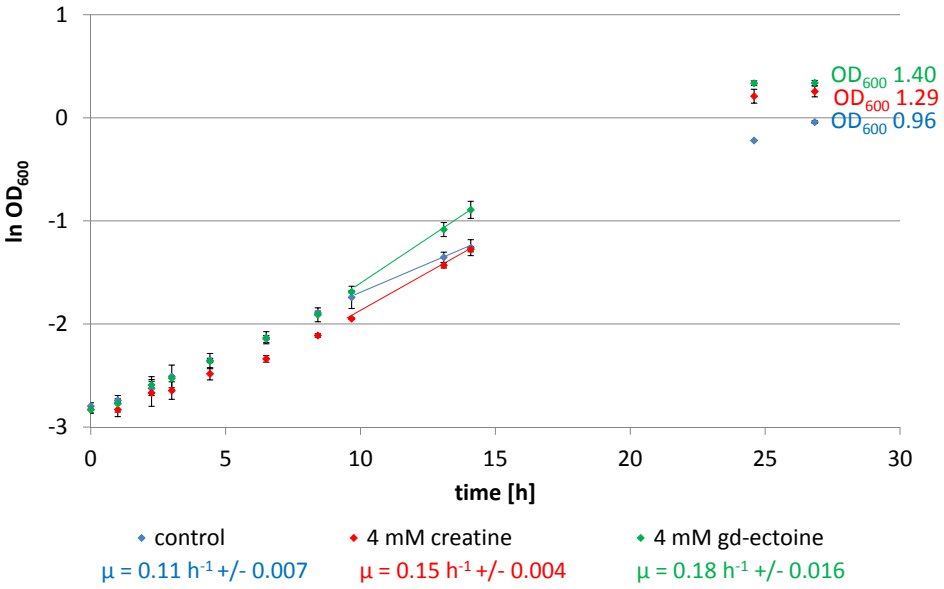

Figure 6.3: Growth of *E. coli* MC4100 in KMM63 containing 3 % KCl (*w*/*v*). Cultures were supplemented with 4 mM creatine or guanidino-ectoine. Unsupplemented cultures served as control. Growth rates (μ) are given in corresponding colours and the range of values from which μ was calculated is indicated by lines in the graphs. Each measuring point reflects the arithmetic mean of 2 cultures with error bars providing the highest and lowest value.

References

Akopyan, K. & Trchounian, A. (2006), '*Escherichia coli* membrane proton conductance and proton efflux depend on growth pH and are sensitive to osmotic stress', *Cell biochemistry and biophysics* **46**(3), 201–208.

Allen, P. J. (2012), 'Creatine metabolism and psychiatric disorders: Does creatine supplementation have therapeutic value?', *Neuroscience Biobehavioral Reviews* **36**(5), 1442 – 1462.

Amendt, B., Stein, M., Fassbender, S., Kunte, J. & Galinski, E. A. (2007), 'Creatine - an incompatible solute: Recovery from fish processing offals and growth inhibitory effects on *E. coli*', *Conference contribution VAAM, Osnabrück* .

Bakker, E. P., Booth, I. R., Dinnbier, U., Epstein, W. & Gajewska, A. (1987), 'Evidence for multiple K^+ export systems in *Escherichia coli*', *Journal of bacteriology* **169**(8), 3743–3749.

Benedict, S. R. & Osterberg, E. (1914), 'Studies in creatine and creatinine metabolism', *Journal of Biological Chemistry* **18**(2), 195–214.

Bertani, G. (1951), 'Studies on Lysogenesis I', *Journal of bacteriology* **62**(3), 293–300.

Blöchl, E., Rachel, R., Burggraf, S., Hafenbradl, D., Jannasch, H. W. & Stetter, K. O. (1997), '*Pyrolobus fumarii*, gen. and sp. nov., represents a novel group of archaea, extending the upper temperature limit for life to 113 °C', *Extremophiles* **1**(1), 14–21.

Bligh, E. & Dyer, W. (1959), 'A rapid method of total lipid extraction and purification', *Canadian journal of biochemistry and physiology* **37**(8), 911–917.

Booth, I. R. (1985), 'Regulation of cytoplasmic pH in bacteria', *Microbiological Reviews* **49**(4), 359–378.

Booth, I. R., Epstein, W., Giffard, P. M. & Rowland, G. C. (1985), 'Roles of the *trk*B and *trk*C gene products of *Escherichia coli* in K^+ transport', *Biochimie* **67**(1), 83–89.

Borges, N., Ramos, A., Raven, N. D., Sharp, R. J. & Santos, H. (2002), 'Comparative study of the thermostabilizing properties of mannosylglycerate and other compatible solutes on model enzymes', *Extremophiles* **6**(3), 209–216.

Bossemeyer, D., Borchard, A., Dosch, D. C., Helmer, G. C., Epstein, W., Booth, I. R. & Bakker, E. P. (1989), 'K^+-transport protein TrkA of *Escherichia coli* is a peripheral

membrane protein that requires other *trk* gene products for attachment to the cytoplasmic membrane', *Journal of Biological Chemistry* **264**(28), 16403–16410.

Bovell, C. R., Packer, L. & Helgerson, R. (1963), 'Permeability of *Escherichia coli* to organic compounds and inorganic salts measured by light-scattering', *Biochimica et Biophysica Acta* **75**(0), 257–266.

Bowman, J. P., McCammon, S. A., Brown, M. V., Nichols, D. S. & McMeekin, T. A. (1997), 'Diversity and association of psychrophilic bacteria in Antarctic sea ice', *Applied and Environmental Microbiology* **63**(8), 3068–3078.

Bradford, M. M. (1976), 'A rapid and sensitive method for the quantitation of microgram quantities of protein utilizing the principle of protein-dye binding', *Analytical biochemistry* **72**(1), 248–254.

Brakier-Ginggras, L. A., Boileau, G., Glorieux, S. & Brisson, N. (1978), 'Streptomycin-induced conformational changes in the 70-S bacterial ribosome', *Biochimica et Biophysica Acta (BBA)-Nucleic Acids and Protein Synthesis* **521**(2), 413–425.

Brown, A. D. (1976), 'Microbial water stress', *Bacteriological Reviews* **40**(4), 803.

Casadaban, M. J. (1976), 'Transposition and fusion of the *lac* genes to selected promoters in *Escherichia coli* using bacteriophage lambda and Mu.', *Journal of molecular biology* **104**(3), 541.

Cashel, M. (1975), 'Regulation of bacterial ppGpp and pppGpp', *Annual Reviews in Microbiology* **29**(1), 301–318.

Cayley, S., Record, M. T. & Lewis, B. A. (1989), 'Accumulation of 3-(N-morpholino) propanesulfonate by osmotically stressed *Escherichia coli* K-12.', *Journal of bacteriology* **171**(7), 3597–3602.

Chappelle, E. W. & Levin, G. V. (1968), 'Use of the firefly bioluminescent reaction for rapid detection and counting of bacteria', *Biochemical medicine* **2**(1), 41–52.

Crowe, J. H., Carpenter, J. F., Crowe, L. M. & Anchordoguy, T. J. (1990), 'Are freezing and dehydration similar stress vectors? A comparison of modes of interaction of stabilizing solutes with biomolecules', *Cryobiology* **27**(3), 219–231.

Crowe, J. H., Hoekstra, F. A. & Crowe, L. M. (1992), 'Anhydrobiosis', *Annual Review of Physiology* **54**(1), 579–599.

Csonka, L. N. (1989), 'Physiological and genetic responses of bacteria to osmotic stress', *Microbiological Reviews* **53**(1), 121–147.

Cui, C., Smith, D. O. & Adler, J. (1995), 'Characterization of mechanosensitive channels in *Escherichia coli* cytoplasmic membrane by whole-cell patch clamp recording', *Journal of Membrane Biology* **144**(1), 31–42.

Da Costa, M., Santos, H. & Galinski, E. A. (1998), 'An overview of the role and diversity of compatible solutes in Bacteria and Archaea', *Advances in Biochemical Engineering/Biotechnology* **61**, 117–153.

Dagert, M. & Ehrlich, S. D. (1979), 'Prolonged incubation in calcium chloride improves the competence of *Escherichia coli* cells.', *Gene* **6**(1), 23.

Dash, A. K. & Sawhney, A. (2002), 'A simple LC method with UV detection for the analysis of creatine and creatinine and its application to several creatine formulations', *Journal of pharmaceutical and biomedical analysis* **29**(5), 939–945.

Davies, J. & Davis, B. D. (1968), 'Misreading of Ribonucleic Acid Code Words Induced by Aminoglycoside Antibiotics: The effect of drug concentration', *Journal of Biological Chemistry* **243**(12), 3312–3316.

Dibrov, P., Rimon, A., Dzioba, J., Winogrodzki, A., Shalitin, Y. & Padan, E. (2005), '2-Aminoperimidine, a specific inhibitor of bacterial NhaA Na^+/H^+ antiporters', *FEBS letters* **579**(2), 373–378.

Dinnbier, U., Limpinsel, E., Schmid, R. & Bakker, E. P. (1988), 'Transient accumulation of potassium glutamate and its replacement by trehalose during adaptation of growing cells of *Escherichia coli* K-12 to elevated sodium chloride concentrations', *Archives of microbiology* **150**(4), 348–357.

Dosch, D. C., Helmer, G. L., Sutton, S. H., Salvacion, F. F. & Epstein, W. (1991), 'Genetic analysis of potassium transport loci in *Escherichia coli*: Evidence for three constitutive systems mediating uptake potassium', *Journal of bacteriology* **173**(2), 687–696.

Douglas, R. M., Roberts, J. A., Munro, A. W., Ritchie, G. Y., Lamb, A. J. & Booth, I. R. (1991), 'The distribution of homologues of the *Escherichia coli* KefC K^+-efflux system in other bacterial species', *Journal of general microbiology* **137**(8), 1999.

Dunn, S. R., Gabuzda, G. M., Superdock, K. R., Kolecki, R. S., Schaedler, R. W. & Simenhoff, M. L. (1997), 'Induction of creatininase activity in chronic renal failure: timing of creatinine degradation and effect of antibiotics', *American journal of kidney diseases* **29**(1), 72–77.

Durell, S. R., Bakker, E. P. & Guy, H. R. (2000), 'Does the KdpA subunit from the high affinity K^+-translocating P-type KDP-ATPase have a structure similar to that of K^+ channels?', *Biophysical journal* **78**(1), 188–199.

Durell, S. R., Hao, Y., Nakamura, T., Bakker, E. P. & Guy, H. R. (1999), 'Evolutionary relationship between K^+ channels and symporters', *Biophysical journal* **77**(2), 775–788.

Edgar, G. & Shiver, H. E. (1925), 'The equilibrium between creatine and creatinine, in aqueous solution. The effect of hydrogen ion', *Journal of the American Chemical Society* **47**(4), 1179–1188.

Elmore, M. J., Lamb, A. J., Ritchie, G. Y., Douglas, R. M., Munro, A., Gajewska, A. & Booth, I. R. (1990), 'Activation potassium efflux from *Escherichia coli* by glutathione metabolites', *Molecular microbiology* **4**(3), 405–412.

Epstein, W. & Davies, M. (1970), 'Potassium-dependant mutants of *Escherichia coli* K-12', *Journal of bacteriology* **101**(3), 836–843.

Epstein, W. & Kim, B. S. (1971), 'Potassium transport loci in *Escherichia coli* K-12', *Journal of bacteriology* **108**(2), 639–644.

Epstein, W. & Laimins, L. (1980), 'Potassium transport in *Escherichia coli*: Diverse systems with common control by osmotic forces', *Trends in Biochemical Sciences* **5**(1), 21–23.

Epstein, W. & Schultz, S. G. (1965), 'Cation transport in *Escherichia coli* V. Regulation of cation content', *The Journal of general physiology* **49**(2), 221–234.

Fassbender, S. (2004), Wertstoffgewinnung aus industriellen Prozess- und Abfallwässern mit Hilfe halophiler Bakterien, PhD thesis, Bonn.

Felitsky, D. J., Cannon, J. G., Michael, W., Hong, J., Van Wynsberghe, A. W., Anderson, C. F. & Record Jr, M. T. (2004), 'The exclusion of glycine betaine from anionic biopolymer surface: Why glycine betaine is an effective osmoprotectant but also a compatible solute', *Biochemistry* **43**(46), 14732–14743.

Galinski, E. A. (1995), 'Osmoadaptation in bacteria', *Advances in microbial physiology* **37**, 273–328.

Galinski, E. A. & Trüper, H. G. (1994), 'Microbial behaviour in salt-stressed ecosystems', *FEMS Microbiology Reviews* **15**(2â3), 95–108.

Gauglitz, U. (1988), *Anaerober mikrobieller Abbau von Kreatin, Kreatinin und N-Methylhydantoin*, Unitext-Verl.

Giaever, H. M., Styrvold, O. B., Kaasen, I. & Strøm, A. R. (1988), 'Biochemical and genetic characterization of osmoregulatory trehalose synthesis in *Escherichia coli*.', *Journal of bacteriology* **170**(6), 2841–2849.

Göller, K. & Galinski, E. A. (1999), 'Protection of a model enzyme (lactate dehydrogenase) against heat, urea and freeze-thaw treatment by compatible solute additives', *Journal of Molecular Catalysis B: Enzymatic* **7**(1), 37–45.

Haardt, M., Kempf, B., Faatz, E. & Bremer, E. (1995), 'The osmoprotectant proline betaine is a major substrate for the binding-protein-dependent transport system ProU of *Escherichia coli* K-12', *Molecular and General Genetics MGG* **246**(6), 783–796.

Hanahan, D. (1983), 'Studies on transformation of *Escherichia coli* with plasmids.', *Journal of molecular biology* **166**(4), 557–580.

Hanson, G. T., McAnaney, T. B., Park, E. S., Rendell, M. E. P., Yarbrough, D. K., Chu, S., Xi, L., Boxer, S. G., Montrose, M. H. & Remington, S. J. (2002), 'Green fluorescent protein variants as ratiometric dual emission pH sensors. 1. Structural characterization and preliminary application', *Biochemistry* **41**(52), 15477–15488.

Harms, C., Domoto, Y., Celik, C., Rahe, E., Stumpe, S., Schmid, R., Nakamura, T. & Bakker, E. P. (2001), 'Identification of the ABC protein SapD as the subunit that confers ATP dependence to the K^+-uptake systems TrkH and TrkG from *Escherichia coli* K-12', *Microbiology* **147**(11), 2991–3003.

Heintz, R., McAllister, H., Arlinghaus, R. & Schweet, R. (1966), Formation and function of the active ribosome complex, *in* 'Cold Spring Harbor symposia on quantitative biology', Vol. 31, Cold Spring Harbor Laboratory Press, pp. 633–639.

Higgins, C. F., Cairney, J., Stirling, D. A., Sutherland, L. & Booth, I. R. (1987), 'Osmotic regulation of gene expression: Ionic strength as an intracellular signal?', *Trends in Biochemical Sciences* **12**, 339–344.

Hill, W. E., Anderegg, J. W. & van Holde, K. E. (1970), 'Effects of solvent environment and mode of preparation on the physical properties of ribosomes from *Escherichia coli*', *Journal of molecular biology* **53**(1), 107–121.

Imhoff, J. F. & Trüper, H. G. (1977), '*Ectothiorhodospira halochloris* sp. nov., a new extremely halophilic phototrophic bacterium containing bacteriochlorophyll b', *Archives of Microbiology* **114**(2), 115–121.

Jäger, R., Purpura, M., Shao, A., Inoue, T. & Kreider, R. B. (2011), 'Analysis of the efficacy, safety, and regulatory status of novel forms of creatine', *Amino acids* **40**(5), 1369–1383.

Kaasen, I., Falkenberg, P., Styrvold, O. B. & Strøm, A. R. (1992), 'Molecular cloning and physical mapping of the *ots*BA genes, which encode the osmoregulatory trehalose pathway of *Escherichia coli*: Evidence that transcription is activated by *kat*F (AppR)', *Journal of bacteriology* **174**(3), 889–898.

Kaempfer, R. (1968), 'Ribosomal subunit exchange during protein synthesis.', *Proceedings of the National Academy of Sciences of the United States of America* **61**(1), 106–113.

Kaplan, A. & Naugler, D. (1974), 'Creatinine hydrolase and creatine amidinohydrolase: I. Presence in cell-free extracts of *Arthrobacter ureafaciens*', *Molecular and cellular biochemistry* **3**(1), 9–15.

Karpel, R., Alon, T., Glaser, G., Schuldiner, S. & Padan, E. (1991), 'Expression of a sodium proton antiporter (NhaA) in *Escherichia coli* is induced by Na^+ and Li^+ ions', *Journal of Biological Chemistry* **266**(32), 21753–21759.

Kempf, B. & Bremer, E. (1998), 'Uptake and synthesis of compatible solutes as microbial stress responses to high-osmolality environments', *Archives of microbiology* **170**(5), 319–330.

Kleyman, T. R. & Cragoe, E. J. (1988), 'Amiloride and its analogs as tools in the study of ion transport', *Journal of Membrane Biology* **105**(1), 1–21.

Kopper, P. H. & Beard, H. H., eds (1947), *Creatinase activity of a strain of Pseudomonas: Federation proceedings*, Vol. 6.

Kreider, R. B. (1999), 'Dietary supplements and the promotion of muscle growth with resistance exercise', *Sports medicine* **27**(2), 97–110.

Kreider, R. B. (2003), 'Effects of creatine supplementation on performance and training adaptations', *Molecular and cellular biochemistry* **244**(1), 89–94.

Kurz, M. (2008), 'Compatible solute influence on nucleic acids: Many questions but few answers', *Saline systems* **4**(6).

Kwon-Chung, K. J., Polacheck, I. & Bennett, J. E. (1982), 'Improved diagnostic medium for separation of *Cryptococcus neoformans var. neoformans* (serotypes A and D) and *Cryptococcus neoformans var. gattii* (serotypes B and C)', *Journal of Clinical Microbiology* **15**(3), 535–537.

Laimins, L. A., Rhoads, D. B. & Epstein, W. (1981), 'Osmotic control of *kdp* operon expression in *Escherichia coli*', *Proceedings of the National Academy of Sciences of the United States of America* **78**(1), 464–468.

Lang, H. J. (2003), Chemistry of NHE inhibitors, *in* 'The Sodium-Hydrogen Exchanger', Springer, pp. 239–253.

Leon, S. A. & Brock, T. D. (1967), 'Effect of streptomycin and neomycin on physical properties of the ribosome', *Journal of Molecular Biology* **24**(3), 391–404.

Levina, N., Tötemeyer, S., Stokes, N. R., Louis, P., Jones, M. A. & Booth, I. R. (1999), 'Protection of *Escherichia coli* cells against extreme turgor by activation of MscS and MscL mechanosensitive channels: identification of genes required for MscS activity', *The EMBO journal* **18**(7), 1730–1737.

Lewinson, O., Padan, E. & Bibi, E. (2004), 'Alkalitolerance: A biological function for a multidrug transporter in pH homeostasis', *Proceedings of the National Academy of Sciences of the United States of America* **101**(39), 14073–14078.

Lippert, K. & Galinski, E. A. (1992), 'Enzyme stabilization by ectoine-type compatible solutes: Protection against heating, freezing and drying', *Applied microbiology and biotechnology* **37**(1), 61–65.

Ludwig, J. (unpublished), Flux measurements with ion selective electrodes. Rheinische Friedrich-Wilhelms-Universität Bonn, Institut für Zelluläre und Molekular Botanik.

Macario, A. J. L., Dugan, C. B. & de Macario, E. C. (1993), 'An archaeal *trk*A homolog near *dna*K and *dna*J', *Biochimica et Biophysica Acta (BBA)-Gene Structure and Expression* **1216**(3), 495–498.

MacDonald, R., Lanyi, J. & Greene, R. (1977), 'Sodium-stimulated glutamate uptake in membrane vesicles of *Escherichia coli*: The role of ion gradients', *Proceedings of the National Academy of Sciences of the United States of America* **74**(8), 3167–3170.

Mackey, B. M., Miles, C. A., Parsons, S. E. & Seymour, D. A. (1991), 'Thermal denaturation of whole cells and cell components of *Escherichia coli* examined by differential scanning calorimetry', *Journal of general microbiology* **137**(10), 2361–2374.

Mangiarotti, G. & Schlessinger, D. (1966), 'Polyribosome metabolism in *Escherichia coli*: Extraction of polyribosomes and ribosomal subunits from fragile, growing *Escherichia coli*', *Journal of molecular biology* **20**(1), 123–143.

Mann, T. (2008), 'Untersuchungen zum Effekt von Kreatin auf Bakterien', *Diploma thesis, Bonn* .

McDonald, T., Drescher, K. M., Weber, A. & Tracy, S. (2012), 'Creatinine inhibits bacterial replication', *The Journal of Antibiotics* **65**, 153–156.

McElroy, W. D. (1947), 'The energy source for bioluminescence in an isolated system', *Proceedings of the National Academy of Sciences of the United States of America* **33**(11), 342.

McLaggan, D., Jones, M. A., Gouesbet, G., Levina, N., Lindey, S., Epstein, W. & Booth, I. R. (2002), 'Analysis of the *kef*A2 mutation suggests that KefA is a cation-specific channel involved in osmotic adaptation in *Escherichia coli*', *Molecular microbiology* **43**(2), 521–536.

McLaggan, D., Naprstek, J., Buurman, E. T. & Epstein, W. (1994), 'Interdependence of K^+ and glutamate accumulation during osmotic adaptation of *Escherichia coli*', *Journal of Biological Chemistry* **269**(3), 1911–1917.

McNicholas, P. M., Najarian, D. J., Mann, P. A., Hesk, D., Hare, R. S., Shaw, K. J. & Black, T. A. (2000), 'Evernimicin binds exclusively to the 50S ribosomal subunit and inhibits translation in cell-free systems derived from both Gram-positive and Gram-negative bacteria', *Antimicrobial Agents and Chemotherapy* **44**(5), 1121–1126.

Measures, J. C. (1975), 'Role of amino acids in osmoregulation of non-halophilic bacteria', *Nature* **257**(3), 398–400.

Médicis de, E. (1986), 'Magnesium, manganese and mutual depletion systems in halophilic bacteria', *FEMS microbiology letters* **39**(1), 137–143.

Meffert, A. (2012), Die Hydroxylierung von Ectoin und Derivaten durch die Hydroxylase EctD aus *Halomonas elongata*, PhD thesis, Rheinische Friedrich-Wilhelms-Universität Bonn.

Meffert, A. (unpublished). Rheinische Friedrich-Wilhelms-Universität Bonn, Insitut für Mikrobiologie und Biotechnologie.

Mergny, J. L. & Lacroix, L. (2003), 'Analysis of thermal melting curves', *Oligonucleotides* **13**(6), 515–537.

Meury, J. (1994), 'Immediate and transient inhibition of the respiration of *Escherichia coli* under hyperosmotic shock', *FEMS microbiology letters* **121**(3), 281–286.

Meury, J. & Kepes, A. (1982), 'Glutathione and the gated potassium channels of *Escherichia coli*', *The EMBO journal* **1**(3), 339.

Meury, J., Lebail, S. & Kepes, A. (1980), 'Opening of potassium channels in *Escherichia coli* membranes by thiol reagents and recovery of potassium tightness', *European Journal of Biochemistry* **113**(1), 33–38.

Möller, B., Hippe, H. & Gottschalk, G. (1986), 'Degradation of various amine compounds by mesophilic *Clostridia*', *Archives of microbiology* **145**(1), 85–90.

Motitschke, P., Driller, D. & Galinski, D. (2003), 'EP Patent 0,671,161. Ectoine and ectoine derivatives as moisturizing agents in cosmetic preparation. 22. October 2003'.

Müller, M. & Blobel, G. (1984), 'In vitro translocation of bacterial proteins across the plasma membrane of *Escherichia coli*', *Proceedings of the National Academy of Sciences of the United States of America* **81**(23), 7421–7425.

Mullis, K. B. & Faloona, F. A. (1987), 'Specific synthesis of DNA *in vitro* via a polymerase-catalyzed chain reaction.', *Methods in enzymology* **155**, 335.

Nakamura, T., Tokuda, H. & Unemoto, T. (1984), 'K^+/H^+ antiporter functions as a regulator of cytoplasmic pH in a marine bacterium, *Vibrio alginolyticus*', *Biochimica et Biophysica Acta (BBA)-Biomembranes* **776**(2), 330–336.

Natochin, Y. V. (1982), 'Mechanism of drugs action on ion and water transport in renal tubular cells.', *Progress in drug research. Fortschritte der Arzneimittelforschung. Progrès des recherches pharmaceutiques* **26**, 87.

Newman, I. (2001), 'Ion transport in roots: Measurement of fluxes using ion-selective microelectrodes to characterize transporter function', *Plant, cell & environment* **24**(1), 1–14.

Nies, D. H. (1995), 'The cobalt, zinc, and cadmium efflux system CzcABC from *Alcaligenes eutrophus* functions as a cation-proton antiporter in *Escherichia coli*', *Journal of bacteriology* **177**(10), 2707–2712.

O'Byrne, C. P. & Karatzas, K. A. G. (2008), 'The Role of Sigma B (σ^{B})in the Stress Adaptations of *Listeria monocytogenes*: Overlaps Between Stress Adaptation and Virulence', *Advances in applied microbiology* **65**, 115–140.

Ohwada, T. & Sagisaka, S. (1987), 'An immediate and steep increase in ATP concentration in response to reduced turgor pressure in *Escherichia coli* B', *Archives of biochemistry and biophysics* **259**(1), 157–163.

Oren, A. (1999), 'Bioenergetic aspects of halophilism', *Microbiology and Molecular Biology Reviews* **63**(2), 334–348.

Oren, A. (2002), 'Diversity of halophilic microorganisms: Environments, phylogeny, physiology, and applications', *Journal of industrial microbiology & biotechnology* **28**(1), 56–63.

Ørskov, F. (1984), 'Genus I. *Escherichia* Castellani and Chalmers 1919, 941AL.', *Bergey's manual of systematic bacteriology* **1**, 420–423.

Padan, E., Maisler, N., Taglicht, D., Karpel, R. & Schuldiner, S. (1989), 'Deletion of *ant* in *Escherichia coli* reveals its function in adaptation to high salinity and an alternative Na^+/H^+ antiporter system', *Journal of Biological Chemistry* **264**(34), 20297–20302.

Page, L. A., Englander, S. W. & Simpson, M. V. (1967), 'Hydrogen Exchange Studies on Ribosomes', *Biochemistry* **6**(4), 968–977.

Paolini, L. (1969), 'Elementary process of nerve conduction and muscle contraction. Ed.: Nachmansohn D, Academic Press 1960 (New York)', *Molecular biology* p. 173.

Pederson, P. L. & Carafoli, E. (1987), 'Ion motive ATPases. Ubiquity, properties, and significance to cell function', *Trends in Biochemical Sciences* **12**, 146–150.

Pinner, E., Kotler, Y., Padan, E. & Schuldiner, S. (1993), 'Physiological role of NhaB, a specific Na^+/H^+ antiporter in *Escherichia coli*.', *Journal of Biological Chemistry* **268**(3), 1729–1734.

Pinner, E., Padan, E. & Schuldiner, S. (1995), 'Amiloride and harmaline are potent inhibitors of NhaB a Na^+/H^+ antiporter from *Escherichia coli*', *FEBS letters* **365**(1), 18–22.

Polacheck, I. & Kwon-Chung, K. J. (1980), 'Creatinine metabolism in *Cryptococcus neoformans* and *Cryptococcus bacillisporus*', *Journal of bacteriology* **142**(1), 15–20.

Potrykus, K., Murphy, H., Philippe, N. & Cashel, M. (2011), 'ppGpp is the major source of growth rate control in *E. coli*', *Environmental microbiology* **13**(3), 563–575.

Radchenko, M. V., Tanaka, K., Waditee, R., Oshimi, S., Matsuzaki, Y., Fukuhara, M., Kobayashi, H., Takabe, T. & Nakamura, T. (2006), 'Potassium/proton antiport system of *Escherichia coli*', *Journal of Biological Chemistry* **281**(29), 19822–19829.

Reed, R. H. & Stewart, W. D. P. (1985), 'Osmotic adjustment and organic solute accumulation in unicellular cyanobacteria from freshwater and marine habitats', *Marine Biology* **88**(1), 1–9.

Rees, W. A., Yager, T. D., Korte, J. & von Hippel, P. H. (1993), 'Betaine can eliminate the base pair composition dependence of DNA melting', *Biochemistry* **32**(1), 137–144.

Richard, H. & Foster, J. W. (2007), 'Sodium regulates *Escherichia coli* acid resistance, and influences GadX- and GadW-dependent activation of gadE', *Microbiology* **153**(9), 3154–3161.

Rod, M. L., Alam, K. Y., Cunningham, P. R. & Clark, D. P. (1988), 'Accumulation of trehalose by *Escherichia coli* K-12 at high osmotic pressure depends on the presence of amber suppressors.', *Journal of bacteriology* **170**(8), 3601–3610.

Roosild, T. P., Miller, S., Booth, I. R. & Choe, S. (2002), 'A mechanism of regulating transmembrane potassium flux through a ligand-mediated conformational switch', *Cell* **109**(6), 781–791.

Sambrook, J., Fritsch, E. F., Maniatis, T. *et al.* (1989), *Molecular cloning: A laboratory manual*, Vol. 2, Cold spring harbor laboratory press New York.

Schleifer, K. H. & Fischer, U. (1982), 'Description of a new species of the genus *Staphylococcus*: *Staphylococcus carnosus*', *International Journal of Systematic Bacteriology* **32**(2), 153–156.

Schleyer, M., Schmid, R. & Bakker, E. P. (1993), 'Transient, specific and extremely rapid release of osmolytes from growing cells of *Escherichia coli* K-12 exposed to hypoosmotic shock', *Archives of microbiology* **160**(6), 424–431.

Schlösser, A., Hamann, A., Bossemeyer, D., Schneider, E. & Bakker, E. P. (1993), 'NAD^+ binding to the *Escherichia coli* K^+ uptake protein TrkA and sequence similarity between TrkA and domains of a family of dehydrogenases suggest a role for NAD^+ in bacterial transport', *Molecular microbiology* **9**(3), 533–543.

Schlösser, A., Kluttig, S., Hamann, A. & Bakker, E. P. (1991), 'Subcloning, nucleotide sequence, and expression of *trk*G, a gene that encodes an integral membrane protein involved in potassium uptake via the Trk system of *Escherichia coli*', *Journal of bacteriology* **173**(10), 3170–3176.

Schlösser, A., Meldorf, M., Stumpe, S., Bakker, E. P. & Epstein, W. (1995), 'TrkH and its homolog, TrkG, determine the specificity and kinetics of cation transport by the Trk system of *Escherichia coli*', *Journal of bacteriology* **177**(7), 1908–1910.

Schönheit, P. & Beimborn, D. B. (1985), 'Presence of a Na^+/H^+ antiporter in Methanobacterium thermoautotrophicum and its role in Na^+ dependent methanogenesis', *Archives of Microbiology* **142**(4), 354–361.

Schröter, C. (2008), 'Gliedergürtelmuskeldystrophien (LGMD). Die Muskeldystrophien vom Gliedergürteltyp. www.gliederguertel-muskeldystrophien.de/ (Klinik Hoher Meissner - Bad Sooden-Allendorf; last access: Arpil, 2013)'.

Schwarz, T. (2005), 'DE Patent 102,004,016,129. Use of combination of osmolyte from extremophilic microorganism, e.g. (hydroxy) ectoine, and evening primrose oil in cosmetics, topical formulations, medical products and pharmaceuticals for skin care and prophylaxis. 14. October 2005'.

Seip, B. (unpublished). Rheinische Friedrich-Wilhelms-Universität Bonn, Insitut für Mikrobiologie und Biotechnologie.

Sell, K. (2009), 'Die antimikrobielle Wirkung von zwitterionischen Guanidiniumverbindungen', *Diploma thesis, Bonn* .

Sell, K. & Galinski, E. A. (2011), 'Guanidino-ectoine: a new member of the incompatible solute family', *Conference contribution VAAM, Karlsruhe* .

Shabala, L., Ross, T., McMeekin, T. & Shabala, S. (2006), 'Non-invasive microelectrode ion flux measurements to study adaptive responses of microorganisms to the environment', *FEMS microbiology reviews* **30**(3), 472–486.

Shabala, S. N., Newman, I. A. & Morris, J. (1997), 'Oscillations in H^+ and Ca^{2+} Ion Fluxes around the Elongation Region of Corn Roots and Effects of External pH', *Plant Physiol.* **113**(1), 111–118.

Sherman, M. I. & Simpson, M. V. (1969), 'The role of ribosomal conformation in protein biosynthesis: the streptomycin-ribosome interaction', *Proceedings of the National Academy of Sciences of the United States of America* **64**(4), 1388–1395.

Smith, N. R. & Gordon, R. (1957), 'Genus I. Bacillus Cohn, 1872', *Bergey's manual of determinative bacteriology. 7th ed. Williams and Wilkins, Baltimore* pp. 613–634.

Spizizen, J. (1958), 'Transformation of biochemically deficient strains of *Bacillus subtilis* by deoxyribonucleate', *Proceedings of the National Academy of Sciences of the United States of America* **44**(10), 1072.

Stent, G. S. & Brenner, S. (1961), 'A genetic locus for the regulation of ribonucleic acid synthesis', *Proceedings of the National Academy of Sciences of the United States of America* **47**(12), 2005.

Stewart, L. M., Bakker, E. P. & Booth, I. R. (1985), 'Energy coupling to K^+ uptake via the Trk system in *Escherichia coli*: the role of ATP', *Journal of general microbiology* **131**(1), 77–85.

Stumpe, S. & Bakker, E. P. (1997), 'Requirement of a large K^+-uptake capacity and of extracytoplasmic protease activity for protamine resistance of Escherichia coli', *Archives of microbiology* **167**(2), 126–136.

Stumpe, S., Schlösser, A., Schleyer, M. & Bakker, E. P. (1996), 'K^+ circulation across the prokaryotic cell membrane: K^+-uptake systems', *Handbook of biological physics* **2**, 473–499.

Styrvold, O. B. & Strøm, A. R. (1991), 'Synthesis, accumulation, and excretion of trehalose in osmotically stressed *Escherichia coli* K-12 strains: Influence of amber suppressors and function of the periplasmic trehalase.', *Journal of bacteriology* **173**(3), 1187–1192.

Sutherland, L., Cairney, J., Elmore, M. J., Booth, I. R. & Higgins, C. F. (1986), 'Osmotic regulation of transcription: induction of the *pro*U betaine transport gene is dependent on accumulation of intracellular potassium', *Journal of bacteriology* **168**(2), 805–814.

Taglicht, D., Padan, E. & Schuldiner, S. (1993), 'Proton-sodium stoichiometry of NhaA, an electrogenic antiporter from *Escherichia coli*', *Journal of Biological Chemistry* **268**(8), 5382–5387.

Tannock, G. W. (1994), *Normal microflora: An introduction to microbes inhabiting the human body*, Springer.

Tempest, D., Meers, J. & Brown, C. (1970), 'Influence of environment on the content and composition of microbial free amino acid pools', *Journal of general microbiology* **64**(2), 171–185.

Tissières, A., Watson, J. D., Schlessinger, D. & Hollingworth, B. R. (1959), 'Ribonucleoprotein particles from *Escherichia coli*', *Journal of Molecular Biology* **1**(3), 221–233.

Trchounian, A. & Kobayashi, H. (1999), 'Kup is the major K^+ uptake system in *Escherichia coli* upon hyper-osmotic stress at a low pH', *FEBS letters* **447**(2-3), 144–148.

Tsuchiya, T., Raven, J. & Wilson, T. (1977), 'Co-transport of Na^+ and methyl-β-D-thiogalactopyranoside mediated by the melibiose transport system of *Escherichia coli*', *Biochemical and biophysical research communications* **76**(1), 26–31.

van der Knaap, M. S., Verhoeven, N. M., Maaswinkel-Mooij, P., Pouwels, P. J. W., Onkenhout, W., Peeters, E. A. J., Stöckler-Ipsiroglu, S. & Jakobs, C. (2000), 'Mental retardation and behavioral problems as presenting signs of a creatine synthesis defect', *Annals of neurology* **47**(4), 540–543.

Ventosa, A., Nieto, J. J. & Oren, A. (1998), 'Biology of moderately halophilic aerobic Bacteria', *Microbiology and Molecular Biology Reviews* **62**(2), 504–544.

Vilhelmsson, O., Hafsteinsson, H. & Kristjánsson, J. K. (1996), 'Isolation and characterization of moderately halophilic bacteria from fully cured salted cod (bachalao)', *Journal of Applied Microbiology* **81**(1), 95–103.

Walderhaug, M. O., Litwack, E. D. & Epstein, W. (1989), 'Wide distribution of homologs of *Escherichia coli* Kdp K^+-ATPase among Gram-negative bacteria', *Journal of bacteriology* **171**(2), 1192–1195.

Waldmann, L. (2005), Effect of L-arginine and guanidinium chloride (GdmCl) on the unfolding and refolding of hen egg-white lysozyme (HEWL), PhD thesis.

Weissensteiner, T. & Lanchbury, J. S. (1996), 'Strategy for controlling preferential amplification and avoiding false negatives in PCR typing', *BioTechniques* **21**(6), 1102–1109.

Whatmore, A. M., Chudek, J. A. & Reed, R. H. (1990), 'The effects of osmotic upshock on the intracellular solute pools of *Bacillus subtilis*', *Journal of general microbiology* **136**(12), 2527–2535.

Zierhut, G., Piepersberg, W. & Böck, A. (1979), 'Comparative Analysis of the Effect of Aminoglycosides on Bacterial Protein Synthesis *in vitro*', *European Journal of Biochemistry* **98**(2), 577–583.

7 Acknowledgement

Ich danke Herrn Prof. Dr. Erwin Galinski für seine Unterstützung und Ratschläge als Doktorvater und die Ermöglichung zur Erstellung dieser Arbeit.
Ich möchte Ihnen besonders danken, dass Sie meinen Tasmanienaufenthalt möglich gemacht haben. Nich zuletzt durch dieses unvergessliche Erfahrung werde ich meine Doktorandenzeit stets als eine tolle Zeit im Gedächtnis bewahren. Vielen Dank!

Frau apl. Prof. Dr. Christiane Dahl danke ich für die freundliche Übernahme des Zweitgutachtens.

I thank all people from the University of Tasmania who supported me during my stay.
I owe special thanks to Prof. Marc Tamplin who organized and agreed to my visit and helped me to find a place to stay.
I am especially indebted to Prof. Tom McMeekin for many interesting discussions and encouragements during my stay at UTas and afterwards. Thank you for sending your promoting ideas to the other side of the world!
Many thanks to Sergey and Svetlana Shabala for introducing the wonderful MIFE system to me and for being very cooperative all the time.
I would like to express my very special gratitude to the amazing Dr. Lyndal Mellefont from Mount Nelson to receive me in her beautiful house and to bestow a most delicious time upon me. I hope to meet you some day again, up in the air or under your porch.

Ich danke Herrn PD Dr. Jost Ludwig sowie Daniel Ganser für die Etablierung und Bereitstellung des FLISE-System. Besonders Daniel danke ich für viele zeitaufwändige Hilfestellungen.

Herrn Jochem Gätgens vom Forschungszentrum Jülich danke ich für die Durchführung der GC/TOF-MS Analysen und die intressante Zusammenarbeit.

Ein besonderer Dank gilt selbsverständilich meiner Arbeitsgruppe.
Der guten Seele Birgit Amendt danke ich natürlich für die gewissenhafte Bereitstellung ihrer Fähigkeiten in Hinblick auf die Lagerung und Wiederbelebung von Bakterienzellen aber vorallem auch für ihre Gutmütigkeit und die stets gefüllten Keks- und Kuchen Vorräte. Ohne dich würde der Tee nur halb so gut schmecken.
Der mehrarmigen und vielköpfigen Elisabeth Witt danke ich für all ihre Ratschläge, sowohl zu meiner Arbeit als auch zum Thema Gartenbau. Ich bin froh dass du mir Finch gezeigt hast und danke dir von Herzen für Mürmelchen und andere Überraschungen!

Mit in die Gruppe der Gartenliebhaber gehört Marlene Hecker, der ich für grüne Abwechslungen, ausgewachsen in Venlo oder auch in Samenform für den Balkon, danke.
Matthias Kurz danke ich für hilfreiche wissenschaftliche Anregungen und die köstlichen Speisen aus fernen Ländern.
Der Hilfsbereitschaft in Person, Elisabeth Schwab danke ich für viele Hilfestellungen im Labor, so vor allem das ständige Wechseln von HPLC-Säulen und zugehörige Messungen. Danke außerdem, dass du es immer wieder schaffst auch in aufregenden Zeiten eine ausgeglichene Atmosphäre zu schaffen und deine Ruhe wenn nötig auf uns überträgst!
Danke Andrea Meffert für deine tolle Betreuung in meinem ersten Laborblock, sowie die erfrischende Zusammenarbeit im Kellerlabor während meiner Diplomarbeit. Du hast mich veranlasst, die AG nicht so schnell zu verlassen.
Dem Kellerkind Christoph Tanne danke ich für etwaige Kopfkino-Vorführungen und viele interessante fachliche und freundschaftliche Unterhaltungen. Ich hoffe wir pendeln in Zukunft noch oft zwischen Rhein und Spree hin und her.
Britta Seip danke ich für viele nette Unterhaltungen während und außerhalb des Unialltags. Danke außerdem, dass du mir gezeigt hast, wie man mit Ribosomen umgeht.
Jhonny Correa danke ich für die Bereicherung meiner Kenntnisse zu Ectoin Hydroxyectoin und allem was dazu gehört. Außerdem die Einladungen zu stets gut besuchten Partys mit immer neuen Gesichtern die in mindestens 5 verschiedenen Sprachen miteinander kommunizieren. Nicht zuletzt, wer hätte sich um Sekt und Käsekuchen gekümmert wenn du nicht aus dem fernen Panama nach Bonn gekommen wärst?
Kathi Moritz, Kathi Werner und Marco Schäfer-Herte danke ich für die gute Zusammenarbeit und ihre Mühe während ihrer Laborblöcke.
Kathi Moritz gilt außerdem ein Dankeschön für das Beitreten in den Club der Teetrinker. Ich bin froh, dass du dich entschieden hast die Arbeitsgruppe noch ein paar weitere Jahre mit deiner Fröhlichkeit zu beglücken.
Sinje Vielgraf danke ich für die vielen schönen und lustigen Momente in den Teepausen und auch nach Feierabend.
Tassilo van Ooyen, nie wäre ich auf die Idee gekommen aus dem Keller einen Blick auf die Baumkronen in Estland zu werfen. Aber es hat sich gelohnt! Danke!
Unserem Mann für alles, Elmer Kopp, danke ich für seine Hilfsbereitschaf in jeder Situation und seine freundschaftliche Art.

Allen Institutsmitglieder danke ich für anregende Diskussionen und eine angenehme Arbeitsatmosphäre.

Danken möchte ich außerdem meiner Familie für viele unterstützende Worte und Hilfestellung wann immer sie nötig waren. Dabei gilt mein besonderer Dank meinem Verlobten Fritz Waßmann für seine Liebe und sein Verständis in jeder Lebenslage.